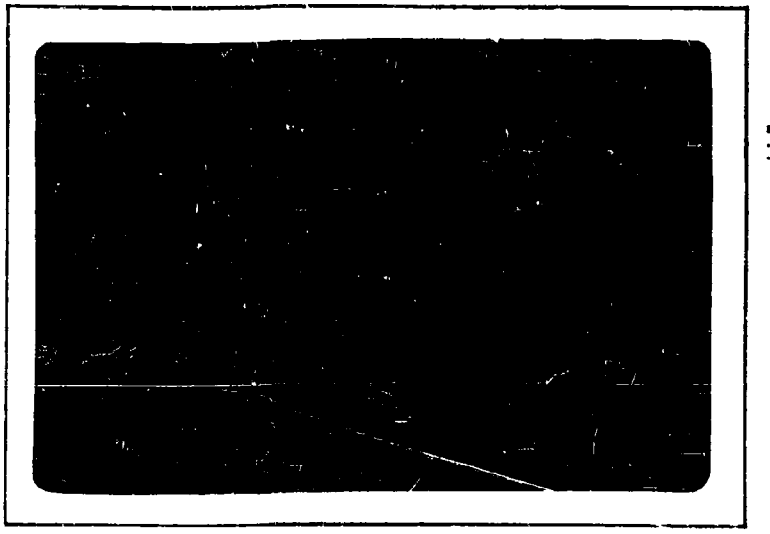

TECHNOLOGY DEPARTMENT

CRUCIBLE STEEL COMPANY OF AMERICA

234 100, 6338, 1452, 1450, 1451, 5951, 5451,
6161, 1273, 3727, 1125, 1159, 1492, 5712, 1184,
6337, 4366, 2975, 295, 6060, 67, 271, 1455,
4128, 4354

THE SALT CORROSION OF TITANIUM ALLOYS AT ELEVATED TEMPERATURES

Final Technical Report

January 15, 1961

Contract No. NOas 60-6004-c

September 21, 1959 to December 30, 1960

E. L. Kochka
V. C. Petersen

CRUCIBLE STEEL COMPANY OF AMERICA
Midland Research Laboratory
Midland, Pennsylvania

THE SALT CORROSION OF TITANIUM ALLOYS AT ELEVATED TEMPERATURES

ABSTRACT

The corrosion of titanium by salt below 1100F is an overall oxidation process that proceeds by the following steps: (1) chloride salt reacts with titanium and surface oxides with the liberation of chlorine; (2) chlorine attacks titanium metal; and (3) titanium chlorides oxidize. The reaction is sustained by (a) diffusion of salt into the oxide layer and (b) continued regeneration of chlorine. Accelerated attack above 1100F is the result of a liquid salt phase that forms and improves contact between alloy and corrodent.

The attack of stressed super-alpha titanium alloys, processed below the beta transus, is centered in the grain boundaries. Alloys processed at higher temperatures corrode more extensively and crack transgranularly indicating that alloy partitioning occurs and results in thermal sensitization. Chlorine is the primary cracking agent.

The extent of the damage contributing to stress failure can be reduced by processing alloys containing minimum amounts of hydrogen, at low temperatures.

Certain minor alloy additions, notably 0.2 percent palladium and 0.1 percent yttrium, slightly improve the resistance of the base alloys to salt. Carefully applied, adherent, non-porous aluminum and nickel plates, although susceptible to mechanical damage, provide adequate protection of stressed super-alpha titanium alloys below 1000F.

TABLE OF CONTENTS

TABLE OF CONTENTS
(Continued)

TABLE OF CONTENTS
(Continued)

TABLE OF CONTENTS
(Continued)

LIST OF TABLES

LIST OF TABLES
(Continued)

LIST OF TABLES
(Continued)

LIST OF FIGURES

LIST OF FIGURES
(Continued)

LIST OF FIGURES
(Continued)

LIST OF FIGURES
(Continued)

I. INTRODUCTION

The corrosion of titanium by salt at elevated temperatures was first reported as a result of investigating an occasional loss in ductility observed after creep testing a particular titanium alloy. When specimens were machined after creep testing to remove about two mils from the surface, no loss in ductility was evident. This surface phenomena was at first explained as "omega" embrittlement. Subsequent work showed that failure was due to salt corrosion. Traces of salt were identified on the fractured surface of a specimen by means of x-ray diffraction techniques. The salt was traced to fingerprints as indicated by their characteristic pattern.

Realizing the potential damage that could be caused by salt corrosion, several laboratories began research work on this problem. Some of the results of this work were published in a cooperative effort by four of the titanium producers and Pratt and Whitney Aircraft Company in 1957(1). Although considerable information is available on the corrosion behavior of titanium in molten salts and in aqueous salt solutions, few reports such as TML Report No. 88(1) and WADD Technical Report 60-191(2) contain information on the dry salt corrosion of titanium and titanium alloys at elevated temperatures.

TML Report No. 88 showed that all titanium alloys produced prior to the middle of 1957 are vulnerable in varying degrees to salt corrosion at high temperatures. The nature and extent of the damage caused by salt corrosion is a function of the load, time, and temperature. The salt attacks the grain boundaries and produces sizeable pits, at above about 750F, which are precursors of the stress corrosion cracking of titanium alloys. This action decreases the cross-sectional area and produces notches which markedly decrease the tensile ductility. Rapid general corrosion of unstressed samples in intimate contact with sodium chloride was reported for temperatures above 1100F.

Some data supported the expectation that anodized films would retard thecorrosion, but WADD Technical Report 60-191(2) shows the protection of the oxide film to be lost in time by direct reaction with the chloride salt. The incubation period for crack initiation depends upon the thickness of the oxide film and on temperature and stress. The reaction is accelerated when corrosion products lower the melting point of salt, flux away the oxide film, and form a liquid layer on the metal surface. After the oxide film is eliminated the corrosion process is basically electrolytic.

---

(1) Numbers in parenthesis identify references appended to this report.

These laboratory tests are conducted under much more severe conditions than would normally be encountered. At the present time, no service failure can be attributed to salt corrosion, nor are there any known applications within the stress and temperature ranges where failures would be expected. The alloys being produced are limited by their high temperature mechanical and strength properties, particularly creep, but not by salt corrosion.

As new performance frontiers are sought, however, the demands increase for materials to withstand operation at increasingly higher temperature and stress levels. Super-alpha and heat-treated alpha-beta alloys, having favorable high-temperature mechanical and strength properties, have been developed recently. However, the high-temperature applications of these new alloys may be limited by their vulnerability to salt corrosion.

The Bureau of Aeronautics, Department of the Navy recognized the seriousness of this problem and awarded Crucible Steel Company of America Contract NOas 60-6004-c to conduct a research study on the salt corrosion phenomena. This research program, based on our proposal ML-59-3G, dated 28 May 1959, had the following objectives.

1. To study the nature and mechanism of the corrosion and cracking of titanium by salt at elevated temperatures.

2. To evaluate the performance characteristics of the newer titanium alloys, especially Ti-8Al-1Mo-1V, Ti-12Zr-7Al, and Ti-8Al-8Zr-1 (Cb + Ta), under conditions which may result in salt corrosion and cracking.

3. To apply coatings for salt corrosion resistance.

4. To study the influence of processing and alloying in an effort to minimize salt damage at high temperature and stress levels.

These objectives were pursued by combining a fundamental study of the hot salt corrosion phenomena to provide a basis for suggesting means of increasing the corrosion resistance of titanium-base materials with an investigation of coatings and special processing designed to protect titanium against salt corrosion at elevated temperature and stress.

II. SUMMARY AND CONCLUSIONS

This report describes research conducted under the Bureau of Aeronautics, Department of the Navy, Contract NOas 60-6004-c. The objectives of this program were to study the basic salt corrosion phenomena, and means for minimizing the damage caused by salt on the super-alpha titanium alloys at elevated temperatures.

The conditions for reaction and the products of reaction were established. The reaction requires oxygen or a reducible oxide, and is accelerated by certain oxides. Chlorine is an important reaction product; it attacks titanium readily and is recycled by the oxidation of the titanium salts. Consequently, a trace of chloride salt can produce extensive damage. The damage is a direct function of time, temperature and stress level. Evidence was also found of a liquid corrosion phase above about 1100F which is coincident with a marked increase in general salt corrosion.

In the super-alpha alloys and Ti-6Al-4V (C120AV), the threshold for general salt attack occurred at 800F. Application of stress reduced this threshold attack to 600F. The upper temperature limit for stress corrosion was found to be alloy dependent, i.e., 800F for Ti-6Al-4V, 900F for Ti-8Al-1Mo-1V and above 1000F for Ti-12Zr-7Al. Stress does not appear to accelerate general attack or promote stress corrosion cracking above these temperatures. The rate of attack is then temperature dependent.

In the study of processing effects, it was discovered that the super-alpha alloys could be sensitized to both aqueous stress corrosion cracking, and to elevated temperature salt attack, by prior excessively high-temperature exposures. As a corollary to this effect, improved resistance to salt attack was obtained by laboratory processing at temperatures below the recrystallization temperatures. Evidence to date indicates that high-temperature sensitization in titanium alloys is associated with alloy partitioning and the formation of a submicroscopic secondary phase.

Of the numerous surface treatments and coatings tested, nickel plating and aluminum coating--both dip and flame spray--offered the best protection against salt attack. When applied with a minimum thickness of 0.002 inches, protection was obtained to 1000F. Nickel-plated, as well as aluminum-coated, material suffered a decrease in room temperature fatigue strength which, however, we believe may be remedied by development of improved techniques for surface preparation and coating.

III. RECOMMENDATIONS FOR FUTURE WORK

The results of this exploratory investigation on the problem of elevated temperature corrosion in titanium alloys has yielded further information on the nature and mechanism of the corrosion phenomena. In addition, the discovery that titanium alloys can be "sensitized" by excessively high temperature exposures is likewise of basic importance. These results together with findings on the special alloying phase of this report strongly suggest the following areas of study for a solution to the salt corrosion problem:

1. A fundamental study to elucidate further the role and significance of the liquid corrosion phase.

2. The composition, nature, and role of the metallurgical phases involved in the sensitizing phenomena. Since all of the studies to date indicate this phenomena to be associated with alloy partitioning and the formation of a fine secondary phase, a study of the phenomena would necessarily include electron micrography and electron probe analyses.

3. A theoretical and empirical study of individual and multiple alloying elements to catalogue their effects on the corrosion phenomena. Here, theoretical consideration of alloy additions would include deoxidation capacity, electrochemical nobility, and atomic size of both the metal addition and its oxide.

4. The application of these and previous findings for the development of additional salt resistance in the important current and new titanium alloys.

IV. LITERATURE SURVEY

The literature was surveyed for the most part from 1950 to the present. Primary importance was placed upon Titanium Abstract Bulletin, Crerar Metals Abstracts, Chemical Abstracts, and the ASM Review of Metal Literature as reference sources. The original articles were consulted when available, but in the case of foreign language articles reliance was usually placed upon the abstracts for an understanding of the text.

With the exception of TML Report No. 88[1] and WADD Technical Report 60-191[2], there is little published information directly related to the problem of the dry salt corrosion of titanium at elevated temperature and stress. A series of articles is available on the corrosion of titanium by molten salts and these will be discussed later. Articles on the corrosion testing of titanium in aqueous salt systems were excluded from consideration except in those few cases where stress corrosion cracking was of primary importance. It would be well to begin by examining the state of the art as it applies to the hot salt corrosion of metals other than titanium before entering into the titanium corrosion problem.

A. Salt Corrosion of Metals Other Than Titanium

Previous investigators of salt corrosion were concerned almost exclusively with the effects of molten salts upon metals. Under these conditions there is limited access of oxygen to the metal surface, and

in many cases the vapors above the salt baths are more corrosive than the salt bath itself.

A recent paper deals with the rapid intergranular attack of 18-8 stainless steels by oxygen and dry sodium chloride at elevated temperature[3]. The corrosion process involves the migration of oxygen and metal vapor to the metal surface where they apparently react with chromium or chromium oxide in the steel to form a non-protective sodium chlorate containing scale. Chromium carbide in the grain boundaries accelerates intergranular attack. Stress appears to have only a minor influence on the rate of reaction.

Several studies were made on the corrosion of metals in fused alkali halides. Inconel electrodes are found to be only slightly attacked by fused sodium chloride-potassium chloride at 1500F unless the bath is made alkaline. However, very large amounts of alkali depress electrode destruction[4]. Russian investigators showed the rate of corrosion of iron increases with temperature in molten carnallite ($KCl \cdot MgCl_2 \cdot 6H_2O$) dehydrated with dry hydrogen chloride, whereas, the rate decreases in molten carnallite dehydrated with ammonium chloride[5]. Gurovich[6] studied the corrosion of nickel, copper, and several steels in molten potassium, sodium, and lithium chlorides and found that corrosion increases for the same metals with the following order of the cation radius: $LiCl > NaCl > KCl$. (The reverse order was found to hold true for titanium.)[36] Electrochemical studies of nickel, copper, and iron versus a platinum electrode in fused alkali halides show the galvanic corrosion to be smaller than the actual corrosion of the metal by the fused salt. The ratio of both types is influenced by the salt ions[7].

The corrosion of nickel-base superalloys by potassium chloride and lithium fluoride was studied at temperatures of 1600 to 1900F[8]. Oxygen was necessary for corrosion to occur, but stress serves mainly to rupture specimens already weakened by severe intergranular attack. The salt prevented the formation of a protective oxide film and the oxide corrosion products differed from those normally formed in the absence of salt.

Investigations on the compatibility of metals with fused fluoride salts show that protective films are fluxed away by molten fluorides exposing the metal surface to an accelerated attack by the salts[9].

Gurovich[10] also investigated the corrosion of nickel, copper, duralumin, and some steels in molten nitrates of lithium, sodium, and potassium. The metals were found to lose weight through solution and gain weight through scaling. Colored surface films were obtained. The cation radius does not have as decided an effect on the rate of

corrosion as Gurovich had found to be the case in an earlier investigation conducted in molten alkali halides[6].

The resistance of sixty-five cast iron-nickel-chromium alloys to corrosion in molten neutral heat treating salts was studied by Jackson and La Chance[11]. Intergranular corrosion along carbide networks is found to be more severe than metal loss by solution.

The effects of molten boron oxide on high-temperature alloys were studied. Some alloy constituents such as titanium at low concentration levels reduce alloy resistance to molten boron oxide[12].

Smith[13,14,15] and his co-workers showed selective leaching of alloying elements to be a predominant aspect of the corrosion of nickel base materials in molten sodium hydroxide. Subsurface porosity develops into a maze of channels which in most cases travel through the bulk of the material. Several review and survey articles are available which are indicative of the interest in the fused hydroxide corrosion of metals[16,17,18].

B. High Temperature Properties of Titanium and Titanium Alloys

Several articles are available which provide information on the high temperature properties of titanium and titanium alloys[19,20,21,22,23]. Information on the high temperature properties of these materials may be of value for comparison purposes in the testing program. TML Report No. 82 also presents an extensive bibliography on the subject.

C. Oxidation of Titanium

Since hot salt corrosion appears to be an oxidation process which proceeds by first destroying the normally protective oxide film, information on the oxidation of titanium is important.

The oxidation of titanium proceeds by two mechanisms: (1) the formation of a surface film, and (2) diffusion of oxide into the metal[24]. Phase boundary reactions are the rate controlling factors in the initial stages of oxidation, but in time the rate of diffusion through the oxide scale gains control[25]. The corrosion occurs in stages involving chemisorption, penetration of oxygen by chemisorption into the metal lattice, diffusion of oxygen in titanium[26], and the apparent diffusion of titanium ions outward through the layers of titanium dioxide[25]. The diffusion processes are not fully understood[27]. The speed of heating and the pressure of oxygen also exert a strong influence on the oxidation of titanium[28].

Kofstad and Hauffe[26] studied earlier work on the oxidation rate of titanium to explain the mathematical relationships that exist between

time and oxidation. Below 575F* they found a slow, logarithmic relationship. Above 575F absorption of oxygen becomes noticeable and between about 650F and 1200F a cubic relationship holds. From about 1300F to 1525F the relationship is parabolic and from 1575F to 1750F it is linear. As oxygen absorption increased the study became more difficult, but above 1750F the results indicate a parabolic relationship.

Kofstad[29] proposes the following mechanism for the oxidation of titanium: the logarithmic rate law is interpreted as oxide film formation possibly governed by a Mott-type mechanism; the cubic rate law is associated with the diffusion of oxygen into the titanium metal; the parabolic rate law is related to the usual high temperature mechanism as described by Wagner; and the linear rate law results from cracks in the oxide scale brought about by stress.

The ultimate product of the high temperature oxidation of titanium is the rutile modification of titanium dioxide (TiO_2), however, the possibility of lower intermediate oxides exists.[2] Trillat[28] found that at temperatures of about 575F and 750F and reduced oxygen pressures of 5×10^{-3} mm Hg and 2×10^{-4} mm Hg, respectively, titanium monoxide (TiO) was formed, but in the same order at temperatures of 750F and 1025F and at the same low oxygen pressures the products are anatase and rutile. Another investigation showed a colored corrosion product, which resembled titanium sesquioxide (Ti_2O_3) and titanium trioxide (TiO_3), to form as a film on titanium in air at around 1475F[30]. An examination of the inner porous layers of titanium samples annealed at about 1475F, 1825F, and 2200F showed them to consist of titanium monoxide, titanium sesquioxide, and titanium dioxide; the outer layer of titanium dioxide has a rutile structure[31].

A recent Russian investigation showed moist air to be less corrosive than dry air below 1300F, but at higher temperatures moist air was more corrosive. The investigator attributed the sharp increase in corrosion rate above 1300F to dissociation of water vapor and its effect upon the reaction[32].

The oxidation behavior of titanium is summed up in the abstracts of a recently published article[33]. Some of the aspects of the oxidation of titanium are:

1. Effect of temperature - rapid oxidation above 1300F.

---

*Centigrade temperatures have been converted to their approximate Fahrenheit equivalents for consistency in this report.

2. Effect of pressure - a minimum oxidation rate exists at a certain pressure for a given temperature.

3. "Whisker" formation on the oxidized surface - maximum development apparently correlates with the above pressure effect.

4. Effect of nitrogen in air - its oxidation inhibiting effect is much stronger than that which could be attributed to dilution.

5. Effect of alloying elements - aluminum, columbium, tantalum, and tungsten decrease the oxidation rate, and tin increases it. Columbium, tantalum, and tungsten, however, do not produce the important oxidation-inhibiting action expected by the theory stressing the importance of unoccupied oxygen sites in the rutile lattice.

6. Diffusion - titanium diffusion through the oxide layer plays a much more important part in the oxidation process than is currently believed.

D. Hot Salt Corrosion of Titanium

Published information on the hot salt corrosion of titanium falls into two categories--the corrosion and cracking of titanium by dry salt and corrosion and pyrosol formation in fused salts. Corrosion in fused salts usually occurs at a higher temperature with limited access of oxygen; corrosion by dry salt occurs above about 600F and in the presence of a large excess of oxygen (air).

1. Dry Salt Corrosion of Titanium at Elevated Temperature and Stress

A report on the dry salt corrosion of titanium alloys at elevated temperatures and stress was prepared by the four major titanium producers and Pratt and Whitney Aircraft and issued as TML Report No. 88 in November 1957[1]. All of the alloys reported in this publication are vulnerable in varying degrees to salt corrosion at elevated temperatures with the extent of the damage dependent upon the load, time and temperature. Stress corrosion cracking per se is reported above 600F; rapid general corrosion of unstressed samples occurs above 1100F. The report proposes the following mechanism to account for the hot salt corrosion of titanium:

(1) a. $2NaCl + Ti + O_2 = Na_2O_2 + TiCl_2$ or

b. $2NaCl + Ti + TiO_2 + \frac{1}{2}O_2 = Na_2TiO_3 + TiCl_2$

(2) $TiCl_2 + O_2 = TiO_2 + Cl_2$

(3) $Ti + Cl_2 = TiCl_2$

Microscopic examination of a sample of Ti-75A a few minutes after removal from a furnace in which the sample was held for two hours at 1100F revealed corrosion pits filled with a black substance. As the specimen cooled, rapid liquefication of this black substance occurred and was followed by the evolution of a gas. The above items are consistent with the chemistry of titanium dichloride. At high temperatures titanium dichloride should react with the oxygen in the air to yield titanium dioxide and free chlorine, however, attempts to detect chlorine in the corrosion studies failed in the presence of pure sodium chloride. Gas having the color and odor of chlorine was observed when the solid corrosion product, resulting from the high temperature exposure of titanium to a mixture of sodium chloride and an acidic oxide, was broken apart. Acidic oxides were reported to accelerate the hot salt corrosion of titanium, but the specific effect of the oxides on the corrosion mechanism is in doubt. The presence of oxygen or a reducible oxide is necessary for continuation of the reaction mechanism. For this reason there was no attack of titanium samples by sodium chloride in experiments conducted under high vacuum or argon atmospheres. However, the concentration of oxygen was found to have little effect on the rate of corrosion. Sodium chloride may not react with titanium dioxide in the absence of titanium metal, but the protection afforded by a dense adherent film of titanium dioxide is not sufficient to protect the metal from hot salt corrosion.

Work done at Armour Research Foundation showed that film protection is lost by direct chemical reaction of the chloride salt with the oxide film[2]. After elimination of the film, sodium chloride and titanium react electrochemically to form titanium dichloride. According to the proposed mechanism, the dichloride disproportionates to form the tri- and tetrachlorides which depress the melting point of the salt layer adjacent to the metal to form a liquid salt mixture. The corrosion rate is proportional to the amount of fused salt present.

2. <u>Corrosion of Titanium in Fused Salts</u>

Most of the related work which may shed light on the salt corrosion of titanium was performed in molten sodium chloride

by Straumanis and his associates[34 thru 41]. It was found that titanium corrodes quickly under the surface of molten sodium chloride in the presence of air. The observed process is an oxidation in which oxygen diffuses through the melt and dissolves in the metal. At a concentration of 6.2 weight per cent oxygen the surface layer breaks off and disperses itself in the melt. The separation of the surface layer of TiO_x from the metal gives rise to the observed rapid corrosion. The weight loss vs time and the rate vs temperature relationships are both linear[34,35]. The chief corrosion products are a dispersion of titanium metal in the molten salt (pyrosols) mixed with titanium oxides. The liquid mixture is dark gray, but appears blue-black in the solid state. Small amounts of white-to-yellowish oxides, which appear on the surface of the salt bath, consist mainly of titanium dioxide. Progressively less corrosion occurs in potassium, sodium, and lithium chloride melts. The most severe corrosion was noted in molten equimolar mixtures of sodium chloride and sodium fluoride[36]. At higher temperatures lower chlorides of titanium are formed, possibly by the reaction of the pyrosols with the melt according to the reaction

$$Ti + 3\ NaCl = TiCl_3 + 3\ Na$$

The sodium partially evaporates at working temperatures of 1650F and greater[37]. The pyrosols have been used to coat ceramic and metal objects with titanium[38,39].

Of twenty metal chlorides tested only the chlorides of iron, nickel, copper, cobalt, and cadmium were found to promote the corrosion of titanium in fused salt. The reaction appears to occur as follows:

$$Ti + 3\ CuCl = 3\ Cu + TiCl_3$$

$$Ti + 2\ CuCl = 2\ Cu + TiCl_2$$

In time, a white vapor, from the hydrolysis or oxidation of titanium tetrachloride, appears above the melt and suggests the following reactions take place[40]:

$$3\ TiCl_2 = Ti + 2\ TiCl_3$$

$$4\ TiCl_3 = Ti + 3\ TiCl_4$$

Measurements of the electrochemical potential of a cell consisting of titanium encased in a porous alumina diaphragm;

sodium chloride, potassium chloride, or an equimolar mixture of the two salts; and platinum were made at temperatures of 1475F and 1650F. An e.m.f. of about 0.5V was consistently measured in the presence of a vacuum or inert gas. In the presence of air, oxygen, or water vapor, e.m.f.'s of 1.42-1.53V were observed. It was presumed that cathodic depolarization was responsible for the change and that the net overall reaction shown below, results in the formation of titanium tetrachloride(41).

$$Ti + 4\ Na^{+} + O_2 = Ti^{4+} + 2\ Na_2O, \text{ or,}$$

$$Ti + 4\ NaCl + O_2 = TiCl_4 + 2\ Na_2O$$

Kreye and Kellogg(42) discussed the equilibrium that exists between titanium metal, titanium dichloride, and titanium trichloride in sodium chloride-potassium chloride melts. In the temperature range of 1300-1475F divalent titanium makes up 87-91 percent of the total titanium dissolved in the salt; the remainder of the dissolved metal with the exception of less than one percent as tetravalent titanium is trivalent titanium. The equilibrium constant for the reaction

$$TiCl_3(\text{NaCl-KCl melt}) + \tfrac{1}{2}Ti^{\circ}(C) = 3/2 TiCl_2(\text{NaCl-KCl melt})$$

is apparently a function of the total titanium concentration in the melt. These results are in agreement with the findings of Mellgren and Opie(43) who found 78-93 percent of divalent titanium in sodium chloride-strontium chloride melts between 1200 and 1475F. Varying the solvent composition in this case markedly affects the equilibrium. The amount of divalent titanium in the melt decreases with increasing sodium chloride content.

Dean, etal(44,45) showed that the relationship between log $TiCl_3/TiCl_2$ and the sodium content of the bath is linear for a constant titanium content of the bath and discussed the mechanism of titanium deposition from fused sodium chloride.

Skinner and Ruehrwein(46) determined the equilibrium in the reaction of titanium with sodium chloride. The following reaction is found to proceed to a measureable extent at temperatures of 2575 to 3325F:

$$2\ NaCl(g) + Ti(c) = 2\ Na(g) + TiCl_2(g)$$

Approximate thermodynamic calculations show that titanium dichloride is the only titanium chloride present in an appreciable amount.

Komarek and Herasymenko[47] presented a phase diagram for the titanium dichloride-sodium chloride system. The eutectic point occurs at 1121F and 50 weight percent of titanium. A peritectic reaction at 1165F results in the formation of $NaCl \cdot TiCl_2$. Another compound, $2NaCl \cdot TiCl_2$ decomposes in the solid state at 1018F.

An investigation of the equilibrium between titanium, titanium tetrachloride, and titanium dichloride revealed that the reaction of titanium with titanium tetrachloride begins at 650F to form titanium dichloride, and that the decomposition of titanium dichloride to titanium and titanium tetrachloride begins at 1200F[48].

E. Fusion Products of Sodium Compounds and Titanium Oxides

Conjeaud[49] made a study of the condensation products of titania vapor on single crystals of heated halides. The thin films of titanium dioxide when condensed on crystals of sodium chloride, potassium chloride, sodium iodide, and potassium iodide and heated above 842F show, by electron diffraction techniques, polycrystalline patterns that do not correspond to anatase, rutile or brookite. Conjeaud believed that an orthotitanate or acid titanate is formed as the reaction product. Thermodynamic calculations, presented in another section of this report, also indicate that sodium titanate is a key product in the corrosion of titanium by salt at elevated temperatures.

The Bureau of Mines provided data on the heat contents and heat capacities of Na_2TiO_3, $Na_2Ti_2O_5$, and $Na_2Ti_3O_7$[50,51]. These compounds are prepared by heating the stoichiometric amounts of sodium carbonate and titanium dioxide in a platinum crucible at 1650 to 2000F for several hours with constant pumping to remove the carbon dioxide. X-ray examination proved the crystalline character of the prepared materials, but no data were available for checking the different patterns.

X-ray powder photographs taken by Barblan[52] indicate that $Na_2Ti_3O_7$ has a structure similar to that of $Na_2Ti_2O_5$, but has a smaller unit cell. Na_2TiO_3 evidently has a different type of structure. Rotation photographs taken around the C-axis of $Na_2Ti_2O_5$ show the unit cell contains eight molecules of $Na_2Ti_2O_5$ with the following dimensions: a, 13.49; b, 16.66; c, 3.80A; d$_{\bar{1}52}$ 3.42. A structure of linked octahedra similar to vanadium pentoxide is suggested.

The formation of sodium titanates from sodium carbonate and titanium dioxide starts with the decomposition of sodium carbonate and diffusion of the resulting sodium oxide into the titanium dioxide. The titanate forms in the solid phase as the culmination of a series of interactions

between the two oxides during which the chemical and physical properties change gradually with time and temperature. The initial product of the reaction has a metatitanate composition (probably a mixed oxide corresponding to a $Na_2O \cdot TiO_2$) regardless of the ultimate product, but mixtures of different proportions form the metatitanate only at temperatures higher than those needed for the formation of the other compounds(53).

The generally accepted melting points for the compounds were reported by Washburn and Bunting(54) and are as follows: Na_2TiO_3, 1886F; $Na_2Ti_2O_5$, 1805F; and $Na_2Ti_3O_7$, 2062F. Budnikov and Tresvyats'kiy(55) reported melting points of 2066F for $Na_2Ti_3O_7$ and 1881F for $Na_8Ti_5O_{14}$. They found no evidence for the existence of Na_2TiO_3 and $Na_2Ti_2O_5$ by thermal analysis in a range of from 100 to 55 mole percent of titanium dioxide.

Lux(56) investigated the equilibrium in the Na_2O-TiO_2 system and found that $Na_2Ti_2O_5$ is less basic than $Na_2Ti_2O_3$ in the eutectic mixture (64 mole percent of titanium dioxide and 1805F)(55) and decomposes to soluble Na_2O-Na_2TiO_3 and an insoluble TiO_2-rich product according to the following reactions:

$$2\ Na_2Ti_2O_5 = Na_2TiO_3 + Na_2Ti_3O_7$$

$$3\ Na_2TiO_3 = 2\ Na_2O + Na_2Ti_3O_7$$

In addition to the compounds already mentioned, a number of sodium titanates of a variety of compositions have been reported in the literature. Viltange(57) reported the preparation of Na_2TiO_4 by heating sodium peroxide and titanium dioxide in the solid state. Bichowsky(58) reported the formation of $Na_4Ti_3O_7$ and $Na_2Ti_3O_6$ by heating titanium carbide, titanium nitride and sodium carbonate below the melting point of sodium carbonate. Sodium cyanide is formed quantitatively during this reaction and is removed by distillation at 2730F. If either $Na_4Ti_3O_7$ or $Na_2Ti_3O_6$ react with water $Na_2Ti_6O_{11}$ and sodium hydroxide are formed. $Na_2Ti_6O_{11}$ is reported to be quite stable. The existence of Na_4TiO_4, $Na_8Ti_5O_{14}$, and $Na_2Ti_5O_{11}$ were detected by reacting titanium dioxide with sodium hydroxide(59). $NaHTiO_3$ is also reported as a product of this reaction(60).

Reaction was reported between a titanium crucible containing a high chromium slag and a flux of sodium peroxide and sodium carbonate at 1400F(61). The reaction was sufficiently exothermic to transform the metal to the acicular structure of beta titanium.

F. Stress Corrosion Cracking of Titanium and Titanium Alloys

In addition to causing general corrosion of an unstressed sample, sodium chloride is also reported to cause cracking of titanium alloys under stress at elevated temperatures. All of the commercial alloys that were tested are susceptible to cracking above certain temperatures (600F) and stresses (about 30,000 psi) in air in the presence of sodium chloride. Neither the limits of the corrosion reaction nor the mechanism has been established, however, the reaction has been shown to be dependent upon stress, temperature, and time and appears to be a form of stress-corrosion cracking attributed to sodium chloride[1].

Titanium is, in general, fairly resistant to stress corrosion[62,63]. Stress corrosion cracking has been observed in only a few environments. The most notable of these environments is anhydrous (less than 1.5 percent of water) red fuming nitric acid. Furthermore, corrosion may proceed with the occurrence of an explosive pyrophoric reaction[64]. The pyrophoric reaction is not, apparently, associated with stress corrosion cracking but depends on the amount of water and nitrogen dioxide present in the acid[65]. The extent of corrosion and the tendency for a pyrophoric reaction to occur increases with increasing nitrogen dioxide concentration and decreases with increasing water concentration in the system: nitric acid-nitrogen dioxide-water. These variables also control the formation of a dark coating of finely divided titanium which preceeds the pyrophoric reaction[66].

Several cases of stress-corrosion cracking have been reported in the presence of small amounts of hydrochloric acid, but all of these cases involve a Ti-5Al-2.5Sn alloy. The alloy, stressed to 90 percent of the proportional limit, failed in 10 weight percent hydrochloric acid at 95F[67]. Cracking resulted from selective attack of the beta phase and propagated along the grain boundaries. It was proposed that hydrogen formed at the local cathodes, embrittling the alloy, and contributing to its failure. The Ti-5Al-2.5Sn alloy developed extensive cracks at the welded joints after immersion in a chlorinated hydrocarbon containing 0.017 percent of free hydrochloric acid at 700F. The cracks were usually transgranular and had a decided tendency to follow the rolling direction. A correlation appeared to exist between the stress level and the susceptibility to cracking[68].

The corrosion of titanium by molten cadmium is a special case of stress corrosion cracking. If the cadmium is molten and the titanium oxide film is ruptured the cadmium penetrates intergranularly. If the titanium is under stress, cracking occurs[69].

C. Surface Coating of Titanium

The susceptibility to salt corrosion can be reduced by the use of coatings serviceable at high temperatures. Anodic coatings give corrosion resistance to titanium at low temperatures while metallic or ceramic coatings seem best suited for high temperature applications. Electroplated metal coatings do not form satisfactorily on titanium unless proper surface treatments are first performed to provide an oxide-free surface essential for the adhesion of the deposit. Sprayed metal coatings tend to be porous and may not provide the desired degree of resistance. Evaporated metal coatings (metal from an electrically heated filament deposits in an inert atmosphere) have low porosity, but the initial investment in coating equipment is high. Titanium alloys have not been coated satisfactorily with ceramic coatings because the metal tends to oxidize and become embrittled when the ceramic is fused on the surface[70]. Nevertheless, developments in each of the above areas make them worth considering for protecting titanium-base alloys from salt corrosion.

1. Anodizing of Titanium

Titanium has been anodized in boric[71], chromic[72], nitric[73], perchloric[71], phosphoric[74], and sulfuric[71,75] acid solutions, and in potassium hydroxide[72] and borax[72] solutions. A rutile coating forms in boric and perchloric acids while in sulfuric acid the coating is a mixture of rutile and anatase[71]. These coatings offer some protection against corrosion in the absence of fluoride salts in aqueous solutions, however, it is doubtful that they would provide adequate protection against salt corrosion at high temperatures.

Electrolysis of titanium in a 0.1N potassium chloride solution at about 12V gives a thixotropic hydrous oxide coating[76]. Anodization was accomplished in a fused salt electrolyte at about 575F[77].

Cathodic hydridation gives titanium a hydride film (TiH_2) which, apparently protects it from attack by up to 24 weight percent of hydrochloric acid at room temperature[78].

2. Metallic Coatings for Titanium

Titanium can be electroplated with such metals as brass, chromium[79], copper[80,81], gold[80], nickel[80,81], platinum, silver[80], and zinc[82] by conventional plating techniques. A large amount of patent literature exists on the subject of the electroplating of titanium. Plating is generally accomplished

by conventional means and the major differences in the patents are the methods of treating the sample prior to electroplating. The pre-treatment is necessary to provide a surface to which the metal being plated adheres readily. Reference to some of the patents is given in the bibliography showing patent number, date, and metal coating[83].

Adherent metal coatings can also be formed chemically by depositing a metal which is electronegative to the base metal. This chemical process is termed "electroless" plating. Coatings of aluminum[84], nickel[85,86], nickel-phosphorous[87], tin[88], and zinc[89] have been formed by this method.

Coatings of molybdenum have been applied to titanium by spray and vapor-deposition methods. The wear-resistant coating does not change the microstructure of the titanium base[90,91,92]

3. Ceramic Coatings for Titanium

In an article which discusses potential applications for enamels and ceramic coatings in the aircraft industry it is stated that coatings for use up to 1500F would be required to prevent gas absorption and protect the titanium metal from corrosion. The development of such coatings should be simplified by the fact that enamels used for sheet steels can be readily applied to titanium[93]. Other coatings designed for use in the aircraft industry, such as a soda-boron-aluminate glass base[94] and a sodium silicate-cobalt oxide-nickel oxide base[95], have been developed. These coatings, applied by dipping, spraying, and other means, are annealed before use, and are said to be resistant to rapid temperature changes, distortion, corrosion, erosion, and moisture encountered in engine and airplane parts.

Heat and oxidation resistant coatings have been formed by oxide systems which form titanates. Oxides of magnesium, zinc, and beryllium have been used in this respect[96,97].

A carbide coating formed by heating titanium in pure hydrocarbon vapor at 1400 to 1800F and covered with a layer of carbon is cited as reducing the oxidation of titanium alloys heated in air at 1400 to 1650F[98].

Ammonia nitriding, reported as improving the creep-rupture properties of titanium alloys in the 1000-1200F range, improves the oxidation resistance of the metal at 1200F as well as its resistance to boiling sulfuric and hydrochloric acids[99].

V. FUNDAMENTAL STUDY

A. Salt Corrosion

1. Thermodynamic Considerations

The free energy changes for a number of reactions pertinent to this investigation are shown as a function of temperature in Figures 1 through 4.

Figure 1 shows the free energy-temperature relationships for reactions of compounds of titanium and oxygen. This figure indicates that the following reactions are important to an investigation of the corrosion mechanism:

	ΔF Reaction (kcal) 440F	1340F
$Ti(s) + O_2(g) = TiO_2(s)$	-203.7	-182.45
$Ti(s) + \frac{1}{2}O_2(g) = TiO(s)$	-112.45	-101.25
$TiO(s) + \frac{1}{2}O_2(g) = TiO_2(s)$	- 89.25	- 81.00
$TiO_2(s) + Ti(s) = 2TiO(s)$	- 20.9	- 20.05

Figure 2 shows the free energy-temperature relationships for reactions of compounds of titanium, oxygen, and chlorine. In this case the reactions important to the corrosion mechanism are:

	ΔF Reaction (kcal) 440F	1340F
$Ti(s) + Cl_2(g) = TiCl_2(s)$	-105.0	-88.3
$TiCl_2(s) + \frac{1}{2}O_2(g) = TiO(s) + Cl_2(g)$	- 7.45	-12.95
$2TiO(s) + Cl_2(g) = TiCl_2(s) + TiO_2(s)$	- 83.8	-68.25
$TiCl_2(s) + O_2(g) = TiO_2(s) + Cl_2(g)$	- 98.7	-94.15

It is seen that the chlorination of the monoxide to form the dichloride and dioxide has a greater thermodynamic probability than does the oxidation of the dichloride to the monoxide and chlorine.

Figure 3 shows the free energy-temperature relationships for reactions of compounds of titanium, oxygen, chlorine, and sodium and illustrates the thermodynamic incompatibility of titanium dichloride and sodium oxides as corrosion products.

	Δ F Reaction (kcal) 440F	1340F
$Ti(s)+2NaCl(s)+\frac{1}{2}O_2(g)=TiCl_2(s)+Na_2O(s)$	- 11.04	+ 9.01
$Ti(s)+2NaCl(s)+O_2(g)=TiCl_2(s)+Na_2O_2(s)$	- 47.00	- 32.00
$TiCl_2(s)+Na_2O(s)=TiO(s)+2NaCl(s)$	-101.41	-110.26
$TiCl_2(s)+Na_2O_2(s)=TiO_2(s)+2NaCl(s)$	-185.10	-183.35

Figure 4 shows the free energy-temperature relationships for reactions which form sodium titanate. It is seen that the most favorable ultimate corrosion products below 875F are sodium titanate, titanium dioxide, and chlorine. There is a thermodynamic probability that chlorine will react with sodium titanate above 875F to form titanium dioxide and sodium chloride.

	Δ F Reaction (kcal) 440F	1340F
$2NaCl(s)+2Ti(s)+3/2O_2(g)=TiCl_2(s)+Na_2TiO_3(s)$	-460.7	-214.45
$2NaCl(s)+2Ti(s)+2O_2(g)=TiO(s)+Na_2TiO_3(s)+Cl_2(g)$	-468.15	-227.40
$2NaCl(s)+2Ti(s)+5/2O_2(g)=TiO_2(s)+Na_2TiO_3(s)+Cl_2(g)$	-559.40	-308.60
$2NaCl(s)+TiO_2(s)+\frac{1}{2}O_2(g)=Na_2TiO_3(s)+Cl_2(g)$	-152.00	+ 56.30

Although thermodynamic considerations favor the formation of sodium titanate, titanium dioxide, and chlorine, it is likely that other compounds will be identified among the corrosion products because of the corrosion mechanism and differences in the reaction rates.

2. Corrosion Mechanism

a. The Role of Oxygen or a Reducible Oxide

An earlier experiment performed in this laboratory demonstrated the need for oxygen or a reducible oxide to maintain the corrosion reaction. A mixture of titanium dioxide and

sodium chloride were welded (in vacuum) in a one-inch thick block of titanium alloy Ti-5Al-2½Sn (A110AT) that was subsequently rolled at 1800F to ¼ inch and held for 100 hours at 900F. The sectional pieces showed the familiar corrosion product and demonstrated that titanium dioxide can support the reaction. However, an adjacent cavity (the control, containing only sodium chloride) indicated that sodium chloride alone will not react with titanium.

b. The Reaction and Reaction Products

The reaction is apparently complex and gives rise to intermediate reaction products, the nature of which depends upon time and temperature. For example, if the unreacted salt is removed from a sample that was generously covered with salt (originally applied as a slurry) and held at 1200F for 24 hours, the reaction products are jet black. If, on the other hand, a minimum amount of salt is used or if a sample similar to the above sample is held for a longer period of time (about 70 hours), the reaction products are white or yellow-white. The products are layered and shown by x-ray analysis to consist of mixtures of sodium chloride and titanium dioxide, with the sodium chloride concentration decreasing in layers closer to the metal surface. In some samples of the corrosion product, titanium monoxide has also been identified by x-ray diffraction techniques.

The reaction products contain a substance that is strongly hygroscopic. Placing some of the corrosion product in water results in gas evolution, and the water gives an acid reaction to litmus. Some of the black material takes on a white to yellow-white appearance while much of it appears to be quite stable. The following reactions are believed to be responsible for the observed behavior.

$$TiCl_2 + (x+1)\ H_2O = TiO \cdot xH_2O + 2HCl$$

$$TiO + (x+1)\ H_2O = TiO_2 \cdot xH_2O + H_2$$

We have not been able to conclusively identify titanium chlorides as corrosion products by physical means presumably because of their instability in moist air. However, a diffraction pattern has been obtained at Armour Research Foundation which contains three lines which are in agreement with the strongest lines for titanium dichloride (2,103). The sample was obtained from a specimen that was corroded by a low-melting chloride salt mixture.

Chemical evidence for the presence of titanium dichloride was obtained through the establishment of chlorine as a product of the reaction. Air was passed at a moderate rate through a Vycor tube containing a strip of titanium sheet coated with sodium chloride. A tube furnace was used to heat the materials to about 1200F. Chlorine was detected in the exit gas passed through a gas-washing bottle containing potassium iodide. The color from the liberated iodine intensified as the run progressed. Since sodium chloride should not oxidize under the above conditions, the chlorine produced should have come from the oxidation of a titanium chloride.

Sodium titanate, thermodynamically believed to be a logical reaction product, has defied conclusive identification. X-ray data are scant and led us to prepare samples of the titrates by fusing stoichiometric proportions of sodium carbonate and titanium dioxide at temperatures above 1950F. The product from the mixture, corresponding to the formula Na_2TiO_3, was pale green, and the products from the mixtures corresponding to $Na_2Ti_2O_5$ and $Na_2Ti_3O_7$ were each an off-shade of white. Analysis by x-ray diffraction showed the sample to have crystalline patterns, but no standards were available for direct comparisons. The d-spacings and relative intensities, given in Table I, were used for comparison with patterns taken of corrosion products. In some patterns, heretofore unidentified lines agreed with several lines for the compound $Na_2Ti_3O_7$, but the preponderance of titanium dioxide in the sample made definite identification difficult. However, because of the large proportion of titanium dioxide relative to the amount of sodium that takes place in the reaction, the higher titanates would be expected to form as the primary titanate, Na_2TiO_3, dissolves increasing amounts of titanium dioxide.

c. <u>The Method of Attack</u>

Figure 5 illustrates some revealing features of sodium chloride attack on Ti-12Zr-7Al sheet. This macrograph was made after 100-hour exposure at 900F and shows the corrosion products to form dark blisters beneath the salt crystals. The dark surface crust was determined by x-ray diffraction to be largely TiO_2 (rutile). This dark crust showed no noticeable growth during the second 100-hours of exposure with a sharp decrease in reaction rate. The sodium chloride crystals were also observed to remain largely intact during the attack with only a small portion being required to

sustain the reaction. These features would support either the existence of a liquid corrosion phase, as suggested by Crossley, etal[2], and/or the transfer of sodium chloride as a vapor, as suggested by Pickering, etal[3], and/or the progressive attack of the metal by the formation, consumption, and regeneration of chlorine.

Efforts to resolve this problem did not yield results that were sufficiently definitive. A 65-hour test at 900F, with an air flow of 2000 ml/minute, did not cause the corrosion blister to assume a significant degree of eccentricity in the direction of the air flow as would be expected in the case of vapor or gas attack. Inclined samples also failed to show a greater degree of attack in one direction than another. However, samples suspended in a furnace for long periods of time showed greater attack at the top of the sample.

Samples of titanium alloys were held above but not in direct contact with (a) mixtures of sodium chloride, titanium, and titanium dioxide, (b) mixtures of sodium chloride and titanium dioxide, and (c) sodium chloride for 24 hours at 1200F and 65 hours at 900F. Samples above (a) and (b) suffered the greatest attack as indicated by the amount of corrosion product on the surface of the sample. Samples above (c) did not show much greater attack than samples exposed to air alone under the same conditions.

The above findings indicate that free chlorine produced by the corrosion reaction causes the most extensive damage to titanium alloys. However, this finding does not preclude the existence of a liquid which, if present, exists as a thin film of contact adjacent to the metal. Attempts to confirm the existence of a liquid phase have not been experimentally accomplished.

d. <u>Effect of Metal Oxides</u>

It was stated in TML Report No. 88[1] that the presence of the acidic oxides accelerated the salt corrosion of titanium. Support of this statement can be obtained from the chemistry of the chloridizing roasting of ores wherein acidic oxides are used to decompose salt and liberate chlorine at high temperatures. The acid oxide then usually fuses with the base formed by the decomposition of salt and shifts the equilibrium to complete the reaction[104,105].

A survey of the effects of different oxides upon the salt corrosion of titanium showed only a few of them to cause extensive damage. Mixtures of salt containing one weight percent of the metal oxides were applied as a slurry to samples of titanium, which were dried and suspended in a furnace for 24 hours at 1200F. Although a complete analysis of each reaction was not made, it was apparent that the oxides causing the most severe damage were those that reacted readily with salt releasing chlorine and/or forming a liquid corrosion product during the reaction. The results of these tests are given in Table II.

Additional tests were made to determine the extent to which different amounts of the oxides of aluminum and chromium accelerate the corrosion reaction (Figure 6). The tests were conducted in the manner described above. Chromic oxide proved to be much more damaging than aluminum oxide and in the higher concentrations perforated the metal samples. It was at first thought that fused chloride salts flowed to the bottom of the sample in the tests involving chromic oxide and formed a bead on cooling, but subsequent analysis proved this to be fused sodium chromate. No evidence of fusion was observed in the tests involving aluminum oxide.

The effect of aluminum oxide and chromic oxide upon the salt corrosion of titanium suggest two different mechanisms by which the reaction can occur. Aluminum oxide apparently increases the yield of chlorine by reaction with the salt, followed by rapid oxidation of aluminum chloride, and/or by fusion with the basic oxide. Chromic oxide, on the other hand, reacts with the salt to form a liquid at the test temperature which acts as a carrier of the corrosion agent and/or a flux and intensifies the damage that would ordinarily occur. Thus, the nature of the oxide that forms on the surface of a titanium alloy, the alloying elements, and their chlorides all have a significant effect on the mode of attack and the extent of the damage caused by salt.

3. General Salt Corrosion

The general corrosion of titanium by salt has been investigated via a thermogravimetric study of the progress of the corrosion reaction with time.

a. Testing Procedures

Samples of the alloy having a total area of 8 square inches, are cut into three pieces with one piece 2.5 x 0.8 and two

pieces 1.25 x 0.8 inches. The sizes were chosen for convenience in fitting them into a porous crucible. The metal is coated liberally on all sides with a concentrated salt slurry and dried overnight before placing in the crucible. The crucible is suspended in a tube furnace by means of a nichrome wire hanging from an analytical balance. A periodic record is made of the change in weight of the system at a fixed temperature.

b. General Salt Corrosion of Commercially Pure Titanium

Data from tests made at 1000 and 1200F are shown in Figure 7. The figure shows the temperature dependence of the reaction. This is also emphasized by comparing the information in Table III and Table IV. Very little corrosion occurred with a salt coated sample at 800F which gained less than 0.001 g/square inch after a 152 hour exposure. The reaction of titanium with air at 1000F (in the absence of salt) is also negligible.

The samples that were attacked by salt at higher temperatures were badly pitted; after 170 hours at 1200F the samples were perforated in several locations. The effect of the amount of salt upon the corrosion rate is less pronounced than the effect of temperature as long as salt is available to support the reaction. A sample of titanium sprayed with a light salt coating showed a small rate difference from a slurry-coated sample when reacted at 1200F. The difference was probably well within experimental error as shown by a duplicate run of a slurry-coated sample. These results are summarized in Table III.

c. General Salt Corrosion of Titanium Alloys

Samples of Ti-12Zr-7Al, Ti-8Al-1Mo-1V, and Ti-8Al-8Zr-1 (Cb+Ta) were liberally coated with salt and exposed at 1000 and 1200F in the same manner as the above samples of A70. The results at 1200F indicate that there is little difference in the resistance to salt attack exhibited by Ti-12Zr-7Al and Ti-8Al-1Mo-1V. The other alloy, Ti-8Al-8Zr-1(Cb + Ta), shows somewhat less resistance to salt corrosion under comparable conditions, but is considerably more resistant than commercially pure titanium. At 1000F, Ti-12Zr-7Al appears to have the best resistance, but the differences between the alloys are less pronounced and are perhaps within the range of experimental error. (A more complete interpretation of results is given in part e of this section.) The results of these tests are summarized in Tables III and IV. Figures 8 and 9 show a graphic comparison of the materials.

d. A Comparison of Salt Corrosion and Normal Oxidation of Titanium and Titanium Alloys

The reaction of titanium with air at 1000F is negligible in the absence of salt. Because of the very small weight changes obtained in the absence of salt, the weighing of a sample suspended in a furnace did not yield satisfactory results and a different procedure was used to present a comparison of the effects of salt corrosion and normal oxidation of titanium alloys.

Two small pieces of each material having a total area of four square inches were placed in combustion boats and put into a furnace at the desired temperature. Daily weighings were made on the system and the weight increase per square-inch of metal surface was determined. In order to make the comparisons under identical conditions, separate runs were made with and without salt at 1000 and 1200F. These data are shown in Tables V and VI. Because of the few data available for each curve and the wide difference in the values obtained for each material with and without salt, it was necessary to take certain liberties in presenting this comparison graphically. Four-cycle semi-logarithmic paper was used to accommodate the information. The best curves, shown in Figures 10 and 11, were visually drawn through the points. The effect of salt upon the oxidation of titanium will be discussed in part e.

e. The Effect of Temperature on the Corrosion Rate

The extent to which titanium is attacked by salt was found to increase rapidly with increasing temperatures. The difference in the behavior of Ti-12Zr-7Al and Ti-8Al-1Mo-1V and unalloyed titanium toward increasing temperatures was determined for sixteen-hour exposures made in the manner described in part c. The data, presented in Table VII and Figure 12, show a very rapid increase in the rate of salt attack at temperatures above 1000F.

f. Discussion and Interpretation of Results

An examination of the data, provided by the study conducted in part b, showed that it is satisfied best by the expression $W = kt^n$, where W equals the increases in weight resulting from the formation of adherent corrosion products, t is time, and k and n are constants. The constants were evaluated for each alloy and at each temperature by the method of averages. These values are shown on the following page.

At 1200F:	n	k	log k
A70	0.952	3.56	0.5518
Ti-12Zr-7Al	0.653	4.52	0.6546
Ti-8Al-1Mo-1V	0.631	4.14	0.6171
Ti-8Zr-8Al-1(Cb+Ta)	0.627	7.22	0.8585
At 1000F:			
A70	1.085	0.498	-0.3026
Ti-12Zr-7Al	0.576	0.417	-0.3795
Ti-8Al-1Mo-1V	0.700	0.401	-0.3970
Ti-8Zr-8Al-1(Cb+Ta)	0.783	0.280	-0.5536

The logarithmic relationship (log W = log k plus n log t) for the variables is a straight line with a slope equal to n, and W equals k when t equals one. When applied to our data, k gives the extent of the corrosion reaction after the first hour, and n should give the rate at which the reaction progresses. However, ignoring errors introduced in performing the experiment, consistent values of n and k are expected only if the corrosion reaction is a simple one. The salt corrosion of titanium alloys is presumed to proceed by an apparently complex mechanism or by several complex, competitive mechanisms. The normal oxidation of titanium is known to proceed by a complex mechanism and is represented by several different rate laws, each valid for a specific temperature range. Different rate laws have been reported for essentially the same temperature range, but the basic difference was the manner in which the results were interpreted[27,29]. In general, a logarithmic oxidation relationship applied up to about 600F, and from there to about 1200F the relationship appears to be cubic. From 1200 to about 1600F the relationship is parabolic but it becomes more linear with increasing temperatures.

We compared the damage caused by salt with the increase in weight given by normal oxidation at 1000 and 1200F in part c. The procedure used in obtaining these data was different than the method used in part b, but it provided the same type curve when shifted to accommodate the change in experimental conditions. Excellent agreement with the previous data was obtained at 1200F, but only fair agreement was obtained at 1000F where the lower temperature produced smaller weight changes which reflect more strongly the errors inherent in the procedure. Errors over and above those

normally encountered in weight change measurements of this type are caused by variable salt adherence. Apparently this influences the data more at low temperatures than at higher temperatures where rates of diffusion and reaction are more rapid. However, the data for both temperatures show that the presence of salt causes considerably more damage than would result from normal oxidation of the alloys.

Oxidation data were included from the literature[106], in Figures 10 and 11 for comparison. These data show the oxygen absorbed by commercial titanium in pure oxygen at the temperatures indicated. This agrees fairly well with our data on A70 at 1200F but it must be remembered that our samples were oxidized in an air atmosphere and not in pure oxygen. At 1000F the agreement was not as good as it was in the above case, but here the weight changes were so small that they approached the sensitivity of the balance.

Above about 1000F, the effect of temperature on the rate of corrosion becomes increasingly important. This is clearly indicated by the sixteen-hour tests shown in Figure 12. It is interesting that below 800F the systems show a consistent loss in weight. Because of the small differences involved this weight loss could result from errors in weighing, from the evolution of chlorine produced in the corrosion reaction, or, more likely, from the loss of moisture present in the salt. The abrupt change in the slope of the curve between 1000 and 1100F indicates a change in the corrosion mechanism. The low temperature mechanism could merely be oxidation of the alloys (a significant difference in this region would be difficult to detect with our present equipment) or the surface of the titanium could be sufficiently passivated to ward off the major effects of general salt attack with only slight damage occurring in the unprotected areas. In Figure 12 we have also plotted data from Reference 106 on the oxidation of commercial titanium in pure oxygen for sixteen hours at different temperatures. Here, only small changes in slope are encountered indicating the different oxidation mechanisms operating between 1100 and 1400F.

In summary, the alloys studied under this contract show improved high-temperature oxidation and salt-corrosion resistance over unalloyed titanium. The alloys show moderate surface attack from salt in the temperature range for which they are designed. Catastrophic damage from general salt

corrosion occurs beyond the high temperature limits of these alloys. However, the salt conditions used in the laboratory tests were severe and an excess of salt was constantly provided for sustaining the reaction during each test. Consequently, service conditions to which these alloys would be subjected are considerably less severe than those employed in the laboratory.

4. Salt Corrosion Cracking

While it was noted above that very little corrosion occurred at temperatures as high as 800F with salt-coated titanium alloys, the effect of stress on hot-salt corrosion is to reduce the limit. In this connection, no attack was observed in Ti-12Zr-7Al material exposed with salt and without stress for 100 hours at 600F. However, samples run in like manner but at 60,000 psi tensile stress showed the start of surface attack after a 100-hour exposure.

a. Metallographic Studies

Metallographic studies on Ti-12Zr-7Al material reveal similarities in modes of salt attack between stressed and unstressed material; i.e., both modes of attack appear to be structure dependent. Figures 13 to 16 show 800F salt attack on the surface of samples representing two conditions of processing. Samples in Figures 13 and 14 were processed in the alpha-plus-beta field and show the nature of salt attack when exposed with and without stress. Figures 15 and 16 represent material processed in the beta field and likewise show the mode of attack with and without stress. It is important to note that while Figures 13 to 15 show intergranular attack, Figure 16 reveals transgranular attack. The beta-rolled material also cracked in five percent hydrochloric acid and in a similar manner. The microstructure of salt corrosion at the surface of a Ti-12Zr-7Al sample after 100-hour exposure at 900F and 30,000 psi stress is given in Figure 17. The attack here is definitely intergranular with preferential attack of the dark-etching grain boundary beta phase.

These studies suggest that beta-rolling or sensitization results in transgranular attack and predicts early failure. Materials rolled in the all-alpha or low in the alpha-plus-beta field give a more desirable structure for resistance to both general corrosion and stress corrosion cracking.

b. Reactions of Titanium Carbide and Titanium Hydride With Salt

A study was made on the effect that the interstitial elements carbon and hydrogen may have upon the salt corrosion of titanium. Titanium carbide and titanium hydride were each mixed with salt in a 1 to 2 mole ratio. Small amounts of these mixtures were placed in a furnace at 600, 800, 1000 and 1200F for 24 hours and then examined for possible signs of a reaction. Up to 1200F there was very little difference in the appearance of titanium carbide regardless of whether or not salt was present. No other qualitative evidence was obtained to indicate that this system reacted. After 24 hours at 600 and 800F, the titanium hydride and salt mixture became lighter in color than the titanium hydride by itself. At 1000F the mixture became mottled white and gray after 16 hours, and ivory after 24 hours. At 1200F the mixture turned ivory-colored in 24 hours while the titanium hydride itself remained a dark gray. No soluble titanium compounds were detected in the reacted mixture. The titanium hydride by itself appeared to be unaffected but in the mixture it appeared to be completely oxidized.

The ease with which titanium hydride, salt, and air react at moderately elevated temperatures suggests that hydrogen has an adverse effect upon the corrosion reaction. Strained areas may cause hydrogen to concentrate in preferred locations in the alloy and promote vulnerability to stress corrosion cracking.

Salt creep testing of hydrogenated tensile samples, discussed in the special processing section of this report, demonstrates the adverse effect that hydrogen had upon the resistance of stressed samples exposed to salt.

c. Role of Chlorine in Stress Corrosion Cracking at Elevated Temperatures

Chlorine is produced when chloride salts attack titanium and its alloys in air. This trace of chlorine is capable of cracking stressed titanium alloys. Figure 18 exemplifies the intergranular attack which accompanied the stress-corrosion cracking failure of a stressed Ti-12Zr-7Al sample during exposure at 500F to dry air containing one percent chlorine gas at atmospheric pressure. The sheet was stressed by bending a 2½ inch long by 3/8 inch wide strip around a

¼ inch radius and clamping the ends. The maximum surface stresses, therefore, exceeded the yield strength. It is significant to note the beta phase attack at the grain boundaries. This behavior is identical to elevated temperature salt corrosion of this alloy under tensile stress as seen in Figure 17.

When argon was substituted for air, cracking also occurred showing that air is not necessary for the cracking mechanism. In previous work we demonstrated that salt and titanium will not react at a significant rate at elevated temperatures unless air is present. However, when air is present, sodium chloride reacts rapidly with titanium at high temperatures and chlorine gas is evolved. Therefore, we now believe that chlorine gas may be the principal stress corrosion cracking medium in these reactions.

B. Aqueous Stress Corrosion Cracking

We hoped that a relationship between aqueous stress corrosion cracking and hot salt corrosion cracking would be readily apparent and thus enable us to simplify our testing procedures by replacing the more involved hot salt creep tests by stress corrosion tests in hydrochloric acid. To determine if a relationship exists between salt corrosion cracking and aqueous stress corrosion cracking it was first necessary to establish the conditions required to make a metal or alloy vulnerable to cracking. Abnormal exposure at very high temperatures for long periods of time usually produce this condition and destroy the normal and desirable properties of the alloys.

The possibility of contamination during the long exposures at high temperatures (although minimized by the use of a proprietary high temperature coating) was present. This possibility, together with a poorly defined relationship to the cracking caused by salt corrosion at high temperatures (reducing acid vs salt oxidation), inaccuracies involved in relating outer fiber-stress to creep-stress, and the time that would have to be spent in developing data on samples given abnormal exposures to increase reliability in comparing results, suggested abandoning this testing procedure after obtaining some preliminary data.

1. Testing Procedures

A. Sample Preparation

Samples of commercially pure titanium (A70) and titanium alloys prepared as longitudinal sheet coupons were

sheared to about 0.037 x 0.6 x 4.2 inches and 0.048 x 0.6 x 4.3 inches, respectively. Materials tested in the "as received" (mill annealed) condition were pickled in the conventional 30% HNO_3-3% HF solution just before testing. Whenever heat treatments were employed the coupons were sheared prior to this operation, and afterwards grit blasted and deskinned in 30% HNO_3-3% HF to remove about 4 mils from the thickness.

b. Sample Testing

A convenient testing apparatus was developed which consists of a channeled Synthane jig. The samples are loaded by placing them inside a channel section somewhat narrower than the length of the specimen and then immersing the bowed sample in the test solution at room temperature.

The maximum stress in the outer fibers of the bowed specimen can be approximated, providing the yield strength is not exceeded, by means of the following equation:

$$S = Et/2r$$

where S = the maximum stress in the outer fibers
E = modulus of elasticity
t = thickness
r = radius of curvature to the center line

Appendix A reviews the methods used to calculate stress for these tests.

c. Test Solution

The most convenient solution found for this work consists of 5 percent hydrochloric acid (by weight). It is very effective and yet not dangerous to handle or very corrosive to the metal.

2. Stress Corrosion Cracking of Commercially Pure Titanium

Samples of commercially pure titanium (A70) stressed to approximately 75,000 psi in five percent hydrochloric acid, did not show a consistent history of failure when annealed at temperatures below 1900F. Exposure times in excess of six hours at 1900F seem necessary to induce vulnerability

to cracking. Since no skin was detected on these samples, after pickling, vulnerability is believed to be associated largely with preferential alloy and impurity partitioning and beta grain coarsening.

The results of these tests are given in Table VIII.

3. Stress Corrosion Cracking of Ti-12Zr-7Al

Samples of Ti-12Zr-7Al, stressed to approximately 80,000 psi (outer fiber stress) in five percent hydrochloric acid, showed a behavior similar to that shown by commercially pure titanium, i.e., susceptibility to cracking was not induced at exposure temperatures of less than 1900F. The major difference shown by these materials is the shorter exposure time of four hours at 1900F required to induce vulnerability to cracking of the Ti-12Zr-7Al alloy. (The results of these tests are given in Table IX.) Since no skin was detected on any of these samples, the vulnerability promoted at 1900F can be credited to metallurgical effects.

A metallographic study of these samples after test exposure revealed that the mode of attack is directly associated with the microstructure. In this study, the surface of the sample on the tension side of the bend was ground and polished lightly to reveal the character of the hydrochloric acid attack. Figure 19 which gives the microstructure of samples in the first condition noted in Table IX (exposed 16 hours at 1800F and tested 20 days under stress in five percent hydrochloric acid), shows the attack to be random. The microstructure is primary alpha (light etching) and transformation alpha (dark etching). The microstructure of samples in the seventh condition (exposed four hours at 1900F with instantaneous failure in five percent hydrochloric acid) is observed in Figure 20. Here, numerous fine stress corrosion cracks are observed, all of which are perpendicular to transformation alpha platelets.

4. Stress Corrosion Cracking of Ti-8Al-1Mo-1V

The effects of high temperature exposure on the stress corrosion cracking of Ti-8Al-1Mo-1V sheet in 5 percent hydrochloric acid are given in Table X. The stress condition was approximately 78,000 psi. It is important to note that a very abnormal treatment of 10 or more hours at 1900F is required to induce stress corrosion cracking in HCl. The cracking was observed to be transgranular and confined to selective areas.

An example of this attack is shown in Figure 21. Figure 22 shows a crack that propagated through the entire width of the specimen. A photomicrograph of a polished surface at the break (Figure 23) indicates that the cracks apparently have their origin in the primary alpha platelets.

5. Miscellaneous Stress Corrosion Cracking Tests

The results of a number of miscellaneous stress corrosion cracking tests are summarized in Table XI. Samples made vulnerable to cracking by high temperature exposures failed rapidly in 5 percent hydrochloric acid and 5 percent titanium trichloride solution. The addition of 2 percent hydrogen peroxide to the hydrochloric acid solution inhibited cracking at least until some time after the oxidant was exhausted. Samples sensitized in a vacuum did not fail in 5 percent hydrochloric acid indicating that a relationship may exist between metal purity and/or oxygen content and the cracking phenomena. Passing an electrical current through samples stressed in 5 percent hydrochloric acid solution resulted in anodic attack at the air-solution interface and the eventual failure, by rapid general corrosion, of both vulnerable and non-vulnerable samples. No cracking was observed.

6. Discussion

In substance, vulnerability to acid corrosion cracking is induced by prior high temperature exposure. The vulnerability temperature appears to be above the beta transus for the respective alloys. Other factors, in addition to the abnormal exposure temperature, are: time at temperature, testing stress, and concentration of the test solution.

A metallographic examination of samples used in these tests established the following relationship between hot salt and aqueous stress corrosion cracking: cracks propagate transgranularly in titanium alloys given high temperature processing on exposure to both salt and 5 percent hydrochloric acid; intergranular attack has been observed under hot salt conditions in titanium alloys processed at low temperatures. High temperature exposure and/or processing appears to result in the diffusion of a susceptible constituent from the grain boundary to preferred planes within the grain. Improved performance of alloys processed at low temperatures emphasizes the advantage of low temperature processing for increased salt resistance. (The effects of processing are discussed later under Part VI B.)

C. Electrode Potential Measurements

An exploratory investigation was made of the electrode potential of the different titanium alloys used in this work to determine if a relationship exists between the corrosion potentials and stress corrosion cracking tendencies.

1. Electrode Potential Measurements of Titanium in Hydrochloric Acid

a. Studies of the Electrode Potential of Titanium in Hydrochloric Acid

Studies of the electrode potential of titanium in hydrochloric acid have been reported by Straumanis and Chen[107], Schlain and Smatko[108], and by Schlain[109]. Their findings show that at low acid concentration (up to 3N) air passivates titanium surfaces to give more noble electrode potentials, and indicate that a reaction involving oxygen, metal ions, or ions containing oxygen occurs on the passive surfaces (which change very little in appearance). The passivity can be destroyed gradually by nascent hydrogen from the corrosion reaction. An inert-gas sweep removes oxygen and some hydrogen from the solution and gives a more stable potential. High acid concentrations also break down the passivity and cause the electrode potential to decrease rapidly with time until a steady-state value is reached after approximately one hour. The rate of change depends upon the rate of film break down and repair which in turn depends upon the relative oxidizing or reducing ability of the solution. The steady-state values varied with the solution, but were otherwise the same regardless of the pre-treatment of the metal surface.

b. Experimental Procedure

For this exploratory work, the measurements were made in 5 percent hydrochloric acid (slightly less than 1.5N) in an open beaker at room temperature against a saturated calomel electrode. The values obtained were later corrected to the hydrogen scale for comparison with the published work discussed above. A small flow of argon was continually passed through a bottle containing 5 percent hydrochloric acid and into the solution in which measurements were made (except for the tests shown in Figure 26.)

The surfaces of the samples were prepared by a light pickle in a solution containing 3 percent of hydrofluoric acid and 30 percent of nitric acid to provide a bright, clear surface. The samples were rinsed with distilled water and quickly transferred to the solution in which measurements were to be made. The initial reading was taken as soon thereafter as possible. Immersion of the samples was not complete and interface effects were inherent in the technique employed.

c. Alloy Comparisons

The electrode potentials of the materials used in this work are compared in Figure 24. The data presented show that all the alloys are more electronegative in 5 percent hydrochloric acid than unalloyed titanium. Other than that, the electrode potentials show no apparent relationship to the stress corrosion cracking tendencies of the materials. The resistance of these samples, as expressed by their electrode potential in 5 percent hydrochloric acid, is the reverse of that exhibited under salt conditions at elevated temperatures. Although this reversal may be coincidental (and no conclusions should be drawn therefrom) it suggests that surfaces which passivate most readily in aqueous solutions may be more vulnerable to salt corrosion at elevated temperatures.

d. Processing Differences

In salt corrosion studies, samples of Ti-12Zr-7Al given alpha-beta processing were found to perform consistently better under stress than samples from beta processed stock. A look at the electrode potential of these samples in 5 percent hydrochloric acid (Figure 25) shows a slightly higher potential for the alpha-beta material signifying increased resistance in the acid solution. However, the difference between the observed potentials is not great and does not necessarily reflect the performance of the alloy under salt-stress conditions. Nevertheless, it indicates that an increase in the amount of beta phase lowers the resistance of titanium base alloys to chloride attack under conditions which tend to destroy the passive film that normally protects the metal.

e. Stress Corrosion Cracking Tendencies

Potential measurements were made on samples from the stress corrosion cracking tests to see if electrochemical

relationships contributed any worthwhile information regarding cracking tendencies. Measurements on unalloyed titanium were made in a stagnant 5 percent hydrochloric acid solution and are recorded in Figure 26. These data show an increased electronegativity for samples which had longer exposures at the sensitizing temperature of 1900F. The sensitized samples also showed a lesser tendency to passivate in the acid solution than the untreated, unalloyed titanium.

The Ti-12Zr-7Al samples showed, on the other hand, that the sensitized samples were more noble than the untreated alloy (Figure 27). The same situation was noted for the Ti-8Al-1Mo-1V alloy (Figure 28). This shift in potential probably resulted from metallurgical changes which occurred during the high temperature exposure and apparently bears no direct relationship to the cracking tendency of the material. Of particular interest, however, is the comparative nobility shown by a sample of Ti-12Zr-7Al that was heated in a vacuum for 100 hours at 1600F.

2. Electrode Potential Measurements in Salt at Elevated Temperatures

The measurement of the potential difference between the alpha and beta phases, using molten salt as the electrolyte, was suggested in the preface to TML Report No. 88[1]. In attempting to obtain these data, a measurable potential was encountered in powdered dry salt at temperatures above 1000F. This system was examined further because it parallels the salt corrosion testing procedures used throughout this work.

a. Experimental Procedure

In the general procedure, nickel wire was welded to the titanium samples (1/4 x 3 in.) which were placed in a refractory crucible. Salt was packed around the electrodes (spaced about 3/4 in. apart) and the crucible was placed in a furnace. The leads were connected to a potentiometer and the temperature was adjusted. The data, recorded as a function of time, are naturally dependent upon the bulk density of the salt (which could not be controlled precisely) as well as the temperature which, even though controlled within the limits of the equipment used, fluctuated because of the necessity of keeping the furnace door slightly ajar to permit access

for the lead wires. Due to the possible magnitude of the error introduced by these items, the results presented in this section are tentative and in need of refinement.

b. Salt Conductivity Measurements

The measurable potential was at first thought to be influenced by the titanium corrosion reaction. Before continuing, the conductance was measured by applying a voltage to two equivalent nickel electrodes and measuring the current. The differences in values at different temperatures with and without titanium present were found to be well within experimental error (Table XII). Therefore, the conductivity of the salt is independent of the chlorine-producing titanium corrosion reaction. The highly erratic ammeter fluctuations at 1400F suggest that, in the vicinity of the electrodes, a phase change results from the lowering of the melting point of salt by the corrosion products.

Similar measurements using titanium electrodes gave ammeter fluctuations above 1300F which were too small to be decisive (Table XIII). Conceivably, a liquid phase forms but oxidizes before an appreciable concentration builds up. (Titanium dichloride and sodium chloride are reported to form a eutectic at 50 weight percent of titanium dichloride and 1121F.)[27]

The change in weight of the electrodes (including recovered corrosion products) as a function of the applied voltage is shown in Figure 29. Both electrodes undergo attack, but the attack of the anode is more severe and a weight gain of approximately twice that of the cathode is obtained.

c. Potential Difference Between Alpha- and Beta-Titanium

A potential difference of about 0.5 volt was found to exist at 1200F between A70 and Ti-13V-11Cr-3Al (B120VCA) after about 4 hours. This potential difference was less than 0.1 volt at 1400F. These data, shown in Figure 30, suggest preferential or anodic attack of the beta phase by dry salt at elevated temperatures when coupled with the alpha phase. However, the effect of the beta stabilizers on the potential of Ti-13V-11Cr-3Al is not taken into account.

The behavior of the cell over an extended period of time would undoubtedly be influenced by the diffusion of oxygen through the salt and dissolution in the metal specimen. For example, Dean, et al[110], show a definite relationship between the oxygen content of a titanium sample and the e.m.f. of the sample measured against a titanium electrode in a molten salt electrolyte. The reduction of the potential difference with increased temperature is probably related to increased reaction rates of both phases.

d. Galvanic Behavior of Titanium and Other Metals

When the potential difference between titanium and nickel was measured at 1200F, a value of 0.9 volt was found to exist after about 7 hours (Figure 31). All of the alpha alloys gave similar results, but the potential of the beta alloy changed more rapidly with time. When nickel was replaced by copper the potential difference was found to decrease rapidly with time (Figure 31). The favorable change appears to be brought about by the development of an oxide coating on the copper, and suggests that a sub-plate of copper may enhance the effectiveness of a nickel plate.

3. Discussion

Our measurements of the electrode potential of unalloyed titanium in hydrochloric acid are essentially in agreement with those reported by other investigators. The differences that exist ("steady-state" values were reached in a much shorter time and were slightly more electronegative) can be attributed to the metal, its pretreatment, and differences in measurement techniques.

These data do not point to any apparent relationship between the net corrosion potential of a specimen as a whole and its vulnerability to cracking when stressed in an aggressive medium. Although there is firm evidence that electrochemical differences play a role in stress corrosion cracking, special techniques, capable of measuring local-cell potentials and potential differences surrounding pre-existing paths of susceptibility, are required to illustrate this role.

The relationship between salt-stress cracking at elevated temperatures and the electrode potential measurements was at first thought to be obscured by the large difference in test

conditions. However, subsequent measurements made in dry sodium chloride at 1200F also failed to show any relationship between the cracking tendency and electrode potential. This agrees with the findings of Crossley, etal,[2] showing the absence of a correlation between electrode potential and susceptibility to chloride salt stress corrosion based on measurements of the potential of various alloys (versus platinum) in molten potassium chloride-lithium chloride at 1000F.

VI. COATINGS AND PROCESSING

Since new high temperature titanium alloys are beginning to appear on the market, it is desirable that these be evaluated for their resistance to salt, and if necessary, modified before extensive test programs get underway in the field. Consequently, screening of these alloys was undertaken using material from production-sized heats.

A. Alloy Screening

The original plans were to confine the work on alloy screening to the three super-alpha alloys: Ti-12Zr-7Al, Ti-8Al-1Mo-1V and Ti-8Al-8Zr-1(Cb + Ta). The Ti-6Al-4V (C120AV) alloy was added at a later date for comparison purposes. The objective was to determine how well these alloys resist salt attack under stress in the 600 to 1000F temperature range. Chemical analysis of these alloys is given in Table XIV.

1. Creep and Creep Stability

A. Ti-12Zr-7Al

Before hot-salt stress-corrosion performance could be evaluated on these alloys, creep data in the prescribed temperature range were required. These data are developed in Figures 32 and 33 for sheet and rod product and give the required stress for 0.1 and 0.2% plastic creep in a 100-hour exposure period over the 600 to 1100F temperature range. These data will be applied in subsequent salt-creep studies.

Creep stability, which is one of the limiting considerations in extending the service temperature of titanium alloys, may be broken down into factors of metallurgical instability and service instability. In this study, evidence of instability was determined by comparison of tensile properties of specimens with and without creep exposure. All tensile samples were cleaned in acetone prior to creep testing. After creep

testing, they were tensile tested without surface conditioning. This procedure was followed to include the effects of surface oxide and corrosion on instability. Creep stability data are given in Tables XV and XVI for Ti-12Zr-7Al sheet and rod over the 600 to 1000F range and indicate the alloy to be quite stable.

b. Ti-8Al-1Mo-1V

The creep data for Ti-8Al-1Mo-1V alloy rod are given in Figure 34. The creep resistance of this alloy is seen to be poorer than the Ti-12Zr-7Al over the entire 600-1100F temperature range. Creep stability data for Ti-8Al-1Mo-1V rod are given in Table XVII and show no evidence of instability.

c. Ti-8Al-8Zr-1(Cb + Ta)

Creep and creep stability data on this alloy are given in Table XVIII and show it to be unstable in the 800 and 900F temperature range. With this evidence and instability results published by others, the Ti-8Al-8Zr-1(Cb + Ta) was dropped from the program with Navy approval and the Ti-6Al-4V (C120AV) alloy was chosen as a substitute for comparison purposes.

d. Ti-6Al-4V (C120AV)

This alloy is a popular heat-treatable alpha + beta type. In the annealed condition, however, it may be regarded as a "near-alpha" with a strength level in the neighborhood of the super-alphas.

The creep properties of the Ti-6Al-4V (C120AV) alloy are given in Figure 35. As may be expected, the creep resistance of the super-alpha and near-alpha alloys decreases with increasing amounts of beta stabilizing elements. Ti-12Zr-7Al shows the highest creep resistance, Ti-6Al-4V (C120AV) the lowest, with Ti-8Al-1Mo-1V in between.

Creep stability data on Ti-6Al-4V (C120AV) are included in Table XIX over the 600 to 900F range and indicate the alloy is quite stable.

2. Elevated Temperature Tensile Properties

Short-time hot-tensile properties are important in designing within the limiting service stresses of an alloy. In this phase of the program, the effects of processing temperature on the hot strength of notch and unnotched Ti-12Zr-7Al and Ti-8Al-1Mo-1V material were evaluated. Four processing techniques were covered:

1) Processing in the beta temperature field (rod),
2) Processing in the alpha-plus-beta field (sheet),
3) Processing in the all-alpha field (sheet), and
4) Tungsten-arc inert gas welding (sheet).

Thus, by a consideration of creep, hot strength, notch sensitivity and salt-creep properties, a measure of the elevated temperature performance of these alloys is obtained.

a. Ti-12Zr-7Al

The technique of sample preparation is given in detail in the following section under salt creep studies. In brief, salt-coated hot-tensile samples were prepared to a standard finish. This finish was described in the following subsection on sample preparation. All welds were ground flush with the base metal. Samples to be salt-coated were then cleaned, held at 140F, and the gage length brushed with a slurry of sodium chloride and water and allowed to dry. During the hot tensile test careful attention was given to maintaining the conditions of time at temperature constant. Samples were brought to test temperature in 15 minutes and held at temperature for an additional five minutes prior to load application. As with room temperature tensile testing, the load was applied at a rate of 0.005 in/in/min to the yield strength and then increased to 0.050 in/in/min.

Data on the effect of salt on the notched and unnotched hot tensile strength of Ti-12Zr-7Al processed under the above techniques 1 to 4 are given in Figures 36 to 39 respectively. From the data in Figure 36 it is apparent that beta-processed rod tests coated with salt suffer no decrease in strength or ductility up to 1000F under the conditions of testing. Sheet samples on the other hand experience a loss in both strength and ductility at 1000F as noted in Figures 37 to 39. The poorer performance in the sheet material is attributed in large part to the increased surface-to-volume ratio. In comparing the salt resistance of sheet material, the alpha-

processed sheet, Figure 37, shows better salt resistance than does the alpha-beta sheet, Figure 38, or the welded sheet, Figure 39. Salt did not appear to influence notch sensitivity in any of the series tested.

b. Ti-8Al-1Mo-1V

Data on the effect of salt on the notched and unnotched hot tensile strength of the Ti-8Al-1Mo-1V alloy are given in Figures 40 to 43. These data represent the same processing techniques studied under the Ti-12Zr-7Al alloy and show parallel trends of salt resistance. In this respect neither alloy shows any particular advantage over the other.

It is important to note that in the 600 to 800F temperature range the yield strength of the Ti-12Zr-7Al alloy is very close to the stress required to give 0.2 percent creep in 100-hours exposure. A similar situation is also observed in the Ti-8Al-1Mo-1V alloy at 600 and 700F. This behavior results from the very low secondary creep rate exhibited in these alloys over the temperature ranges noted.

3. Salt-Creep Studies (Ti-12Zr-7Al, Ti-8Al-1Mo-1V, Ti-6Al-4V)

The following salt corrosion and salt-creep tests were designed to provide data on the severity of attack and information on the mechanism of corrosion. In the latter study, optical and x-ray metallography were employed to provide information on the mechanism of stress corrosion.

a. Sample Preparation

Both round and flat tensile samples were included in this program for comparison study. The round tensile samples were polished in the gage length to a 6 to 10 micro-inch finish with polishing cloth. They were then cleaned in acetone and pickled lightly in an aqueous solution of 30% nitric acid - 3% hydrofluoric acid. This latter treatment provided good salt adhesion without destroying the 6 to 10 micro-inch finish. Figure 44 illustrates a tensile coupon so treated. Flat tensile coupons were not polished but were cleaned with acetone and acid dipped lightly, as above, after machining. The test samples were heated at 140F over a hot plate and brushed with a slurry of demineralized water and powdered reagent-grade NaCl. After coating, heating was continued at 140F to insure complete dryness prior to testing.

b. Sample Testing

The dry, coated samples were loaded in a creep testing machine with normal air circulation and stressed to give 0, 0.1 and 0.2 percent plastic strain after 100-hours exposure at temperature. Loads were selected from creep curves given in Figures 32 to 35. The test program proposed to cover the 600 to 1100F temperature range, but under those conditions where the lower end of this range showed poor results, the testing was not continued into the higher range.

After salt-creep exposure, the samples were tensile tested at room temperature and the fractures examined for salt penetration. Figure 45 shows the appearance of a series of Ti-8Al-1Mo-1V samples after salt exposure and tensile testing. The depth of salt attack is designated by the code letters VL, L, M and H, described in the footnote of Table XX.

c. Metallographic Study

A metallographic study was made on both hot-salt, and aqueous-stress-corrosion samples as a means of establishing the mode of attack and thereby possibly suggesting remedial measures. The microstructure of salt corrosion at the surface of a Ti-12Zr-7Al sample after 100-hours exposure at 900F and 30 ksi stress is given in Figure 17. The attack in this alpha-plus-beta processed material is observed to be definitely intergranular with preferential attack of dark-etching grain-boundary beta phase. This feature suggests that a complete all-alpha working of the material for elimination of the grain boundary beta plate should increase salt corrosion resistance.

The nature of salt attack in Ti-6Al-4V (C120AV) is illustrated likewise in Figure 46 to be intergranular with a preferential attack of the dark-etching transformation (beta plus alpha) structure.

d. Test Results

Salt corrosion tests were conducted on the Ti-12Zr-7Al, Ti-8Al-1Mo-1V, and Ti-6Al-4V alloy with and without stress in the 600 to 1100F temperature range. The stresses were chosen from creep data in Figures 32 to 35 to give 0.1 and 0.2 percent creep in 100-hours exposure. In addition, for the Ti-12Zr-7Al alloy, parallel salt exposures were made between sheet and rod material for comparison of performance.

The results of these tests are given in Tables XX to XXIV. The unexpected high creep rates--above 0.1 and 0.2 percent target values--observed in some of these tests were undoubtedly due to the propagation of minute corrosion cracks which decrease the effective cross-sectional area of the samples. These data also indicate that these specific materials at very high stress levels can be expected to experience a little salt attack at as low as 600F. However, with unstressed material, the temperature limit extends to 700F for rod and 800F for sheet. Above these temperatures surface pitting becomes pronounced and may be objectionable in certain applications. It is interesting to note that sheet material generally shows better salt-creep resistance than does the rod as measured by the degree of salt attack on the fractured surface in break, even though the former has a higher surface to volume ratio. This difference in behavior can be attributed to metallurgical differences between the rod and sheet. The rod was rolled at 1950F in the beta range while the sheet was rolled at 1800F in the alpha-plus-beta range.

There is little difference between the salt results given in Table XX on the Ti-12Zr-7Al rod and in Table XXII on the Ti-8Al-1Mo-1V rod. Both alloys appear to have similar salt resistance.

The salt resistance of the Ti-6Al-4V (C120AV) alloy, noted in Table XXIII, follows the same pattern as observed in the super alphas. In stressed material, some salt attack was found at temperatures as low as 600F. Since the stresses to give 0.1 and 0.2 percent creep in the Ti-6Al-4V sheet are lower than for the super alphas, the salt attack over the 600-1000F temperature range studied is observed to be less in like measure. For Ti-6Al-4V sheet in the unstressed condition, the surface pitting from salt attack becomes pronounced (about 0.001" depth) at 800F as with the super alphas.

Apparent threshold temperature and stress conditions that would produce a measurable loss of ductility in salt coated samples were arrived at by screening 100-hour salt-creep data given in Tables XX to XXII. From these data, the maximum practical load (20 and 30 ksi) and temperature (600F) were selected for 300 and 500-hour, salt-creep tests for each of the two alloys. Tensile properties after these exposures are given in Table XXIV and verify the marginal nature of the salt attack at 600F under low stress levels. These

results are in agreement with the conclusions of Crossley[2] that titanium oxide is resistant to salt attack up to 550F.

While the threshold conditions for salt attack in current titanium alloys appear to be fairly constant the upper limit for stress attack was found to be alloy dependent. Crossley[2] reports a maximum temperature of 900F for hot-salt stress-corrosion attack in titanium alloys. Our work in Tables XX, XXI, XXII and XXIII shows that a stress factor exists up to 1000F for Ti-12Zr-7Al, up to 900F for Ti-8Al-1Mo-1V, and up to 800F for Ti-6Al-4V. Thus, a wide range of salt-stress corrosion may be expected with titanium depending on the alloy, temperature, time and stress.

B. Special Processing (Ti-12Zr-7Al, Ti-8Al-1Mo-1V)

The completion of the alloy screening phase of this work provided basic background data on creep rates, severity of salt attack, and the magnitude of the stress factor in this attack. The following special processing phase screens both processing and metal-purity factors in an attempt to mitigate salt attack.

1. Effect of Purity

In the study of metal purity, two super-pure, 25-gram buttons of Ti-12Zr-7Al were melted from electrolytic titanium, iodide zirconium and Raffinal aluminum and processed to 0.050" thick sheet at 1500F. This processing was on an experimental laboratory level since this temperature is below the recrystallization temperature. A one-inch section of commercial-grade Ti-12Zr-7Al (analysis given in Table XIV) was reduced to sheet in a similar manner and served as a control.

As a basis for evaluation of hot-salt creep performance a condition of 100-hours creep exposure at 700F and 70 ksi stress was established arbitrarily. This condition, which is used extensively throughout the program, is of moderate severity and as such permits a desirable spread in data.

Salt-creep results on these samples, given in Table XXV show no benefit of super-purity over commercial-purity material under equivalent processing conditions.

2. Effect of Hydrogen

As a beta stabilizing element, hydrogen may be expected to migrate to grain boundaries in a two-phase region and conceivably accelerate intergranular attack.

In this work five levels of hydrogen were chosen. These levels ranged from a vacuum annealed condition to 660 ppm. A complete cycle of 2 hours at 1400F was chosen for the vacuum annealing and the thermal addition of hydrogen. Accordingly each sample had the same thermal history.

Several interesting features are observed in the salt-test results of this series given in Figure 47. At 445 ppm hydrogen and above, salt exposures of 100 hours at 700F result in a notable strength loss due to accelerated surface attack. With the addition of 70 ksi creep stress the general trend is for increased salt attack as reflected by a deterioration of residual strength and ductility. In substance, vacuum annealed material gave the best salt resistance in both the stressed and unstressed condition.

3. Effect of Thermal History

Data were developed in the fundamental study phase of this work which illustrate the effect of thermal history on aqueous-stress-corrosion cracking. In this respect extreme high temperature dwells were found to sensitize the material to this form of attack. This trend likewise followed in the alloy screening work where it was noted that sheet material processed at 1800F generally gave better salt-creep resistance than did rod material rolled at 1950F even though the former had a higher surface to volume ratio.

Similar results are illustrated in Table XXV. Here it is noted that high temperature dwells in the beta region (the beta transus for Ti-12Zr-7Al is 1825F) further lowers resistance to attack. Long time (100 hour) dwells in the alpha range are also damaging.

These data point up an important similarity between aqueous-stress-corrosion cracking and elevated-temperature-salt-stress attack, namely that both are accelerated by high time-temperature parameter values.

4. Welding (Ti-12Zr-7Al, Ti-8Al-1Mo-1V)

Welds were included under this grouping as specially conditioned material with high thermal history. As with the short-time elevated-temperature tests, the welds were ground flush with the base metal. In the salt tests the salt was applied to cover the weld and heat-affected zones.

Salt-creep tests were conducted at 700F for 100 hours at stresses calculated to give 0.0 and 0.2 percent plastic creep. The results of this series are given in Table XXVI. Here, salt-coated tests exposed without stress suffered only mild pitting with no significant loss of tensile properties. On the other hand, several of the stressed samples did not survive the 100-hour salt exposure. All of these early failures were found to occur in the heat-affected zone of the weld. Also, the Ti-12Zr-7Al welds gave poorer salt resistance under stress than did alpha-beta processed sheet in Table XXI, even though the latter required higher stresses to give the target 0.2 percent plastic creep. The effect of welding appears to be similar to that of other forms of high-temperature exposures in increasing the rate of salt attack.

The explanation for the above failures in the heat-affected zone is not definitely known. Aside from the high thermal history of the weld, the increased interstitial content from welding, which influences both strength and creep rates, may also impair salt resistance.

These data also show a consistent trend with short-time elevated-temperature test results where it was found that welds were less resistant to salt than unwelded sheet. Accordingly, high-temperature processing may be expected to favor a decrease in the salt resistance of these alloys. Indeed, low-temperature processing (in the all-alpha range) provides the best salt resistance.

C. Effect of Surface Treatments on Salt Resistance and Mechanical Properties of Ti-12Zr-7Al and Ti-8Al-1Mo-1V

1. Surface Treatments

The general objective of this phase of the program was to apply test coatings for improved resistance to salt. This effort is secondary to the basic problem of base-metal inhibition since, unfortunately, coatings are vulnerable to mechanical damage and, in consequence, cannot be considered completely reliable.

The ideal coating should be ductile, adherent, easy to apply, and resistant to salt attack under hot salt-creep conditions. In approaching this problem, numerous surface treatments and techniques were first evaluated for protection against salt attack. A salt exposure of 100 hours under stress at 900F was chosen to measure performance. From these results, the best

coatings were given more rigorous salt reliability tests and more extensive mechanical tests.

a. Electrolyzing Treatments

Treatments with alternating current in phosphoric acid have been reported to show promise for salt protection of titanium at temperatures up to 700F. The procedure which we followed was developed by Boeing Airplane Company (111). Salt creep tests on material so treated are given in Table XXVII and indicate no protection over uncoated material at the same temperature and stress level.

b. Electroplating

The plating metals chosen were those of known resistance to salt up to 1000F. Plated coupons were subsequently salt-creep tested.

The plating pretreatments generally consisted of a 10 minute immersion of the specimens in a mixture containing 25 ml of hydrofluoric acid (52%), 175 ml of glacial acetic acid, and 20 ml of acetic anhydride. Transfers to the plating bath were made in glacial acetic acid. References to the various plating procedures are given in Table XXVII along with salt-creep results.

Preliminary screening of the various metal plates led to the selection of the nickel bath for further evaluation. Chromium plates were brittle, silver plates blistered at high temperatures, while other plates were porous.

In the selection of nickel plating baths we avoided those baths containing chlorides to minimize the danger of entrapped chloride salts. In the screening tests nickel showed good salt resistance in many cases. When failures occurred they could be associated with porosity and other plate defects. The sulfamate plating bath showed the most promise of the nickel baths studied and was selected for more extensive testing.

In the study of nickel plates the general problem of plate porosity was overcome by introducing three cycles of plating and buffing. The buffing serves to decrease the porosity of the plate. A muslin buffing wheel was used which was loaded with a stick compound designed for polishing stainless steel. After each buffing the sample was cleaned with a solvent to remove residual waxes. The thickness of nickel plate was 0.002".

Tensile samples nickel plated and buffed in this manner were given a more rigorous salt-creep exposure in which the time was increased from 100 to 300 hours. The stresses chosen were estimated to give 0.2% creep. The results of these tests, presented in Table XXVIII, demonstrate excellent salt protection up to and including 1000F. At 1100F the nickel plate is attacked to a moderate extent with the formation of a green corrosion product--presumably a nickel chloride.

Because of the low creep strength of Ti-8Al-1Mo-1V at 1100F, it is not anticipated that this alloy would be used for extended times at this temperature.

c. Aluminum Coating

The relatively good resistance of aluminum to hot sodium chloride attack suggested the use of this metal as a protective coating for titanium. The investigation included three types of coatings: paint, hot metal dip, and flame spray.

Both general-purpose and high-temperature aluminum paints were tested. Sheffield Super-Krome Aluminum Paint, the general-purpose brand tested was applied with three coatings, allowing 16-hours drying time between coats. Ti-12Zr-7Al sheet thus coated gave no measurable improvement in resistance to salt attack as noted in Table XXIX. Samples were also double coated with Fuller's Hi-Temperature Aluminum Paint No. 171-A-28 with a five-minute bakeat 400F between coats. This treatment likewise gave no real improvement in salt resistance as seen in the Table. The poor performance of the aluminum paints was attributed to lack of adequate bonding under stress during salt creep exposure.

Aluminum coating by hot metal dipping promised to give an improved bond over aluminum painting. In this work, a potassium chloride-cryolite flux (m.p. approximately 1180F) was used which had been developed by D. K. Hanink[119]. Titanium test samples were coated by dipping them without preheating into a crucible of fused flux and molten aluminum at 1400F. The flux proved adequate in dissolving the oxides of aluminum and titanium and promoting the desired wetting action. The aluminum coat obtained averaged 0.002" thick but was less than 0.0005" at the corners.

At the corners, there was some tendency for shrinkage cracks to occur with resultant exposure of the base metal. The inadequate edge protection thus resulted in premature failure of these samples during subsequent salt-creep testing as noted in Table XXIX. Figure 48 shows an aluminum-coated specimen which failed during a salt-creep test. Here, dark corrosion products are observed at the sample edges where the aluminum coating was thin. The lack of corrosion on the flat surfaces is noteworthy and indicates adequate salt protection if sharp corners are eliminated and a minimum 0.002" coating thickness is maintained.

In preliminary studies the flame-sprayed aluminum coatings appeared promising so that this coating method was accepted as a candidate for more extensive testing. Coatings were in the order of 0.004" thick and were applied with a portable metallizing gun with one-eighth-inch diameter aluminum wire. In order to improve adhesion of the aluminum it was found necessary to preheat the sample to about 1400F with the wire-gun torch prior to flame spraying. The results of salt-creep tests on these samples are included in Table XXIX. Early failures in some of the preliminary tests were attributed to inadequate bonding. However, when applied with sufficient preheating, aluminum flame spraying shows promise of adequate salt protection up to 1000F, and up to 1100F for limited periods (300 hours).

d. Shot Peening

Of the two types of salt attack, general corrosion and stress corrosion, the latter results in the greater loss of strength and ductility in the super-alpha titanium alloys and is potentially the more troublesome. In order for stress corrosion cracking to occur, surface tensile stresses must be present. Thus, the application of surface compressive stresses may be expected to preclude stress corrosion failure. Shot peening offers a convenient method for introducing surface stresses and may serve as a means to minimize stress-corrosion cracking.

Variables studied were: peening intensity, sheet vs rod, and base metal processing. The peening intensity was varied by using four different shot sizes ranging from S-70 to S-230. (The former gave a shot-peened surface layer 0.002 inches in depth and the latter 0.003 inches depth.) The peening intensity in all cases was to saturation. The two tensile types used, $\frac{1}{4}$" diameter rounds, and 0.050" thick microflats,

were peened in the reduced section only. The base metal condition covered beta and alpha-plus-beta processed material for the $\frac{1}{4}$" diameter rounds and alpha-plus-beta and alpha processed sheet.

Table XXX, which gives the test results on this series after 100-hour, 70 ksi, 700F salt-creep exposure, shows no benefit of shot-peening under these limited conditions of testing. It is concluded, therefore, that the beneficial compressive stresses introduced by shot-peening were nullified by relaxation over the 100-hour - 700F test period and by the superposition of tensile creep stress.

e. Test Results

Under the relatively severe conditions of salt-creep exposure chosen, only three of the surface treatments evaluated showed promise of offering satisfactory protection. These were: Nickel plating from a sulfamate bath, aluminum dipping, and aluminum flame spraying. When properly applied these coatings promise protection under conditions of salt and creep for temperatures up to 1000F.

As a result of this study, these three coatings were chosen to be included in the fatigue testing phase of this program which follows.

2. Fatigue Testing of Ti-12Zr-7Al and Ti-8Al-1Mo-1V Alloy

The purpose of the surface treatment phase of this program was to evaluate the more promising coatings for salt protection and to perform a few critical performance tests on these coatings so that one or more may eventually emerge for unreserved use. The first performance test of this series covered salt-creep exposure. The best performers in this test were nickel plating, aluminum dipping and aluminum flame spraying. These coatings applied to optimum processed base metal were chosen for a few critical fatigue tests both with and without prior salt exposure.

a. Endurance Limits

The endurance limits of the alloys under study were established as a necessary prelude to the fatigue testing of surface coatings. These data are given in Figure 49 for the Ti-12Zr-7Al, Ti-8Al-1Mo-1V, and Ti-6Al-4V alloys. Ti-8Al-1Mo-1V is observed here to have the highest endurance

limit with Ti-6Al-4V and Ti-12Zr-7Al following. It is anticipated that a lower annealing cycle would improve the endurance limit of Ti-12Zr-7Al.

b. Effect of Surface Treatments and Prior Elevated Temperature Salt Exposure

In this study sections of Ti-12Zr-7Al and Ti-8Al-1Mo-1V were hot rolled from 1700F to one-half-inch thick plate and annealed in the all-alpha temperature range. Rotating-beam fatigue coupons cut from this material were all prepared to a 16-microinch finish. Those scheduled for nickel-plating, aluminum-dipping, and aluminum flame spraying were so coated in the stressed area of the sample in accordance with the procedure established under the section on Surface Treatment. Samples in both the as-machined and coated conditions are illustrated in Figure 50. These were tested in fatigue with stresses at, and somewhat below, the endurance limit. A second similar series was salt coated in the reduced area, exposed 100 hours at 1000F and likewise tested in fatigue. The results of these tests are given in Table XXXI.

From an examination of samples after testing and a study of the fatigue data it was apparent that the surface coated samples were not adversely affected by the salt exposure. But, the material did suffer a loss in fatigue strength as a result of surface coating. The probable causes of this performance are associated with the coating interface. In the case of the nickel plated material, an acid pickle was used as a pretreatment to plating. Heavy pickling would be expected to lower fatigue life. Furthermore, the formation of a critical amount of brittle, intermetallic, interface layer from both the nickel and aluminum plates would lower the fatigue resistance. Presumably all of these effects could be minimized and improvements in fatigue resistance realized with further study. These results point up the need for a study on the effect of surface coating techniques on fatigue life.

VII. ALLOY DEVELOPMENT STUDIES

The study of the effect of alloying upon the salt corrosion behavior of the super-alpha alloys is divided into three categories. The first category deals with the behavior of the super-alpha alloying elements in binary combination with titanium; in the second category a small study of the effect of composition changes is made; and in the last

category the effect of small alloy additions to the super-alpha alloys is studied.

The alloys were prepared as 50 gram melts which were processed as follows: hot rolled at 1800F to 0.2 in.; 1600F to 0.1 in.; 1500F to 0.060 in. and annealed for 30 minutes at 1400F and air cooled.

A. Binary Alloy Compositions

Binary alloys of titanium and the constituent elements present in the super-alpha alloys were prepared using high purity titanium sponge and alloying elements. The effect of these elements on the salt corrosion of titanium was studied by following the weight increase of salt coated samples as a function of time at 1200F.

Coupons of titanium and the super-alpha alloys were prepared from identical source materials and tested for comparison. Their behavior is shown in Figure 51(a). Figure 51(b) shows the same information on a smaller scale that can be more easily compared with the data on the binary alloys.

1. Effect of Zirconium

As seen in Figure 52(a), increasing amounts of zirconium in titanium increase the initial corrosion rate. Amounts less than 8 weight percent appear to reduce the initial rate when compared with the corrosion rate of unalloyed titanium. However, a phenomena similar to the "breakaway" phenomena was observed after a period of time and accelerated the corrosion rate. (The "breakaway" phenomena[120] can be explained in terms of the volume ratio of metal oxide to metal, e.g.: Vol. TiO_2:Vol. Ti::1.77:1. Since this ratio is greater than one, the oxide grows under compressive strain until it reaches a critical film thickness. At this point it cracks to release the compression stresses and gives the manifold increase in rate or breakaway. Soluble addition elements having an ionic radius which differs by about 15 percent or more from the ionic radius of the solvent metal will distort the normal oxide film and cause breakaway to occur at a much lower film thickness. Insoluble alloying elements give a film of the base metal and separate agglomerates of the oxide of the addition element. In this case breakaway will occur if the addition metal oxide interferes with the adherency of the base metal oxide to the metal.)

2. Effect of Aluminum

The effect of additions of aluminum to titanium is to reduce

the rate of salt corrosion (Figure 53(b)). The lower concentration, 6 percent, appears to have less inhibiting effect than do concentrations of 8 percent or more. The addition of more than 8 percent of aluminum impairs workability and thermal stability.

3. Effects of Molybdenum and Vanadium

Increasing amounts of molybdenum and vanadium lower the salt resistance of titanium. Molybdenum additions appear to have less effect on the general weight increase of the alloy than vanadium additions (Figure 53).

4. Effects of Columbium and Tantalum

Columbium and tantalum accelerate the corrosion of titanium (Figure 54). Columbium seems to be significantly better than tantalum in retarding the accelerated corrosion considering the relative amounts of each element present. However, the improvement that results from increasing the amount of columbium in the alloy may be anomalous.

5. Effects of Iron and Oxygen

The data on iron and oxygen, as shown in Figure 55, indicate that small amounts of these elements can decrease corrosion resistance.

6. Discussion

Of all of the elements present in various super-alpha alloys, only aluminum in binary combination with titanium appears to improve the salt resistance of the titanium. Aluminum stabilizes the alpha phase, reduces the lattice parameter, and has an ionic radius only one percent smaller than titanium. High aluminum additions tend to embrittle the alloy and, since this markedly affects its performance under stress, the addition of other elements are necessary to counteract the effect of aluminum.

Although zirconium is completely soluble in alpha-titanium, its ionic radius is 35.4 percent larger than titanium, a factor that may affect oxide porosity, destroy surface passivity, and cause the observed change in slope. However, the large amounts of zirconium in the alloy are less damaging than the smaller amounts of the other elements which, with the exception of oxygen, prefer the beta phase and have restricted solubilities

in the alpha phase. Preferential attack of the beta phases by salt has been observed on a number of previous occasions.

The relative oxide-chloride stability is a prime factor not only in determining the surface passivity of the alloys, but also in determining the mode of attack and controlling the reaction rate. A non-porous, non-reactive oxide film would be a deterrent to the reaction, but such a film does not form. If the chloride products are stable (or oxidize slowly enough for an appreciable concentration to build up), they will dissolve in the corrodent and change its melting point--possibly lower it to the point where the corrosive mixture is liquid. If, on the other hand, the chloride oxidizes rapidly, gaseous chlorine will be the corrosive agent. A change from one mode of attack to the other would appear as a change of slope on a rate curve.

In looking at the binary data, titanium dichloride (which forms a eutectic at 50 weight percent of sodium chloride and 1121F)[47] and aluminum chloride (which forms a eutectic at 21 weight percent of sodium chloride and 230F)[121] may oxidize rapidly to give a rate curve having a uniform shape. (Aluminum, it is reported, is not volatilized as a chloride in an oxidizing atmosphere.)[104] The other binaries show a change in slope after short periods of time. This time delay could signify a build up in concentration of the corrosion products to the point where they lower the melting point of salt sufficiently for a liquid phase to form and accelerate the general attack. (Zirconium tetrachloride forms a eutectic at 12 weight percent of sodium chloride and 320F; information has not been found on the other systems.)

B. Composition Modification

Based on previous findings, some changes were made in the composition of the super-alpha alloys by increasing or decreasing the amounts of the constituent elements. Data from the studies of the binary alloys indicated that corrosion damage increases with increasing amounts of zirconium and that aluminum increases resistance to salt. Therefore, we reduced the amount of zirconium in the alloy and prepared Ti-10Zr-7Al. Tests with this alloy in moving air confirmed the findings of the binary study, but Ti-10Zr-7.5Al was, for an unknown reason, less resistant. However, the improvement in salt resistance given by Ti-10Zr-7Al is not conclusive enough to recommend a change without an additional and more complete investigation.

Vanadium in binary combination with titanium was also found to lower resistance. Therefore, an alloy with a reduced vanadium content, Ti-8Al-1.5Mo-0.5V was prepared. Salt tests of this alloy in moving air gave an improved corrosion resistance compared to that of Ti-8Al-1Mo-1V. Again, however, additional and more complete tests are advisable to confirm the indication provided by these data.

The data from these and other tests are shown in Table XXXII. Data are presented for each alloy for tests made in a furnace through which air was passed (at 525 ml/minute, a rate sufficient to change the air in the furnace once every three minutes), and also in a stagnant furnace atmosphere. Because of better control of the variables, the tests in moving air are considered more reliable for comparing alloys. The tests in the stagnant furnace atmosphere reflect the variable and generally more severe conditions present in the furnace. This is especially true since volatile compounds and/or gases are evolved during the corrosion reaction and are retained for uncertain periods of time by the refractory brick in the furnace.

Theoretical considerations indicated that a titanium alloy containing 15 weight percent of zirconium and 3 weight percent of aluminum should on the basis of ionic radii and a number of approximations give a strain-free surface oxide at normal temperatures and possibly impart greater protection against salt. Tests at 1200F in a moving atmosphere showed this alloy to corrode more slowly. The corrosion rate curve has a plateau that may signify a halt that occurs after surface oxides build up to a maximum thickness and before dissolution of the oxide film by salt. An alloy containing twice the amount of zirconium and aluminum in the above sample completely deteriorated during the test. It is believed that the passivity of this alloy was destroyed by the excessive amount of zirconium. Because of the high zirconium-to-aluminum ratios neither of the above alloys would possess the mechanical properties required of the super-alpha alloys.

Also included in Table XXXII are tests made on different melts of the super-alpha alloys. Very little difference was noted in the corrosion rate of Ti-12Zr-7Al prepared from pure alloying elements and a sample from the sheet which supplied the base to which minor alloying additions were made. This was not true in the case of Ti-8Al-1Mo-1V. A sample prepared from alloying elements had a much smaller corrosion rate than did a sample from the sheet which supplied the base for minor alloying additions. Although both materials had the same processing schedule, a metallographic examination showed the sample with the lower corrosion rate had been worked to a slightly greater degree than the other material. This feature is observed in Figure 56(a) and (b) for the two Ti-8Al-1Mo-1V alloys listed in Table XXXII. Here the fine-grained worked structure in Figure 56(b) gave a lower salt corrosion

rate than the coarser structure in Figure 56(a). These data and the data from tests on the effect of minor alloying additions suggest that small processing differences may have a large effect on the salt corrosion resistance of Ti-8Al-1Mo-1V.

C. Effect of Minor Alloy Additions

1. Effect of Additions to Ti-12Zr-7Al and Ti-8Al-1Mo-1V

a. General Salt Corrosion

The effect of some minor alloy additions upon the general salt corrosion of Ti-12Zr-7Al and Ti-8Al-1Mo-1V is shown in Tables XXXIII and XXXIV, and in Figures 57 and 58. The figures show the extent of the corrosion of the modified alloys after 24 hours at 1200F. The tables give data for periods of 2, 4, 6 and 24 hours at 1200F. These data were taken from weighings made on a salt-coated sample that was suspended from a balance into a vertical tube furnace at 1200F. Air was dried and passed through the furnace at 525 ml/minute, a rate sufficient to change the air in the furnace once every three minutes. Corrosion of most of the alloys followed the rate law $W = kt^n$, where W equals the increase in weight resulting from the formation of adherent corrosion products, t is time, and k and n are constants.

Data are also given in the tables for tests conducted in a muffle furnace without forced circulation of air. In about every case the furnace atmosphere accelerates the attack and especially with samples containing additions which yield volatile chlorides.

b. Salt Corrosion of Stressed Samples

The behavior of a sample towards general salt corrosion does not necessarily indicate how the material will perform when stressed under corrosive conditions. An addition that increases the normal corrosion resistance of an alloy may have an adverse effect upon its mechanical properties or increase its susceptibility to stress corrosion. The effect of stress upon the salt corrosion of the modified alloys was examined by coating tensile specimens between the gage marks with salt and creep testing them at 700F under a load of 70 ksi for 100 hours. The results of these tests are given in Tables XXXV and XXXVI.

2. Discussion

Data were collected on the general corrosion resistance of the alloys by measuring the weight change of salt coated samples during a fixed period of time. Small net weight changes in themselves are not an adequate measure of the damage caused by salt because part of a weight increase could represent the development of a protective or semi-protective oxide film that retards the reaction. At the same time a sample is gaining weight due to salt attack and oxidation of the metal it is losing weight as chlorine is evolved during the oxidation of some of the metal chlorides formed in the corrosion reaction. The rapid intergranular attack that contributes to stress corrosion failure is not necessarily represented by a measurable weight change. Therefore, a correlation between the results of the general salt corrosion tests and the data from the salt-creep tests cannot be expected. The former tests represent the change in the surface characteristics produced by alloying while the latter tests measure the effect of the alloying element upon the behavior of the alloy when stressed in a corrosive atmosphere.

The general corrosion resistance and the stress corrosion resistance as measured by creep resistance of the salted sample, salt penetration, and residual ductility were all used to evaluate the effect of minor alloy additions upon the salt corrosion of the super-alpha alloys. Data were collected on control samples run without salt in order to assess the effect of the addition upon the mechanical properties of the base alloys so that these effects could be separated from those which affect the stress corrosion resistance of the alloys.

In general, taking into account factors such as variable salt adherence and other sources of experimental error, the corrosion resistance of unstressed Ti-12Zr-7Al was found to be good and, with the exception of additions of copper and nickel, not altered to any large degree by small alloy additions. Additions of antimony, gadolinium, and yttrium resulted in the most significant reduction in the corrosion rate at 1200F in moving air while additions of palladium and yttrium showed significant improvements in a corrosive atmosphere in which circulation was limited. An examination of the fractures of tensile tested samples from the salt-creep tests showed additions of manganese and palladium to result in the smallest amount of salt penetration.

The dependence of the salt corrosion resistance of Ti-8Al-1Mo-1V upon the amount that it was worked during processing, mentioned in a previous section of this report, was brought to light during these alloy studies. The alloys prepared for these tests were processed by a uniform procedure, but apparently suffered from a smaller amount of work and gave higher corrosion rates than had been observed in earlier work. Additions of yttrium, nickel, and antimony gave the greatest improvement in the general salt corrosion resistance of Ti-8Al-1Mo-1V in moving air while manganese and columbium improved the resistance in a corrosive atmosphere having limited circulation. Although many of the additions considerably lessened the creep resistance of the alloy, they did not, with the exception of nickel, show a prominent penetration as indicated by an examination of the break of tensile-tested samples from the salt-creep tests.

The following alloys could not be processed using the rolling schedule given in the beginning of this section: Additions of 1.0 and 0.5 percent yttrium, 0.5 percent beryllium, 0.1 percent mischmetal, and 1.0 percent thorium to Ti-12Zr-7Al; Additions of 1.0 and 0.5 percent yttrium, 0.5 percent beryllium, 0.1 percent gadolinium, and 0.1 percent mischmetal to Ti-8Al-1Mo-1V. With higher rolling temperatures it is possible that some of these alloys could be converted to sheet.

This survey of the effect of small alloying additions upon the salt-stress behavior of the super-alpha alloys at elevated temperatures indicates that subtle effects are produced. Because of the many variables encountered in salt testing these alloys, some of these effects are masked. Therefore, analyses of these effects is difficult unless each alloy or the most promising alloy systems are studied more extensively with the variables separated and/or reduced in number.

D. Study of Selected Alloys

Five pound ingots of alloys selected from the above study were prepared as follows:

Ti-12Zr-7Al	Ti-8Al-1Mo-1V
Ti-12Zr-7Al-1Mn	Ti-8Al-1Mo-1V-1Mn
Ti-12Zr-7Al-0.2Pd	Ti-8Al-1Mo-1V-0.2Pd
Ti-12Zr-7Al-0.1Y	Ti-8Al-1Mo-1V-0.1Y
Ti-10Zr-7Al	Ti-8Al-1Mo-1Cb

The ingots from the Ti-12Zr-7Al series were processed as follows: hot rolled 50 percent at 1850F to 3/4 in., cross-rolled at 1650F to ½ in., with final rolling at 1500F to 0.060 in.; annealed 30 minutes at 1400F and air cooled.

The ingots from the Ti-8Al-1Mo-1V series were processed as follows: hot rolled 10 percent at 1850F--cracking developed and the rolling was therefore continued at 1950F with 40% reduction to 3/4"--cross-rolled at 1750F to ½ in. with final rolling at 1500F to 0.060 in.; annealed 30 minutes at 1400F and air cooled.

Pieces were cut from the sheet to prepare samples for studying the general and stress corrosion behavior of the alloys. Data from the general corrosion tests are given in Table XXXVII and Figures 59 and 60. Creep, salt-creep and tensile test data are given in Table XXXVIII.

General salt corrosion tests of samples of sheet prepared from the five pound ingots showed a varied behavior. The addition of small amounts of manganese and yttrium to the Ti-12Zr-7Al alloy failed to impart the corrosion resistance that was observed in earlier tests. The reduction in the amount of zirconium in the alloy had a greater effect in reducing the rate of salt attack than the addition of small amounts of alloying elements, and it also gave the most significant improvement in performance in the salt-creep tests. The addition of palladium and yttrium improved the salt-creep performance of both Ti-12Zr-7Al and Ti-8Al-1Mo-1V. The addition of palladium to Ti-8Al-1Mo-1V gave better results in the general corrosion tests than were observed earlier. The addition of manganese and the substitution of columbium for vanadium in this alloy gave materials having a higher rate of attack.

E. L. Kochka
E. L. Kochka
Staff Chemist

V. C. Petersen
V. C. Petersen
Staff Metallurgist

Approved:

H. B. Bomberger
H. B. Bomberger, Supervisor
Fundamental Research Section

H. T. Clark
H. T. Clark, Manager
Midland Research Laboratory

REFERENCES

1. Mallory-Sharon Titanium Corporation, Pratt and Whitney Aircraft, Rem-Cru Titanium, Inc., Republic Steel Corporation, and Titanium Metals Corporation of America, "Progress Report on the Salt Corrosion of Titanium Alloys at Elevated Temperature and Stress," Titanium Metallurgical Laboratory, Battelle Memorial Institute, TML Report No. 88, 50 pp., November 20, 1957.

2. F. A. Crossley, C. J. Reichel, and C. R. Simcoe, Armour Research Foundation, "The Determination of the Effects of Elevated Temperatures on the Stress Corrosion Behavior of Structural Materials," WADD Technical Report 60-191, May 1960.

3. H. W. Pickering, F. H. Beck, and M. G. Fontana, "Rapid Intergranular Oxidation of 18-8 Stainless Steels by Oxygen and Dry Sodium Chloride at Elevated Temperatures," ASM Preprint No. 232, 1960.

4. H. R. Copson, "Corrosion of Heating Electrodes in Molten Chloride Baths," J. Electrochem. Soc. 100, 257-64 (1953).

5. V. P. Kochergin, A. V. Kabirov, and D. M. Skornyakova, "Corrosion of Iron in Molten Salt Mixtures," J. Appl. Chem. U.S.S.R. 27, 883-8 (1954).

6. E. I. Gurovich, "Reaction of Molten Lithium, Sodium, and Potassium Chloride with Nickel, Copper and Some Steels," J. Appl. Chem. U.S.S.R. 27, 395-400 (1954).

7. K. Smrcek, I. Sekerka, and V. Seifert, "Corrosion Studies. VII. The Corrosion Cell Metal-Platinum in Fused Alkali Halides," Chem. Listy 50, 721-5 (1956).

8. A. Moskowitz and L. Redmerski, Crucible Steel Company of America, "Corrosion of Superalloys by Selected Fused Salts," WADD Technical Report No. 60-115, March 1960.

9. W. D. Manly, J. H. Coobs, J. H. DeVan, D. A. Douglas, H. Inouye, P. Patriarca, T. K. Roche, and J. L. Scott, "Metallurgical Problems in Molten Fluoride Systems," Proceedings, Second World Nuclear Congress, Geneva, 1958.

10. E. I. Gurovich, "Effect of Molten Nitrates of Lithium, Sodium, and Potassium on Nickel, Copper, Duralumin, and Some Steels," Zhur. Priklad. Khim. 29, 1358-65 (1956).

11. J. H. Jackson and M. H. LaChance, "Resistance of Cast Fe-Ni-Cr Alloys to Corrosion in Molten Neutral Heat-Treating Salts," Trans. Am. Soc. Metals 46, 157-83 (1954).

12. D. Roller and C. R. Andrews, "Effect of Molten Boron Oxide on Selected High Temperature Alloys," Corrosion 15, 85t-96t (1959).

13. G. P. Smith, M. E. Steidlitz, and E. E. Hoffman, "Corrosion and Metal Transport in Fused Sodium Hydroxide. I. Experimental Procedures," Corrosion 13, 561t-4t (1957).

14. G. P. Smith and E. E. Hoffman, "Corrosion and Metal Transport in Fused Sodium Hydroxide. II. Corrosion of Nickel, Molybdenum, Iron Alloys," Corrosion 13, 627t-30t (1957).

15. G. P. Smith, M. E. Steidlitz, and E. E. Hoffman, "Corrosion and Metal Transport in Fused Sodium Hydroxide. III. Formation of Composite Scales on Inconel," Corrosion 14, 47t-52t (1958).

16. G. P. Smith, "Corrosion of Materials in Fused Hydroxides," Am. Inst. Mining Met. Engr., Inst. Metals Div., Spec. Report No. 2, 71-94 (1956).

17. C. M. Craighead, L. A. Smith and R. I. Jaffee, "Screening Tests on Metals and Alloys in Contact with Sodium Hydroxide at 1000 and 1500F," U.S. Atomic Energy Comm. BMI-706, 3-35 (1951).

18. D. D. Williams, J. A. Grand, and R. R. Miller, "The Reactions of Molten Sodium Hydroxide with Various Metals," J. Am. Chem. Soc. 78, 5150-5 (1956).

19. F. R. Schwartzberg, F. C. Holden, H. R. Ogden, and R. I. Jaffee, "Report on the Properties of Titanium Alloys at Elevated Temperatures," Titanium Metallurgical Laboratory, Battelle Memorial Institute, TML Report No. 82, 216 pp. September 10, 1957.

20. J. W. Suiter, "Tensile Properties of Some Titanium Alpha-Solid Solutions up to 600C," J. Inst. Metals 83, 460-4 (1955).

21. W. L. Williams, "Behavior of Titanium at Temperatures to 900F," Iron Age 167, No. 24, 81-4 (1951).

22. R. L. Bickerdike and D. A. Sutcliffe, "The Physical Properties of Titanium at Various Temperatures," Metall 4, 191-3 (1950).

23. R. L. Bickerdike and D. A. Sutcliffe, "Tensile Strength of Titanium at Various Temperatures," Metallurgica 39, 303-4 (1944).

24. W. A. Alexander and L. M. Pidgeon, "Kinetics of the Oxidation of Titanium," Can. J. Research 28B, 60-72 (1950).

25. I. M. Adachi and T. Tsujimoto," On the Oxidation of Titanium Metal and Ti-Al Alloys," J. of the Japanese Institute of Metals 22, 379-82 (1958).

26. P. Kofstad and K. Hauffe, "Oxidation of Titanium," Werkstoffe and Korrosion 7, 642-9 (1956).

27. D. W. Stough, F. W. Fink, and R. S. Peoples, "The Oxidation of Titanium and Titanium Alloys," Titanium Metallurgical Laboratory, Battelle Memorial Institute, TML Report No. 29, 60 pp., January 30, 1956.

28. J. J. Trillat, "Kinetic Study by Electron Diffraction of Structural Transformations and of Oxidation Processes," Rev. met. 53 497-502 (1956).

29. P. Kofstad, "Investigation of the Mechanism of the Oxidation of Titanium and Titanium Alloys at High Temperatures. Period covered: 1 October 1955 to 31 March 1957," AD-130779, WADC-TN-57-231, 92 pp., June 1957.

30. O. N. Carlson, D. Bare, and F. H. Spedding, "Corrosion Properties of Some of the Refractory Metals and Their Alloys," U. S. Atomic Energy Commission, ISC-977, 54 pp. October 15, 1958.

31. W. Kinna and W. Knorr, "On the Oxidation of Titanium," Zeitschrift fur Metallkunde 47, 594-8 (1956).

32. V. A. Yakovlev and Ya. I. Spektor, "Gaseous Corrosion of Titanium Alloys in Furnace and Induction Heating," Metallovedenie i Obrabotka Metallov. No. 6, 55-6 (1958).

33. T. Hurlen, H. Kjollesdal, and J. Markali, "Oxidation of Titanium and Titanium Alloys," Teknisk Ukeblad 105, No. 18, 423-31 (May 1, 1958).

34. M. E. Straumanis and Ch. Chiou, "Rates of Oxidation of Titanium in Fused Salt Baths," J. Electrochem. Soc. 104, 76c (1957).

35. M. E. Straumanis and Ch. Chiou, "The Rate of Oxidation (Corrosion) of Titanium in Molten Salt and the Composition of the Oxidation Products," Z. Elektrochem. 62, 201-9 (1958).

36. C. B. Gill, M. E. Straumanis, and A. W. Schlechten, "Corrosion of Titanium in Fused Chlorides. Formation of Pyrosols," J. Electrochem. Soc. 102, 42-5 (1955).

37. M. E. Straumanis, S. T. Shih, and A. W. Schlechten, "Mechanism of Deposition of Titanium Coatings from Fused Salt Baths," J. Electrochem. Soc. 104, 17-20 (1957).

38. M. E. Straumanis and A. W. Schlechten, "Titanium Coatings on Metals and Ceramic Objects," Metall 10, 901-9 (1956).

39. A. W. Schlechten, M. E. Straumanis, and C. B. Gill, "Deposition of Titanium Coatings from Pyrosols," J. Electrochem. Soc. 102, 81-5 (1955).

40. M. E. Straumanis and Y. P. Huang, "Corrosion of Titanium in Molten Salt Baths," Metall 11, 1029-32 (1957).

41. M. E. Straumanis and A. W. Schlechten, "Electrochemical Behavior of a Titanium-Fused Salt-Platinum Cell," J. Electrochem. Soc. 102, 131-6 (1955).

42. W. C. Kreye and H. H. Kellogg, "The Equilibrium Between Titanium Metal, $TiCl_2$, and $TiCl_3$ in NaCl-KCl Melts," J. Electrochem. Soc., 104, 504-8 (1957).

43. S. Mellgren and W. Opie, "Equilibrium Between Titanium Metal, Titanium Dichloride, and Titanium Trichloride in Molten Sodium Chloride-Strontium Chloride Melts," J. Metals 9, No. 2, 266-9 (1957).

44. R. S. Dean, L. D. Resnik and I. Hornstein, "Titanium Metallurgy - Part 3, Reduced Titanium Chloride of Alkalinous Metals," Industrial Lab 8 (6), 93-5 (1957).

45. R. S. Dean, W. W. Gullet, and F. X. McCauley, "Titanium Metallurgy - Part 2, Structure of Titanium Deposits Formed in Electrolytic Cells Using Fused Alkali Chloride Baths," Industrial Lab 8 (5), 10-2 (1957).

46. G. B. Skinner and R. A. Ruehrwein, "Thermodynamic Properties of the Titanium Chlorides," J. Phys. Chem. 59, 113-7 (1955).

47. K. Komorek and P. Herasymenko, "Equilibria Between Titanium Metal and Solutions of Titanium Dichloride in Fused Sodium Chloride," J. Electrochem. Soc. 105, 216-9 (1958).

48. K. Funaki and K. Uchimura, "System Titanium-Titanium Tetrachloride," J. Chem. Soc. Japan, Ind. Chem. Sect. 57, 538-40 (1954).

49. P. Conjeaud, "Electron-Diffraction Study of the Condensation Products of Titania Vapor on Single Crystals of Heated Halides," Compt. rend. 239, 1210-3 (1954).

50. B. F. Naylor, "High Temperature Heat Contents of Na_2TiO_3, $Na_2Ti_2O_5$ and $Na_2Ti_3O_7$," J. Am. Chem. Soc. 67, 2120-2 (1945).

51. C. H. Shomate, "Heat Capacities at Low Temperatures of Na_2TiO_3, $Na_2Ti_2O_5$ and $Na_2Ti_3O_7$," J. Am. Chem. Soc. 68, 1643-6 (1946).

52. F. F. Barblan, "The Crystal Chemistry of Fe_2O_3 and TiO_2 and Their Alkali Compounds," Schweiz. Minerolog, Petrog, Mitt. 23, 295-352 (1943).

53. V. Gottardi, "The Formation in the Solid Phase of Sodium Titanate and Barium Titanate," Gazz. chim. ital. 85, 1520-34 (1955).

54. E. W. Washburn and E. N. Bunting, "Note on Phase Equilibria in the System Na_2O-TiO_2," Bur. Standards J. Research 12, 239 (1934) (Research Paper No. 648).

55. P. P. Budinikov and S. G. Tresvyats'kiy, "Phase Diagram of the System Na_2O-TiO_2," Dopovidi Akad. Nauk, Ukr. R.S.R. 1954, 371-6.

56. H. Lux, "Reactions in Fused Masses. VI. Equilibrium in the System Na_2O-TiO_2, Z. Elektrochem. 53, 45-7 (1949).

57. M. Viltange, "Some Reactions between Sodium Peroxide and Different Oxides in the Solid State. II" Compt. rend. 239, 61-3 (1954).

58. F. V. Bichowsky, "Nitrides as a Possible Route to Commercial Production of Cyanides," Chem. Met. Eng. 29, 1098-1101 (1923).

59. J. D'Ans and J. Loffler, "Metallic Oxides and Sodium Hydroxide" Ber. 63B, 1446-55 (1930).

60. E. Herrmann, I. Dvornik, O. Koreic and V. Matkovic, "Decantation of Red Silt from Druis (Croatia) Bauxite," Arkiv. Kem. 23, 82-103 (1951).

61. C. E. Armantrout and J. E. Hauger, "Explosion of a Titanium Crucible," Metal Progress 72, 94-5 (September 1957).

62. H. H. Uhlig and J. R. Cobb, Jr., "Titanium Resists Stress Corrosion," Metal Progress 59, No. 6, 816 (1951).

63. G. C. Kiefer and W. W. Harple, "Stress-Corrosion Cracking of Commercially Pure Titanium," Metal Progress 63, No. 2, 74-6 (1953).

64. P. M. Ambrose, J. C. Barrett, R. W. Huber, D. Schlain, and V. C. Petersen, "Investigation of Accident Involving Titanium and Red Fuming Nitric Acid, December 29, 1953," U. S. Bur. Mines, Inform. Circ. 7711, 34 pp. (1955).

65. L. L. Gilbert and C. W. Funk, "Explosion of Titanium and Fuming Nitric Acid Mixtures," Metal Progress 70, No. 11, 93-6 (1956).

66. J. B. Rittenhouse, "The Corrosion, Pyrophoricity, and Stress Corrosion Cracking of Titanium Alloys in Fuming Nitric Acid," Trans. ASM 51, 871-99 (1959).

67. M. G. Fontana, "Stress Corrosion in Titanium and Its Alloys," Ind. Eng. Chem. 48, No. 9, 59A-60A (1956).

68. R. Meredith and W. L. Arter, "Stress Corrosion of Titanium Weldments," Welding J. (N.Y.) 36, 415s-418s (1957).

69. D. W. Stough, F. W. Fink, and R. S. Peoples, "The Stress Corrosion and Pyrophoric Behavior of Titanium and Titanium Alloys," Titanium Metallurgical Laboratory, Battelle Memorial Institute, TML Report No. 84, 46 pp., September 15, 1957.

70. J. Starr, "Comments on the Finishing of Titanium," Products Finishing 17, No. 6, 38-42 (1953).

71. B. Rivolta, "Study of the Anodic Behavior of Titanium. II. Study of the Properties of Passivating Coatings Formed on Titanium by Means of Anodic Treatments," Metallurgia Italians 50, No. 7, 255-62 (1958).

72. H. Bohm, "Anodic Oxidation of Titanium," Metalloberflache 11, 197-200 (1951).

73. R. D. Misch and W. E. Ruther, "The Anodizing of Zirconium and Other Transition Metals in Nitric Acid," J. Electrochem. Soc. 100, 531-7 (1953).

74. Imperial Chemical Industries, Ltd., S. Hands, and J. Hampage, "Oxidation Protection of Titanium and Titanium-Base Alloys at High Temperatures," Brit. 774,598, May 15, 1957.

75. C. C. Ma and E. M. Peres, Jr., "Corrosion Resistance of Anodized and Unanodized Titanium," Ind. Eng. Chem. 43, 675-9 (1951).

76. R. Otsuka, "Thixotropic Protective Layer on a Metal," Kolloid Z. 153, 59 (1957).

77. K. Nagasaki and H. Ishida, "Anodic Oxidation of Titanium," Light Metals (Tokyo), No. 26, 70-2 (1957).

78. R. Otsuka, "Protective Film on Titanium in Hydrochloric Acid," J. Sci. Research Inst. (Tokyo) 49, 319-24 (1955).

79. C. Levy, "Chromium Plating on Titanium Alloys," J. Electrochem. Soc. 105, No. 8, 161C (1958).

80. T. A. Dickinson, "Plating of Titanium and Its Alloys," Metal Finishing 5, No. 49, 24-5, 28 (1959).

81. E. B. Saubestre, "Electroplating on Certain Transition Metals," J. Electrochem. Soc. 106, 305-9 (1959).

82. H. Richaud, "Titanium Surface Treatments," Corrosion et anticorrosion 4, 400-3 (1957).

83. Belgian 559,886, February 7, 1958 - pretreatment of metals which oxidize readily.
British 814,326, June 3, 1959 - nickel plating.
U.S. 2,825,682, March 4, 1958 - chromium plating.
U.S. 2,829,901, April 1, 1958 - chromium or copper plating.
U.S. 2,856,333, October 14, 1958 - chromium, nickel, copper or brass plating.

84. H. Lundin, "Coating Ferrous and Other Metals with Aluminum," U.S. 2,785,084, March 12, 1957.

85. H. J. West, "Electroless Nickel Plating on Nonferrous Metals," Metal Finishing 52, No. 7, 72 (1954).

86. U.S. 2,658,841, November 10, 1953.
U.S. 2,766,138, October 9, 1956.
U.S. 2,774,688, December 18, 1956.

87. W. J. Hyink, "Plated Coating on Titanium Gears," J. Electrochem. Soc. 105, No. 8, 161C (1958).

88. Imperial Chemical Industries, Ltd., "Improvements in Coating Titanium and Titanium-Base Alloys and Zirconium and Zirconium-Base Alloys," Belgian 564,494, August 4, 1958.

89. Horizons, Inc., "Coating Metal Objects with Metals by Dipping," British 803,316, October 22, 1958.

90. A. P. Shepard, "Molybdenum Coatings Expand Uses of Metallizing," Iron Age 173, No. 26, 105-7 (1954).

91. H. W. Schultze, R. R. Freeman, and J. Z. Briggs, "Molybdenum Coatings," Materials in Design Engineering 49, No. 1, 76-81, (1959).

92. S. Tour, A. Styka, and G. Fischer, "Molybdenum Deposition on Titanium," J. Metals 7, AIME Trans. 203, 291-6 (1955).

93. W. M. Sterry, "Ceramics Holds Key to Aircraft Development," Ceramic Industry 68, No. 5, 92-4, 113 (1957).

94. "Glass Protective Coating," Financial Times, No. 21, 521, p. 9, July 15, 1958.

95. A. H. Happe, "Coatings for Metals," U.S. 2,711,974, June 28, 1955.

96. M. Yanagisawa, "Heat Resistant Coating on Titanium," Japan 3656 ('56), May 19, 1956.

97. T. Hibino, M. Nakamura, Y. Wakao, M. Yanagisawa, and C. Noguch, "Oxidation of Titanium and its Protecting Method. II. Surface Coating of Titanium by $MgO-TiO_2$, $ZnO-TiO_2$ and $BeO-TiO_2$ System," Repts. Govt. Ind. Research Inst., Nagoya 4, 328-33 (1955).

98. F. X. McCawley, "Method of Forming Carbonaceous Protective Coatings on Titanium and Zirconium," U.S. 2,865,797, December 23, 1958.

99. J. L. Wyatt and N. J. Grant, "Nitriding Improves Properties of Titanium," Iron Age 173, No. 4, 124-7 (1954).

100. K. K. Kelley and A. D. Mah, "Metallurgical Thermochemistry of Titanium," U. S. Bur. Mines, Rept. Investigations 5490, 48 pp. (1959).

101. K. K. Kelley, U. S. Bureau of Mines Bulletin 476, 241 pp., (1949).

102. F. D. Rossini, et al, U.S. National Bureau of Standards Circular 500, 1268 pp. (1950).

103. M. Farber, A. J. Darnell and F. Brown, "X-Ray Diffraction Patterns of $TiCl_2$ and $TiCl_3$," J. Chem. Physics 23, 1556 (1955).

104. D. M. Liddell, ed., "Handbook of Non-Ferrous Metallurgy," 1945, New York, McGraw-Hill Book Company, Inc., p. 544.

105. W. J. Kroll, "The Pyrometallurgy of Halides," Metallurgical Reviews, 1 (3) 293 (1956).

106. A. E. Jenkins, "The Oxidation of Titanium at High Temperatures in an Atmosphere of Pure Oxygen," Journal of the Institute of Metals, 82, 213 (1954).

107. M. E. Straumanis and P. C. Chen, "The Corrosion of Titanium in Acids," Corrosion 7, 229-37 (1951).

108. D. Schlain and J. S. Smatko, "Passivity of Titanium in Hydrochloric Acid Solutions," J. Electrochem. Soc. 99, 417-22 (1952).

109. D. Schlain, "Certain Aspects of the Galvanic Corrosion Behavior of Titanium," U.S. Bur. Mines, Rept. Investigations 4965, 22 pp., April 1953.

110. R. S. Dean, I. Hornstein and W. W. Gullett, "Electrode Potential of Titanium-Oxygen Alloys in Molten Salt Electrolytes," J. Electrochem. Soc. 105 (3), 55C (1958).

111. E. D. Parr, "Protective Coatings for Titanium," Document No. D2-2522, p. 10-12, 1958, Boeing Airplane Company, Seattle, Wash.

112. D. Halpert, "Electroplating Titanium and Titanium Alloys," U.S. 2,921,888, January 19, 1960 (assigned to Vertol Aircraft Corp.)

113. "Practical Nickel Plating," The International Nickel Company, N.Y., 1959.

114. E. J. Roehl and W. A. Wesley, "Nickel Plating from a Fluoborate Bath," Plating 37, 142-6 (1950).

115. R. F. Ledford, "Cobalt-Nickel Deposition in Electrotyping," Plating 36, 560 (1949).

116. R. C. Barrett, "Nickel Plating from the Sulfamate Bath," Proc. Am. Electroplater's Soc. 41, 169 (1954).

117. M. F. Quaely, "Black-Chromium Base Electroplating," Proc. Am. Electroplater's Soc. 40, 982-5 (1953).

118. W. Blum and G. B. Hogaboom, "Principle of Electroplating and Electroforming," McGraw-Hill Book Company, N. Y., 1949.

119. D. K. Hanink, "Improvements Relating to the Coating of Titanium or Titanium Alloy with Aluminum or Aluminum Alloy," British Patent 740,268.

120. H. A. Porte, J. G. Schnizlein, R. C. Vogel and D. F. Fischer, "Oxidation of Zirconium and Zirconium Alloys," J. Electrochem. Soc. 107, 506-15 (1960).

121. E. M. Levin, ed., "Phase Diagrams for Ceramists," 1956, Ohio, The American Ceramic Society.

122. Derivations and discussion by J. P. Catlin and E. L. Kochka.

123. F. A. Champion., "Corrosion Testing Procedures," pp. 137-52, John Wiley & Sons, N.Y., 1952.

124. H. W. Hatfield and G. L. Thirkell, J. Inst. Met. (London) 22, 83-5 (1919).

125. P. Brenner, Z. Metallkunde 24, 145 (1932).

126. H. L. Logan and H. Hessing, J. Research Natl. Bur Standards 41, No. 1, 69 (1948).

APPENDIX A

Methods of Calculating Stress for Cracking Tests[122]

Several methods were studied for calculating the maximum stresses in samples stressed in an arc as indicated in Figure 61. Champion's book[123] contains a very complete assembly of formulas and techniques for stress corrosion cracking studies. Several of the simpler equations are derived and their applicability to this study is discussed.

A. Equation of Hatfield and Thirkell[124] (see also Brenner[125])

The equation given by the above authors for calculating the stress in a curved specimen is:

$$S = Et/2r \qquad (1)$$

where S = the maximum stress in the outer fibers
E = Modulus of elasticity
t = thickness
r = radius of curvature to the center line

The equation is derived in the following manner with reference to Figure 61:

$$a = r\theta \qquad (2)$$

$$a_1 = (r+t/2)\theta \qquad (3)$$

therefore, the elongation in the outer fibers resulting from the application of stress is:

$$a_1 - a = (t/2)\theta \qquad (4)$$

but, E = stress/strain = load per unit area/(elongation/original length) therefore, stress = (E x elongation)/original length, or

$$S = Et/2r \qquad (5)$$

B. Equation of Logan and Hessing[126]

The above authors give the following equation for calculating the maximum stress in the outer fibers of the central section of a specimen formed to the arc of a circle:

$$S = 4Etd/L^2 \qquad (6)$$

where S = the maximum stress in the outer fibers
E = Young's modulus
t = thickness
d = distance from the outer fibers of the arc to the chord
L = length of chord

This equation can be derived from equation (1) again with reference to Figure 61:

$$r^2 = (r-d)^2 + (L/2)^2 \qquad (7)$$

expanding this gives:

$$-2rd+d^2+L^2/4 = 0 \qquad (8)$$

since d is small compared to L and r, d^2 is neglected, and

$$rd = L^2/8, \text{ or,} \qquad (9)$$

$$r = L^2/8d \qquad (10)$$

substituting (10) into equation (1) gives:

$$S = 4Etd/L^2 \qquad (11)$$

For their measurements, the authors used a dial gauge reading to 0.0001 inch attached to a plunger centered between two fixed pointers spaced two inches apart. The equation reduces to S = Etd for a two-inch chord. They found the stress to differ by less than two percent at 3/4 of the yield strength from the true stress in the outer fibers as determined by strain gage measurements. Of course, the accuracy of the answer depends largely upon the amount of defiection of a sample relative to its length.

C. Equation Used in Column Loading

When the yield strength is not exceeded, the maximum stress in the outer fiber can be calculated by means of the following equation:

$$S = Etd\pi^2/2L^2 \qquad (12)$$

where the symbols employed are the same as in section B.

This equation is derived from Euler's equation for a pin ended long column in which the critical buckling load, Pcr, is given by:

$$Pcr = \pi EI/L^2 \qquad (13)$$

where I = the moment of inertia of the strip cross-section.

The bending moment M concentrated at the point of maximum deflection is given by:

$$M = Pcr \times d \qquad (14)$$

From the elementary beam stress formula

$$S = Mt/2I \qquad (15)$$

By making the appropriate substitutions equation (16) is obtained.

$$S = Etd\pi^2/2L^2 \qquad (16)$$

D. Comparing the Above Equations

Equation 16 has been found to be accurate only if very precise conditions are known (such as: specimen straightness, alignment, and load application). A discussion of column loading in strength of material texts indicates that excessively high values can be expected by the use of this equation, particularly since the actual buckling load is usually much less than the calculated value. Consequently, equation (16) is not the best for stress calculations. Equation (11), because it neglects d^2 on the assumption that d is small compared to L, is less accurate than equation (5).

Equation (5) was considered the best for this work and was used. This equation is based on the strip specimen bent into a circular arc and, although this is not actually the case with the present testing apparatus, the approximation is quite good. The radius of curvature was measured with sufficient accuracy for our needs by using a geometric construction and elementary mathematics.

TABLE I

X-Ray Data on Fusion Products of Sodium Carbonate and Titanium Dioxide*

Na_2TiO_3		$Na_2Ti_3O_7$		$Na_2Ti_2O_5$	
d-Spacing (Å)	Intensity**	d-Spacing (Å)	Intensity	d-Spacing (Å)	Intensity
5.2	MW	8.0	MS	8.0	VW
4.4	W	5.5	M	6.2	M
3.20	S	3.41	W	4.35	MW
2.70	MW	2.95	MW	2.6	MW
2.60	W	2.60	MW	2.40	VW
2.50	VW	2.50	VW	2.21	MW
2.41	W	2.05	S	2.13	W
2.20	MS	1.90	VW	2.06	M
2.06	W	1.80	W	1.68	W
1.90	W	1.64	VW		
1.86	MS	1.56	VW		
1.81	W	1.535	VW		
1.61	VW	1.47	W		
1.58	VW	1.44	W		
1.535	VW	1.39	W		
1.515	VW	1.372	MW		
1.495	W	1.195	MW		
1.39	MW				
1.30	W				
1.22	W				
1.195	W				
1.185	W				

*Sodium carbonate and titanium dioxide were mixed in the stoichiometric properties required to give the compounds indicated and reacted for 4 hours at 1960F.

**S = strong, M = medium, W = weak, VW = very weak

TABLE II

Effect of Metal Oxides on the Salt Corrosion of Titanium

Weight Increase (g/square inch)*	Metal Oxide (1% Metal Oxide in Sodium Chloride)*
Less than 0.05	As_2O_3, Co_3O_4, Cb_2O_5, Cu_2O, MoO_3, NiO, SnO_2
0.5 to 0.10	Al_2O_3, Sb_2O_3, Bi_2O_3, CdO, CuO, Didymium Oxide, Nd_2O_3, Pr_2O_3, SnO, ZnO
	Titanium Metal + Salt for 24 Hours at 1200F
0.10 to 0.15	Fe_2O_3, NiO_2, TeO_2, TiO_2, ZrO_2, Y_2O_3
0.15 to 0.20	V_2O_3, V_2O_5
Greater than 0.20	Cr_2O_3, PbO, PbO_2, MnO_2, Ag_2O, Ta_2O_5 VO_2

*Mixture of 1% metal oxide in NaCl applied as a slurry to samples of titanium which were dried and suspended in a furnace for 24 hours at 1200F.

**The weight increase does not necessarily reflect the degree of damage to the titanium metal, but the change in the overall system. The weight change can indicate volatilization, oxidation, or some other effect, but samples which increased more than 0.1 g/square inch generally showed a significantly greater attack of the metal in the presence of the oxide than without the oxide present.

TABLE III

Tests Showing the Accelerated Oxidation of Titanium Alloys by Salt at 1200F

	Ti(A70)	Ti(A70)	Ti(A70)	Ti-12Zr-7Al	Ti-8Al-1Mo-1V	Ti-8Al-8Zr-1(Cb+Ta)
Time (Hours)	170	167	164	172	143	167
Initial weight of metal (g/square inch)	1.358	1.415	1.348	1.759	1.284	1.882
Initial weight of salt coating (g/square inch)	1.263	0.045	1.082	0.879	0.873	0.818
Increase in weight from corrosion product (g/square inch)	0.563	0.339	0.360	0.141	0.095	0.159
Increase in weight per hour (g/square inch/hour)	0.0033	0.0020	0.0022	0.0008	0.0007	0.0010
Final weight of recovered metal (g/square inch)	0.489	0.883	0.841	1.453	1.075	1.412
Metal loss (g/square in.)	0.869	0.532	0.507	0.306	0.209	0.470
Metal loss per hour (g/square inch/hour)	0.0051	0.0032	0.0031	0.0018	0.0015	0.0028

TABLE IV

Tests Showing the Accelerated Oxidation of Titanium Alloys by Salt at 1000F

	Ti(A70)	Ti-12Zr-7Al	Ti-12Zr-7Al	Ti-8Al-8Zr-1(Cb+Ta)
Time (Hours)	144	102	120	120
Initial weight of metal (g/square inch)	1.361	1.611	1.282	1.799
Initial weight of salt coating (g/square inch)	0.913	0.622	0.536	1.105
Increase in weight from corrosion product (g/square inch)	0.092	0.005	0.009	0.011
Increase in weight per hour (g/square inch/hour)	0.0006	< 0.0001	0.0001	0.0001
Final weight of recovered metal (g/square inch)	1.199	1.603	1.261	1.771
Metal loss (g/square in.)	0.162	0.008	0.021	0.028
Metal loss per hour (g/square inch/hour)	0.0011	0.0001	0.0002	0.0002

TABLE V

Oxidation of Titanium Alloys at 1000F and 1200F

Temperature °F	Time (Hours)	Weight Gain (g/square inch)			
		A70	Ti-12Zr-7Al	Ti-8Al-1Mo-1V	Ti-8Al-8Zr-1(Cb+Ta)
1000	2½	0.00000	0.00013	0.00000	0.00005
	48	0.00013	0.00020	0.00000	0.00015
	72	0.00018	0.00033	0.00013	0.00025
	96	0.00018	0.00033	0.00013	0.00025
1200	25	0.0025	0.0015	0.0017	0.0007
	48	0.0036	0.0023	0.0030	0.0011
	72	0.0042	0.0025	0.0035	0.0013
	96	0.0051	0.0033	0.0043	0.0016

TABLE VI

Salt Corrosion of Titanium Alloys at 1000F and 1200F

Temperature °F	Time (Hours)	Weight Gain (g/square inch)			
		A70	Ti-12Zr-7Al	Ti-8Al-1Mo-1V	Ti-8Al-8Zr-1(Cb+Ta)
1000	16	0.0054	0.0060	0.0111	-
	24	0.0069	0.0090	0.0086	-*
	48	0.0173	0.0163	0.0128	-
	72	0.0279	0.0199	0.0163	-
	96	0.0419	0.0229	0.0189	-
1200	16	0.0864	0.0162	0.0420	-
	24	0.2396	0.0832	0.0832	0.0917
	48	0.4005	0.1412	0.1350	0.1679
	72	0.5105	0.1868	0.1758	-**
	96	0.5884	0.2241	0.2083	-**

*Not tested.
**Salt coating did not adhere to surface after the second weighing.

TABLE VII

The Effect of Temperature on the Salt Corrosion of Titanium Alloys for 16-Hour Exposures

Temperature °F	Weight Gain (g/square inch)		
	A70	Ti-12Zr-7Al	Ti-8Al-1Mo-1V
700	-0.0005	-0.0010	-0.0011
800	+0.0002	-0.0002	-0.0003
900	0.0015	+0.0029	+0.0013
1000	0.0054	0.0060	0.0111
1100	0.0242	0.0140	0.0179
1200	0.0864	0.0162	0.0420
1300	0.1517	0.0485	0.0893
1400	0.5426	0.2097	0.0902

TABLE VIII

Effect of High Temperature Exposure on the Stress Corrosion Cracking of Commercially Pure Titanium Sheet in 5% HCl

Condition of Material*	Time of Test**	Remarks
As received	20 days	None cracked.
24 hours at 1700F	20 days	None cracked.
16 hours at 1800F	20 days	One cracked in 1¼ days; five did not crack.
24 hours at 1800F	20 days	None cracked.
40 hours at 1800F	20 days	One cracked in 1½ days; two did not crack.
1 hour at 1900F	20 days	None cracked.
2 hours at 1900F	20 days	None cracked.
4 hours at 1900F	20 days	Six tested; none cracked.
5 hours at 1900F	20 days	Six tested; none cracked.
6 hours at 1900F	2½ hr; 1 day; 1 day 5 hr; 20 days; 20 days	Six tested; all but two cracked.
7 hours at 1900F	inst; ½ hr; ½ hr	All cracked.
8 hours at 1900F	inst; inst; inst	All cracked immediately upon contact with the aggressive medium.

*Heat Number T6-176630-5. All samples were in the mill-annealed (as-received) condition and given additional treatment as indicated, grit blasted, and deskinned a minimum of 4 mils per side.

**Tested in triplicate or as indicated at approximately 75,000 psi in 5% HCl for 20 days or until failure occurred.

TABLE IX

Effect of High Temperature Exposure on the Stress Corrosion Cracking of Ti-12Zr-7Al Sheet in 5% HCl

Condition of Material*	Time of Test**	Remarks
As received	20 days	None cracked.
16 hours at 1800F	20 days	None cracked.
24 hours at 1800F	20 days	None cracked.
1 hour at 1900F	20 days	None cracked.
2 hours at 1900F	20 days	None cracked.
3 hours at 1900F	20 days	None cracked.
4 hours at 1900F	inst; inst; inst	All cracked immediately upon contact with the test medium.
4 hours at 1900F	½, 2½, 2½ hours	All cracked.
4 hours at 1900F	20 days	Calculated stress of 68,000 psi
6 hours at 1900F	inst; inst; 1 day	All cracked.
½ hour at 2000F	20 days	None cracked.

*Heat Number R98321-1. All samples had been annealed 1 hour at 1600F (i.e., as received) and then given additional high temperature exposures as indicated, grit-blasted, and deskinned a minimum of 4 mils per side.

**Tested in triplicate at 80,000 psi, or as indicated, in 5% HCl for 20 days or until failure occurred.

TABLE X

Effect of High Temperature Exposures on the Stress Corrosion Cracking of Ti-8Al-1Mo-1V Sheet in 5% HCl

Condition of Material*	Time of Test**	Remarks
2 hours at 1900F	20 days	None cracked.
4 hours at 1900F	20 days	None cracked.
6 hours at 1900F	20 days	None cracked.
8 hours at 1900F	20 days	None cracked.
10 hours at 1900F	20 days; 20 days; 5-1/6 days	All specimens showed some attack, but in only one was crack propagation complete.
12 hours at 1900F	20 days; 20 days; 17½ days	
16 hours at 1900F	2 days; 12½ days; broke on loading	All cracked.

*Heat Number R98369. All samples had been annealed one hour at 1800F, air cooled to 1100F, held 8 hours and air cooled to ambient temperature and then given additional exposures as indicated, grit-blasted, and deskinned a minimum of 3 mils per side prior to stressing in 5% HCl.

**Tested in triplicate at about 78,000 psi in 5% HCl for 20 days or until failure occurred.

TABLE XI

Summary of Data from Miscellaneous Cracking Tests

Material	Additional Conditioning*	Stress psi	Medium	Remarks
Ti-12Zr-7Al	4 hours at 1900F in vacuum	98,000	5% HCl	No failures.
"	100 hours at 1600F in vacuum	98,000	5% HCl	No failures.
"	4 hours at 1900F	80,000	Air	No failures.
Ti-8Al-1Mo-1V	16 hours at 1900F	80,000	Air	No failures.
A70	8 hours at 1900F	75,000	Air	No failures.
"	8 hours at 1900F	70,000	5% HCl	No failures.
"	7 hours at 1900F	85,000	5% HCl	1 instantly; 2 in ½ hour
"	7 hours at 1900F	85,000	Air	1 failed in 10½ days possibly from HCl fumes in the area.
"	7 hours at 1900F	85,000	Tap Water	1 failed in 4½ days. HCl fumes caused pH to change from 6 to 3 during test.
"	7 hours at 1900F	85,000	5%HCl-2%H_2O_2	1 failure after 7 days.
"	7 hours at 1900F	75,000	5% $TiCl_3$	2 failed instantly, 1 failed in ½ day.
"	7 hours at 1900F	75,000	5% HCl + Applied Current	Anode attacked.

*Note that all of these treatments are very abnormal and were intentionally selected to study cracking and the conditions required to promote cracking.

TABLE XII

The Conductivity of Dry Salt at Elevated Temperatures Measured with Nickel Electrcdes*

Time (Hrs.)	Temperature (°F)	Applied Potential (millivolts)	Titanium Absent		Titanium Present	
			Measured Current (milliamps)	Calculated Resistance (milliohms)	Measured Current (milliamps)	Calculated Resistance (milliohms)
0	1000	15,000	0.03	500,000	0.03	500,000
1	1100	15,000	0.08	187,500	0.12	125,000
2	1200	15,000	0.38	39,500	0.34	44,000
3	1300	15,000	1.8	8,350	1.7	8,825
4	1400	15,000	3.8(erratic)	3,950	4.(erratic)	3,750

*Nickel Electrodes Spaced 3/4 Inch Apart.

TABLE XIII

The Conductivity of Dry Salt at Elevated Temperatures
Measured with Titanium Electrodes

Time (Hrs.)	Temperature °F	Applied Potential (millivolts)	Measured Current (milliamps)	Calculated Resistance (milliohms)	Remarks
0	950	15,000	0.01	1,500,000	-
0.5	1000	15,000	0.02	750,000	-
1.0	1050	15,000	0.04	375,000	-
1.5	1100	15,000	0.09	166,666	-
2.0	1150	15,000	0.21	71,500	-
2.5	1200	15,000	0.43	34,900	-
3.0	1250	15,000	0.78	19,250	-
3.5	1300	15,000	1.4	10,600	-
4.0	1350	15,000	3.2	4,675	slight fluctuations
4.5	1400	15,000	4.3	3,490	increasing fluctuations
5.0	1450	15,000	14-21	-	very erratic
5.5	1500	15,000	-	-	decreased when salt contracted and pulled away from electrode

TABLE XIV

Chemical Analyses (Weight Percent) and Beta Transi of Super-Alpha Alloys and Ti-6Al-4V

Alloy	Al	Mo	V	Zr	(Cb+Ta)	C	Fe	H_2	N	O	Beta Transus °F	Alpha Transus °F
Ti-12Zr-7Al (Sheet Bar)	6.7			12.2		.025	.03	.0069	.01	.07	1820	1690
Ti-8Al-1Mo-1V (Sheet Bar)	8.0	.95	1.00			.030	.06	.0096	.02	.07	1870	1740*
Ti-8Al-8Zr-1(Cb+Ta) (5/8" Diameter)	7.8			7.8	.98	.030	.26	.0400**	.01	.08	1850	1725*
Ti-6Al-4V (0.050" t Sheet)	5.6		3.9			.030	.08	.0132	.01	.11	1775	1650*

*Temperature represents 10 percent beta.

**As forged condition. After VA 6 hours 1400F, H_2 = .0086%.

TABLE XV

Creep Stability Data on Ti-12Zr-7Al Sheet
(0.050" thick, hot rolled 1800F, annealed 1 hour 1650F)

Creep Tests				Room Temperature Tensile Properties After Creep Exposure				
Creep Temperature °F	Creep Stress ksi	Exposure Time (Hrs.)	Plastic Creep %	Ultimate Tensile Strength ksi	0.2% Offset Yield Strength ksi	Elongation % in 2"	Reduction in Area %	Break*
600	85.0	100	0.082	150.8	139.9	11.0	21.3	2
	90.0	100	0.247	158.8	146.6	5.0	11.2	GM
700	57.0	100	0.015	142.7	136.0	9.5	27.1	3
	75.0	100	0.055	148.0	139.6	12.0	30.7	4
	90.0	100	1.490	148.5	148.5	10.0	25.0	3
800	75.0	100	0.085	146.5	145.3	8.0	17.3	3
	80.0	100	0.197	150.8	146.7	8.0	15.1	OGM
900	30.0	100	0.017	143.5	140.6	12.0	25.4	4
	30.0	100	0.022	144.5	139.9	16.5	25.4	2
	38.0	100	0.030	142.4	140.0	11.0	28.9	3
	54.0	100	0.150	153.3	143.6	5.0	13.1	4
1000	30.0	100	0.210	147.6	137.8	8.0	14.8	2
	35.0	100	0.340	150.0	137.8	9.5	19.8	3
1100	12.0	100	0.195	143.3	131.9	13.0	25.4	3
	25.0	100	0.262	146.9	134.2	10.0	25.8	4
Specimen Not Creep Tested				148.1	137.4	12.5	28.8	3
				145.9	135.9	10.5	28.6	3

*Break code: 1 = center break (midway between gage marks; 2-4 = break between center and gage mark; GM = break at gage mark; OGM = break between gage mark and grips.

TABLE XVI

Creep Stability Data on Ti-12Zr-7Al Rod*
(7/8" Diameter, Hot Rolled 1950F, Annealed 1 hour 1650F)

Creep Tests				Room Temperature Tensile Properties After Creep Exposure				
Creep Temperature °F	Creep Stress ksi	Exposure Time (Hrs.)	Plastic Creep %	Ultimate Tensile Strength ksi	0.2% Offset Yield Strength ksi	Elongation % in 1"	Reduction in Area %	Break**
600	75.0	100	0.11	135.9	127.4	20.0	43.4	2
	79.0	100	0.23	133.5	127.4	18.0	42.2	2
700	73.0	100	0.12	134.9	129.1	20.0	44.3	2
	77.0	100	0.32	132.6	132.6	19.0	39.6	2
800	68.0	100	0.09	135.4	134.2	19.0	41.5	2
	72.0	100	0.19	136.8	130.0	16.0	26.7	3
900	45.0	100	0.09	140.0	131.7	12.0	25.5	2
	51.0	100						
1000	23.0	100	0.07	142.3	131.2	13.0	23.7	1
	28.0	100	0.18	139.5	129.0	15.0	29.6	1
Specimen Not Creep Tested				135.0	123.3	18.0	41.1	2
				137.6	126.2	18.0	43.5	2

*All samples were ¼" round tensiles: 1" gage length x ¼" diameter.

**See Break Code - Table XV.

TABLE XVII

Creep Stability Data on Ti-8Al-1Mo-1V Rod*
(7/8" Diameter, Annealed 1 hour 1800F + 8 hours 1100F)

Creep Tests				Room Temperature Tensile Properties After Creep Exposure			
Creep Temperature °F	Creep Stress ksi	Exposure Time (Hrs.)	Plastic Creep %	Ultimate Tensile Strength ksi	0.2% Offset Yield Strength ksi	Elongation % in 1"	Reduction in Area %
600	79.0	100	0.07	138.3	128.6	17.0	31.4
	82.0	100	0.25	138.7	130.2	17.0	33.5
	88.0	100	0.92	138.7	132.2	20.0	35.9
700	64.0	100	0.07	136.6	126.0	17.0	35.6
	73.0	100	0.12	139.0	129.3	17.0	35.4
800	52.0	100	0.15	138.8	126.9	18.0	32.8
	58.0	100	0.20	140.4	128.9	17.0	35.0
900	23.0	100	0.13	138.2	127.9	19.0	32.5
	35.0	100	0.21	140.4	130.7	18.0	32.4
	45.0	100	0.59	166.9	155.9	13.0	33.7
	56.0	100	1.65	162.8	149.6	14.0	35.5
1000	10.0	100	0.12	140.4	131.7	18.0	32.1
	15.0	100	0.25	138.3	133.5	20.0	29.6
Specimen Not Creep Tested				140.3	131.9	18.0	37.3
				140.9	133.3	18.0	41.5

*All samples were ¼" round tensiles: 1" gage length x ¼" diameter.

TABLE XVIII

Creep and Creep Stability Data on Ti-8Al-8Zr-1(Cb+Ta) Rod*
(7/8" Diameter, Forged at 1925F, Vacuum Annealed 6 Hours at 1400F, Furnace Cooled plus 1 hour 1650F, air cooled)

Creep Tests				Room Temperature Tensile Properties After Creep Exposure			
Creep Temperature °F	Creep Stress ksi	Exposure Time (Hrs.)	Plastic Creep %	Ultimate Tensile Strength ksi	0.2% Offset Yield Strength ksi	Elongation % in 1"	Reduction in Area %
800	75.0	100	0.12	137.1	137.1	2.0	5.6
900	50.0	100	0.00	133.5	125.0	3.0	6.0
Specimen Not Creep Tested				130.8	117.8	12.0	19.1
				134.9	120.5	18.0	29.5

*All tensiles were ¼" round tensiles: 1" gage length x ¼" diameter.

TABLE XIX

Creep Stability Data on Ti-6Al-4V Sheet
(0.050" Thick - Mill Annealed)

Creep Tests				Room Temperature Tensile Properties After Creep Exposure				
Creep Temperature °F	Creep Stress ksi	Exposure Time (Hrs.)	Plastic Creep %	Ultimate Tensile Strength ksi	0.2% Offset Yield Strength ksi	Elongation % in 0.6"	Reduction in Area %	Break*
600	0.0	100	0.0	143.9	121.6	15.0	34.6	3
	75.0	100	0.13	144.4	121.7	15.0	33.8	3
700	0.0	100	0.0	145.2	123.4	15.8	35.6	3
	67.0	100	0.14	148.0	122.1	13.2	32.0	2
800	0.0	100	0.0	146.9	127.3	16.7	34.0	3
	39.0	100	0.28	148.1	122.5	18.3	35.9	3
900	0.0	100	0.0	146.9	123.0	13.4	30.2	4
	24.0	100	0.24	147.4	123.9	18.3	27.6	3
1000	0.0	100	0.0	148.5	130.4	16.7	30.7	3
	7.0	100	0.41	146.7	125.9	15.0	30.4	3
Specimen Not Creep Tested				141.3	120.2	18.3	41.0	3
				140.4	118.6	14.5	42.1	3

*See Break Code - Table XV.

TABLE XX

Salt Creep Corrosion Behavior of Ti-12Zr-7Al Rod
(7/8" Diameter, Hot Rolled at 1950F, Anneal 1 hour at 1650F)

100 Hour Creep Tests					Room Temperature Tensile Properties After Creep Exposure				
Creep Temperature °F	Creep Stress ksi	Coating	Target Plastic Creep %	Measured Plastic Creep %	Ultimate Tensile Strength ksi	0.2% Offset Yield Strength ksi	Elongation % in 1"	Reduction in Area %	Salt* Attack in Break
600	0.0	Salt	0.0	-	135.0	124.7	18.0	41.7	VL
			0.0	-	135.6	124.8	18.0	42.2	VL
		None	0.0	-	135.1	123.5	17.0	42.4	
			0.0	-	134.8	122.5	17.0	41.9	
	75.0	Salt	0.1	.07	130.9	124.7	9.0	15.4	L
			0.1	.43	129.1	122.4	6.0	5.5	L
		None	0.1	.11	135.9	127.4	20.0	43.4	
			0.1	.09	135.8	127.7	19.0	46.6	
	79.0	Salt	0.2	.20	128.2	127.8	4.0	11.7	L
			0.2	.74	132.2	123.3	9.0	13.1	L
		None	0.2	.23	133.5	127.4	18.0	42.2	
			0.2	.24	134.6	127.2	14.0	29.5	
700	0.0	Salt	0.0	-	135.4	123.7	20.0	37.3	VL
			0.0	-	130.9	116.1	16.0	29.2	VL
		None	0.0	-	132.0	120.1	22.0	37.5	
			0.0	-	133.5	122.4	19.0	34.3	
	73.0	Salt	0.1	.10	129.4	122.9	3.0	7.1	L
			0.1	.15	115.5	111.5	2.0	2.9	M
		None	0.1	.12	134.9	129.1	20.0	44.3	
			0.1	.11	133.5	129.1	17.0	38.0	
	77.0	Salt	0.2	.32	118.6	113.9	2.0	4.7	M
			0.2	.18	121.9	118.7	3.0	3.6	M
		None	0.2	.15	133.4	127.1	20.0	44.4	
			0.2	.32	132.6	132.6	19.0	39.6	

TABLE XX
(Continued)

100 Hour Creep Tests					Room Temperature Tensile Properties After Creep Exposure				
Creep Temperature °F	Creep Stress ksi	Coating	Target Plastic Creep %	Measured Plastic Creep %	Ultimate Tensile Strength ksi	0.2% Offset Yield Strength ksi	Elongation % in 1"	Reduction in Area %	Salt* Attack in Break
800	0.0	Salt	0.0	-	131.6	127.9	12.0	20.4	VL
			0.0	-	134.0	125.4	19.0	45.8	VL
		None	0.0	-	139.3	135.6	19.0	40.1	
			0.0	-	138.4	132.3	19.0	39.8	
	68.0	Salt	0.1	Broke 35h					
			0.1	.77	75.7	75.7	0.0	0.0	H
		None	0.1	.09	135.4	134.2	19.0	41.5	
			0.1	.07	132.5	130.6	20.0	45.5	
	72.0	Salt	0.2	Broke 22h					
			0.2	.35	108.6	108.3	0.0	0.0	M
		None	0.2	.22	133.8	133.8	19.0	44.1	
			0.2	.19	136.8	130.0	16.0	26.7	
900	0.0	Salt	0.0	-	136.1	132.3	2.0	5.6	VL
			0.0	-	137.9	134.5	7.0	13.1	VL
		None	0.0	-	141.9	132.6	12.0	26.9	
			0.0	-	142.9	135.5	13.0	27.5	
	45.0	Salt	0.1	Broke 15h					
			0.1	Broke 16h					
		None	0.1	.09	140.0	131.7	12.0	25.5	
			0.1	.08	137.7	129.8	18.0	31.4	
	51.0	Salt	0.2	Broke 43h					
			0.2	Broke 15h					
		None	0.2	.15	137.8	127.6	7.0	15.4	
1000	0.0	Salt	0.0	0.0	140.4	132.2	4.0	6.0	VL
			0.0	0.0	141.0	130.3	10.0	13.1	VL
		None	0.0	0.0	140.1	130.3	12.0	21.8	
			0.0	0.0	142.6	132.2	12.0	16.8	

TABLE XX
(Continued)

100 Hour Creep Tests					Room Temperature Tensile Properties After Creep Exposure				
Creep Temperature °F	Creep Stress ksi	Coating	Target Plastic Creep %	Measured Plastic Creep %	Ultimate Tensile Strength ksi	0.2% Plastic Yield Strength ksi	Elongation % in 1"	Reduction in Area %	Salt* Attack in Break
1000	23.0	Salt	0.1	Broke 8h					
			0.1	Broke 14h					
		None	0.1	.07	142.3	131.2	13.0	23.7	
			0.1	.12	142.6	130.5	8.0	12.3	
	28.0	Salt	0.2	Broke 62h					
			0.2	Broke 26h					
			0.2	.18	139.5	129.0	15.0	29.6	

*Salt Penetration Code:

VL = Very low <.005"
L = Low (1/64")
M = Medium (1/32")
H = High (1/16" +)

TABLE XXI

Salt-Creep Corrosion Behavior of Ti-12Zr-7Al Sheet
(0.050" Thick, Hot Rolled 1800F, Anneal 1 Hour 1650F)

100 Hour Creep Tests					Room Temperature Tensile Properties After Creep Exposure				
Creep Temperature °F	Creep Stress ksi	Coating	Target Plastic Creep %	Measured Plastic Creep %	Ultimate Tensile Strength ksi	0.2% Offset Yield Strength ksi	Elongation % in 0.6"	Reduction in Area %	Salt Attack in Break
600	0.0	Salt	0.0	-	154.5	135.9	20.8	28.6	VL
		None	0.0	-	152.8	138.3	20.8	31.2	
	86.0	Salt	0.1	.38	145.5	140.2	5.5	9.5	L
		None	0.1	.08	150.8	139.9	17.5	21.3	
	88.0	Salt	0.2	.58	139.3	137.0	5.4	9.6	L
		None	0.2	.25	158.8	146.6	8.1	11.2	
700	0.0	Salt	0.0	-	148.3	135.2	28.0	29.0	VL
		None	0.0	-	148.8	140.5	28.3	27.3	
	80.0	Salt	0.1	.17	118.4	118.4	2.0	6.8	L
		None	0.1	.12	134.1	133.6	19.0	43.7	
	86.0	Salt	0.2	.45	136.6	134.5	3.0	1.4	L
		None	0.2	.20	148.6	143.6	20.8	30.1	
800	0.0	Salt	0.0	-	139.2	136.3	18.8	32.9	VL
		None	0.0	-	146.8	142.2	15.8	32.9	
	76.0	Salt	0.1	Broke 18h					
		None	0.1	.09	146.5	145.3	12.8	17.3	
	80.0	Salt	0.2	Broke 22h					
		None	0.2	.20	150.8	146.7	12.8	15.1	
900	0.0	Salt	0.0	-	148.6	142.8	11.3	19.2	VL
		None	0.0	-	142.4	132.9	23.4	28.4	
	50.0	Salt	0.1	Broke 19h					
		None	0.1						
	56.0	Salt	0.2	Broke 8h					
		None	0.2	.15	153.3	143.6	8.2	13.1	

TABLE XXI
(Continued)

100 Hour Creep Tests					Room Temperature Tensile Properties After Creep Exposure				
Creep Temperature °F	Creep Stress ksi	Coating	Target Plastic Creep %	Measured Plastic Creep %	Ultimate Tensile Strength ksi	0.2% Offset Yield Strength ksi	Elongation % in 0.6"	Reduction in Area %	Salt* Attack in Break
1000	0.0	Salt	0.0	0.0	145.2	132.7	5.0	14.7	VL
		None	0.0	0.0	150.0	136.7	15.0	22.1	
	23.0	Salt	0.1	Broke 48h					
		None	0.1	.20	147.2	136.1	3.3	6.5	
	28.0	Salt	0.2	Broke 2h					
		None	0.2	.21	147.6	137.8	8.0	14.8	

*Code - See Table XX.

TABLE XXII

Salt Creep Corrosion Behavior of Ti-8Al-1Mo-1V Rod
(7/8" Diameter, Hot Rolled 1950F, Anneal 1 hour 1800F + 8 hours 1100F)

100 Hour Creep Tests					Room Temperature Tensile Properties After Creep Exposure				
Creep Temperature °F	Creep Stress ksi	Coating	Target Plastic Creep %	Measured Plastic Creep %	Ultimate Tensile Strength ksi	0.2% Offset Yield Strength ksi	Elongation % in 1"	Reduction in Area %	Salt* Attack in Break
600	0.0	Salt	0.0	-	143.1	133.1	18.0	41.4	VL
			0.0	-	141.2	132.5	19.0	43.3	VL
		None	0.0	-	141.1	131.5	18.0	41.3	
			0.0	-	141.6	131.7	19.0	40.1	
	80.0	Salt	0.1	.04	135.9	128.3	6.0	12.2	VL
		None	0.1	.07	138.3	128.6	17.0	31.4	
			0.1	.06	139.1	130.2	19.0	42.9	
	82.0	Salt	0.2	.15	130.3	123.8	11.0	24.0	VL-L
		None	0.2	.25	138.7	130.2	17.0	33.5	
			0.2	.17	142.8	131.6	20.0	39.8	
700	0.0	Salt	0.0	-	135.5	117.4	10.0	20.6	VL
			0.0	-	135.2	118.1	10.0	15.4	VL
		None	0.0	-	130.4	114.5	9.0	17.4	
			0.0	-	134.6	116.2	9.0	16.6	
	70.0	Salt	0.1	.05	133.1	126.8	3.0	7.0	L
			0.1	.13	129.8	120.8	2.0	3.3	M
		None	0.1	.09	139.7	131.4	20.0	42.7	
			0.1	.12	139.0	129.3	17.0	35.4	
	77.0	Salt	0.2	.22	136.0	129.1	6.0	12.1	L
			0.2	.39	134.1	124.8	5.0	6.4	L
		None	0.2	.20	142.4	132.8	20.0	40.7	
			0.2	.23	135.4	124.3	18.0	32.2	

TABLE XXII
(Continued)

100 Hour Creep Tests					Room Temperature Tensile Properties After Creep Exposure				
Creep Temperature °F	Creep Stress ksi	Coating	Target Plastic Creep %	Measured Plastic Creep %	Ultimate Tensile Strength ksi	0.2% Offset Yield Strength ksi	Elongation % in 1"	Reduction in Area %	Salt* Attack in Break
800	0.0	Salt	0.0	-	139.6	131.0	17.0	30.0	VL
			0.0	-	138.7	128.6	18.0	29.0	VL
		None	0.0	-	141.3	132.3	18.0	43.8	
			0.0	-	142.1	132.3	18.0	38.8	
	43.0	Salt	0.1	.26	120.8	111.4	2.0	4.5	M
			0.1	.19	129.4	120.1	2.0	3.3	M
		None	0.1	.15	138.8	126.9	18.0	32.8	
			0.1	.14	133.3	120.9	18.0	40.6	
	58.0	Salt	0.2	.38	102.7	102.7	1.0	3.3	H
			0.2	.61	92.4	92.4	1.0	1.6	H
		None	0.2	.20	140.4	128.9	17.0	35.0	
			0.2	.16	134.3	124.3	18.0	41.8	
900	0.0	Salt	0.0	-	138.0	128.4	18.0	30.2	VL
			0.0	-	138.6	129.1	14.0	19.1	VL
		None	0.0	-	141.9	133.3	18.0	42.7	
			0.0	-	142.7	134.5	18.0	43.1	
	18.0	Salt	0.1	.11	122.7	105.9	12.0	15.9	VL
			0.1	.20	88.5	87.2	3.0	2.5	M
		None	0.1	.13	138.2	127.9	19.0	32.5	
			0.1	.15	137.7	132.7	18.0	38.7	
	34.0	Salt	0.2	.20	103.8	-	0.5	3.9	M
			0.2	.20	107.4	-	0.5	1.2	M
		None	0.2	.21	140.4	130.7	18.0	32.4	
			0.2	.25	139.0	127.1	18.0	29.6	

TABLE XXII
(Continued)

100 Hour Creep Tests					Room Temperature Tensile Properties After Creep Exposure				
Creep Temperature °F	Creep Stress ksi	Coating	Target Plastic Creep %	Measured Plastic Creep %	Ultimate Tensile Strength ksi	0.2% Offset Yield Strength ksi	Elongation % in 1"	Reduction in Area %	Salt* Attack in Break
1000	0.0	Salt	0.0	0.0	136.7	127.2	16.0	21.5	VL
			0.0	0.0	136.8	127.3	12.0	16.6	VL
		None	0.0	0.0	137.7	128.0	18.0	33.1	
			0.0	0.0	138.2	128.2	16.0	27.3	
	9.0	Salt	0.1	0.17	139.5	131.3	12.0	18.5	VL
			0.1	0.26	140.2	132.7	19.0	35.0	VL
		None	0.1	0.12	140.4	131.7	18.0	32.1	
	15.0	Salt	0.2	0.29	141.7	134.0	18.0	33.5	VL
			0.2	0.37	137.3	130.4	10.0	16.9	VL
		None	0.2	0.25	138.3	133.5	20.0	29.6	
			0.2	0.20	143.1	135.6	20.0	39.0	

*Code - See Table XX.

TABLE XXIII

Salt-Creep Corrosion Behavior of Ti-6Al-4V Sheet
(0.050" thick - Mill Annealed)

100 Hour Creep Tests					Room Temperature Tensile Properties After Creep Exposure				
Creep Temperature °F	Creep Stress ksi	Coating	Target Plastic Creep %	Measured Plastic Creep %	Ultimate Tensile Strength ksi	0.2% Offset Yield Strength ksi	Elongation % in 0.6"	Reduction in Area %	Salt* Attack in Break
600	0.0	Salt	0.0	0.0	145.2	122.6	13.3	34.8	VL
		None	0.0	0.0	143.9	121.6	15.0	34.6	
	75.0	Salt	0.2	0.13	146.1	120.6	15.0	28.6	VL
		None	0.2	0.13	144.4	121.7	15.0	33.8	
700	0.0	Salt	0.0	0.0	143.8	123.9	13.3	35.8	VL
		None	0.0	0.0	145.2	123.4	15.8	35.6	
	67.0	Salt	0.2	0.23	148.5	124.5	8.2	19.5	VL
		None	0.2	0.14	148.0	122.1	13.2	32.0	
800	0.0	Salt	0.0	0.0	149.1	128.4	14.1	36.4	VL
		None	0.0	0.0	146.9	127.3	16.7	34.0	
	39.0	Salt	0.2	0.30	147.5	123.0	13.4	28.0	VL
		None	0.2	0.28	148.1	123.9	15.8	34.4	
900	0.0	Salt	0.0	0.0	143.1	124.2	15.0	48.1	VL
		None	0.0	0.0	147.9	124.7	15.0	37.5	
	25.0	Salt	0.2	0.35	145.5	125.9	15.0	32.9	VL
		None	0.2	0.28	145.5	123.7	16.7	30.8	
1000	0.0	Salt	0.0	0.0	143.4	125.4	12.5	20.0	VL
		None	0.0	0.0	148.5	130.4	16.7	30.7	
	4.4	None	0.2	0.21	145.6	125.7	15.0	33.3	
	7.0	Salt	-	0.45	142.5	122.0	9.2	24.7	VL
		None	-	0.41	146.7	125.9	15.0	30.4	
Specimens Not Creep Tested					141.3	120.2	18.3	41.0	
					140.4	118.6	14.5	42.1	

*Code - See Table XX.

TABLE XXIV

Threshold Temperature and Stress for Salt-Creep Corrosion of Ti-12Zr-7Al and Ti-8Al-1Mo-1V

	Salt-Creep Exposure at 600F				Room Temperature Tensile Properties After Creep Exposure				
Alloy	Tensile* Form	Creep Stress ksi	Time hrs.	Measured Plastic Creep %	Ultimate Tensile Strength ksi	0.2% Offset Yield Strength ksi	Elongation %	Reduction in Area %	Salt** Attack in Break
Ti-8-1-1	Round	30	300	0.02	141.5	130.6	17.0	24.4	VL
HR 1950F		30	300	0.01	142.2	132.4	16.0	34.9	VL
Ann 1 Hr		20	500	0.00	140.5	130.6	12.0	19.7	L
1800F+8 Hr 1100F		20	500	0.00	139.0	129.1	17.0	30.8	L
Ti-12-7	Round	30	300	0.00	130.3	111.6	16.0	35.4	VL
HR 1950F		30	300	0.00	125.3	115.5	4.0	7.9	L
Ann 1 Hr		20	500	0.00	136.2	124.0	9.0	13.3	L
1650F		20	500	0.00	134.6	122.5	7.0	16.8	L
Ti-12-7	Sheet	30	300	0.00	148.6	136.1	10.0	23.6	VL
HR 1800F		30	300	0.00	152.4	137.2	11.7	28.2	VL
Ann 1 Hr		20	500	0.00	151.2	136.1	6.7	12.3	L
1650F		20	500	0.00	150.9	136.5	15.0	23.5	VL

*Round rod 7/8" diameter; tensiles ¼" diameter x 1" G.L.
Sheet 0.050" thick, tensiles 0.150" width x 0.6" G.L.

**Codes - See Table XX.

TABLE XXV

Effect of Metal Purity and Thermal History on the Salt Creep Performance of Ti-12Zr-7Al Sheet (0.050" Thick)

Material	Rolling Temp. °F	Anneal Cycle (in Argon)	Creep Exposure 100 hours, 70 ksi, 700F Coating	Creep %	Room Temperature Tensile Properties After Creep Exposure: Ultimate Tensile Strength ksi	0.2% Offset Yield Strength ksi	Elongation % in 0.6"	Reduction in Area %	Salt* Attack in Break
Super Purity	1500	½ hour 1400F	Salt	0.11	111.7	102.3	6.7	14.1	VL
			None	0.05	131.3	119.1	13.3	23.4	
	1600	2 hour 1600F	Salt	0.11	107.1	101.4	1.4	10.2	VL-L
			None	0.00	119.0	114.9	15.0	37.3	
Commercial Purity	1500	2 hour 1500F	Salt	0.09	113.9	108.1	8.3	16.7	VL
			None	0.03	120.2	119.4	20.0	46.4	
	1800	100 hour 1600F	Salt	Broke 37h					
			Salt	0.32	110.8	109.8	5.0	11.1	L
			None	0.13	124.2	121.6	16.7	26.1	
	1800	8 hour 1800F	Salt	0.08	106.7	106.3	1.7	4.3	L-M
			Salt	Broke 87h					
			None	0.15	132.7	119.0	16.7	22.5	
	1800	8 hour 1875F	Salt	0.36	93.6	93.6	0.0	7.1	L-M
			Salt	Broke 98h					
			None	0.08	134.8	120.3	16.7	23.8	

*Code - See Table XX.

TABLE XXVI

Salt Creep Corrosion Behavior of Ti-12Zr-7Al and Ti-8Al-1Mo-1V Welded Sheet
(0.050" Thick, Hot Rolled 1800F, Anneal 1 Hour 1650F)

100-Hour Creep Tests at 700F					Room Temperature Tensile Properties After Creep Exposure				
Alloy	Creep* Stress ksi	Weld Direction	Coating	Measured Plastic Creep %	Ultimate Tensile Strength ksi	0.2% Offset Yield Strength ksi	Elongation % in 0.6"	Reduction in Area %	Salt** Attack in Break
Ti-12Zr-7Al (HR 1650F, Ann 2 hours 1500F)	0	Long	Salt	0.0	134.8	118.8	6.7+	33.8	VL
			Salt	0.0	103.6	103.6	3.3	14.5	VL
			None	0.0	132.7	110.3	13.3	38.0	
			None	0.0	131.8	114.3	11.7	39.2	
	0	Trans	Salt	0.0	128.3	113.6	13.3	31.9	VL
			Salt	0.0	141.9	124.8	10.0	32.4	VL
			None	0.0	142.0	129.8	11.7+	29.0	
			None	0.0	139.9	127.8	6.7+	31.9	
	78	Long	Salt	Broke 66h					
			Salt	Broke 57h					
			None	0.23					
			None	0.25					
	78	Trans	Salt	Broke 65h					
			Salt	Broke 65h					
			None	0.20	137.6	129.1	11.7	29.6	
			None	0.27	129.7	125.1	10.0	32.9	
Ti-8Al-1Mo-1V (HR 1650F, Ann 1 hour 1600F+8 hour 1100F)	0	Long	Salt	0.0	148.1	125.8	10.0	28.8	VL
			Salt	0.0	150.6	124.6	10.0	29.1	VL
			None	0.0	146.5	126.0	6.7+	24.7	
			None	0.0	148.4	126.6	10.0	26.8	

TABLE XXVI
(Continued)

100-Hour Creep Tests at 700F					Room Temperature Tensile Properties After Creep Exposure				
Alloy	Creep* Stress ksi	Weld Direction	Coating	Measured Plastic Creep %	Ultimate Tensile Strength ksi	0.2% Offset Yield Strength ksi	Elongation % in 0.6"	Reduction in Area %	Salt** Attack in Break
Ti-8Al-1Mo-1V (HR 1650F, Ann 1 hour 1600F+8 hour 1100F)	0	Trans	Salt	0.0	138.5	126.0	10.0	28.9	VL
			Salt	0.0	143.0	125.6	6.7	25.3	VL
			None	0.0	141.3	119.0	10.0	29.3	
			None	0.0	139.7	120.9	6.7	31.6	
	76	Long	Salt	Broke 94h					
			Salt	0.35	114.3	114.3	3.3	3.7	L
			None	0.28	152.4	132.0	3.0+	25.6	
			None	0.21	147.7	130.0	10.0	30.4	
	76	Trans	Salt	0.29	107.1	107.1	1.7	3.9	L
			Salt	0.33	112.0	112.0	3.3	6.7	L
			None	0.16	140.4	128.5	8.3	36.8	
			None	0.24	144.5	150.9	3.3+	25.6	

* Creep stresses were chosen to give 0 and 0.2% plastic creep.
** Code - See Table XX.
\+ Gage mark break.

NOTE: Welds were ground flush with base metal before thermal exposure.

TABLE XXVII

Effectiveness of Surface Preparations for Elevated Temperature Salt Protection of Ti-12Zr-7Al Sheet
(Sheet Hot Rolled 1800F, anneal 1 Hour 1650F)

	100-Hour Salt-Creep Exposure at 900F			Room Temperature Tensile Properties After Creep Exposure				
Surface Preparation	Creep Stress ksi	Target Plastic Creep %	Measured Plastic Creep %	Ultimate Tensile Strength ksi	0.2% Offset Yield Strength ksi	Elongation % in 0.6"	Reduction in Area %	Salt* Attack in Break
(a) Phos. Acid Conversion Coat(111)	15	0.01	Broke 15h					
	30	0.02	Broke 12h					
(b) All Sulfate Ni Plate (112)	50	0.10	0.18	137.3	132.3	3.5	8.2	L
	50	0.10	0.15	150.1	140.0	13.3	19.0	VL
(c) Low pH Watt's Ni Plate (113)	50	0.10	0.17	109.7	-	2.0	-	M
	50	0.10	0.10	117.5	-	2.0	-	L
(d) Fluoborate Ni Plate (114)	50	0.10	0.11	145.8	135.9	18.2	23.1	VL
(e) Ni-Co Plate(115)	50	0.10	0.10	147.6	140.7	6.6	13.5	L
	50	0.10	0.15	133.1	132.4	2.0	5.9	L
(f) Sulfamate Ni Plate + Anneal 15 Minutes 1400F(116)	50	0.10	0.02	149.6	142.4	23.5	27.8	VL
	50	0.10	0.06	150.3	139.0	28.2	23.3	VL
	50	0.10	0.09	89.5	89.5	0.0	0.0	M
(g) Sulfamate Ni Plate with Buffing	50	0.10	0.23	145.6	131.8	17.3	18.5	VL
	50	0.10	0.23	118.7	-	2.0	2.6	M
(h) Black Chrome Plate (117)	50	0.10	Broke 2h	Cr plate showed poor ductility.				

TABLE XXVII
(Continued)

Surface Preparation	100-Hour Salt-Creep Exposure at 900F: Creep Stress ksi	Target Plastic Creep %	Measured Plastic Creep %	Room Temperature Tensile Properties After Creep Exposure: Ultimate Tensile Strength ksi	0.2% Offset Yield Strength ksi	Elongation % in 0.6"	Reduction in Area %	Salt* Attack in Break
(i) Silver CN Plate (118)	50	0.10	Broke 5h	Ag plate blistered after 900F exposures.				
(j) Cobalt Plate(118)	50	0.10	0.26	135.5	-	2.0	-	L
	50	0.10	0.20	127.7	-	2.0	-	M

Notes: (a) Surface preparations are described in detail in the numbered references.
(b) All test samples were microtensile flats: 0.6" gage length x 0.150" width x 0.050" thickness.
(c) All test samples were painted with 1/16" thick salt layer prior to creep exposure.
(d) * Coie - See Table XX.

TABLE XXVIII

Effectiveness of Nickel Plating for Elevated-Temperature Salt Protection of Ti-8Al-1Mo-1V 7/8" Diameter Rod
(¼" Diameter x 1" G.L. Tensiles)

300-Hour Salt Creep Exposure			Room Temperature Tensile Properties After Creep Exposure				
Creep Temperature °F	Creep Stress ksi	Measured Plastic Creep %	Ultimate Tensile Strength ksi	0.2% Offset Yield Strength ksi	Elongation % in 1"	Reduction in Area %	Salt** Attack in Break
700	75	0.13	136.0	132.3	19.0	41.8	VL
		0.10	141.3	134.4	15.0	21.5	VL
800	40	0.13	137.0	130.3	17.0	40.1	VL
		0.23	137.4	132.4	17.0	37.4	VL
900	20	0.17	131.8	131.8	19.0	40.5	VL
		0.31	131.4	127.6	19.0	38.8	VL
1000	8	0.71	141.5	137.5	17.0	37.1	VL
		0.33	140.0	138.4	16.0	21.8	VL
1100	3	0.71	140.7	136.5	8.0	11.0	L
		0.70	141.7	139.5	4.0	8.6	L
		0.57*	141.0	135.8	15.0	35.0	

* Control sample creep tested without nickel plate and without salt coating.
**Code - See Table XX.

TABLE XXIX

Effectiveness of Aluminum Coating for Elevated Temperature Salt Protection of Ti-12Zr-7Al Sheet

(Sheet 0.050" Thick, Hot Rolled 1800F, Annealed 1 Hour 1600F)

Salt-Creep Exposure					Room Temperature Tensile Properties After Creep Exposure				
Aluminum Coating Method	Creep Temperature °F	Creep Stress ksi	Creep Time Hours	Measured Plastic Creep %	Ultimate Tensile Strength ksi	0.2% Offset Yield Strength ksi	Elongation % in 0.6"	Reduction in Area %	Salt* Attack in Break
Al Paint (General Purpose)	900	50	Broke 13h						
		56	Broke 13h						
Al Paint (High Temperature)	900	50	Broke 3h						
		50	Broke 4h						
Molten Al Dip	700	75	300	0.09	133.4	131.0	3.3	11.6	L**
	800	40	300	0.15	62.6	62.6	0.0	1.3	M**
	900	50	Broke 70h**						
	1000	8	Broke 116h**						
Al Flame Spray	700	75	300	0.22	136.6	131.9	3.3	14.7	L
	800	40	Broke 200h						
	900	20	300	0.08	132.7	132.7	0.0	11.5	L
	1000	8	300	0.04	146.4	130.7	6.7	21.8	VL
	1100	3	300	0.07	138.4	130.2	13.3	9.6	VL

* Code - See Table XX.
** Salt attack occurred at sample corners where aluminum coating was thin.

TABLE XXX

Salt-Creep Behavior of Shot Peened Ti-12Zr-7Al Rod and Sheet

Material	Condition	Shot Size	Almen No. To Peening Saturation (A2 Strip)	Plastic* Creep %	Room Temperature Tensile Properties After Creep Exposure				Salt** Attack in Break
					Ultimate Tensile Strength ksi	0.2% Offset Yield Strength ksi	Elongation %	Reduction in Area %	
7/8" Diameter Rod (0.25" D x 1" G.L.)	HR 1950F Ann 1 Hr 1650F	S-110	.006-.008	0.18	135.4	123.9	18.0	39.7	L
		S-170	.010-.012	0.13	113.0	108.3	3.0	7.1	M
		S-230	.010-.012	0.33	114.9	114.9	3.0	3.3	M
		None		0.34	117.5	112.2	3.0	3.6	M
	HR 1760F Ann 1 Hr 1650F	S-170	.010-.012	0.04	133.7	124.9	19.0	36.8	VL
		S-230	.010-.012	0.06	131.5	123.2	5.0	8.7	VL
		None		0.06	130.0	123.2	2.0	4.8	L
0.050" Thick Sheet (0.150" width x 0.6" G.L.)	HR 1800F Ann 1 Hr 1600F	S-70	.003-.004	0.09	115.8	115.8	0.0	4.1	L
		S-170	.006-.008	0.21	117.6	117.6	1.7	5.4	VL
		S-230	.006-.008	Broke 81h					
		None		0.12	126.7	125.0	1.7	4.1	L
	HR 1500F Ann 2 Hr 1500F	S-170	.006-.008	Broke 74h					
		S-230	.006-.008	0.00	120.0	112.8	19.0	47.5	VL
		None		0.03	113.9	108.1	8.3	16.7	VL

* Plastic creep after salt-creep exposure of 100 hours at 700F with 70 ksi tensile stress.
**Code - See Table XX.

TABLE XXXI

Effect of Surface Treatment and Salt Exposure on the Fatigue Properties of Ti-12Zr-7Al and Ti-8Al-1Mo-1V Bar

Surface Preparation	Ti-12Zr-7Al		Ti-8Al-1Mo-1V	
	Fatigue* Stress ksi Maximum	Cycles at 10,000 rpm	Fatigue* Stress ksi Maximum	Cycles at 10,000 rpm
Polished	55	10^7 (Endurance Limit)	90	10^7 (Endurance Limit)
Polished + 100 hr at 1000F w salt	55	1.7×10^5	90	2.8×10^4
Polished + 100 hr at 1000F w salt	45	2.7×10^5	70	4.2×10^4
Al Dip (0.002" thick)	55	2.5×10^5	90	4.4×10^4
Al Dip + 100 hr at 1000F w salt	55	1.4×10^5	90	4.2×10^4
Al Flame Spray (0.004" thick)	55	4.1×10^5	90	8.5×10^4
Al Flame Spray + 100 hr at 1000F w salt	55	1.5×10^5	90	2.6×10^4
Ni Plate (0.002" thick)	55	1.9×10^5	90	4.2×10^4
Ni Plate + 100 hr at 1000F w salt	55	1.7×10^5	90	2.8×10^4
Ni Plate + 100 hr at 1000F w salt	45	1.7×10^6	70	7.0×10^4

Note: (a) Ti-12Zr-7Al bar hot rolled at 1700F, annealed 2 hours at 1500F.
(b) Ti-8Al-1Mo-1V bar hot rolled at 1700F, annealed 1 hour at 1600F + 8 hours at 1100F.

*R. R. Moore-Type Rotating-Beam Fatigue-Testing Machine; neck diameter of specimen = 0.250".

TABLE XXXII

Salt Corrosion of Alloys of Variable Composition Based on the Elements Present in the Super-Alpha Alloys

	Weight Gain (g/square inch) at 1200F				
	Air Flow (525 ml/minute)				Stagnant Furnace Atmosphere
Alloy	2 hours	4 hours	6 hours	24 hours	24 hours
Ti-12Zr-7Al	0.0078	0.0106	0.0113	0.0196	0.0220
Ti-12Zr-7Al*	0.0046	0.0069	0.0092	0.0208	0.0284
Ti-10Zr-7Al	0.0076	0.0093	0.0109	0.0177	0.0342
Ti-10Zr-7.5Al	0.0035	0.0079	0.0097	0.0298	0.0251
Ti-15Zr-3Al	0.0038	0.0058	0.0058	0.0144	0.0310
Ti-30Zr-6Al**	0.0157	0.0494	0.0712	0.1140	0.2998
Ti-8Al-1Mo-1V	0.0053	0.0090	0.0100	0.0253	0.0233
Ti-8Al-1Mo-1V*	0.0057	0.0128	0.0175	0.0795	0.0720
Ti-8Al-1.5Mo-0.5V	0.0012	0.0024	0.0047	0.0117	0.0394
Ti-8Zr-8Al-0.75Cb-0.25Ta	0.0085	0.0116	0.0140	0.0241	0.1445

*Heats to which minor alloy additions were made.
**Sample completely deteriorated.

TABLE XXXIII

Effect of Minor Alloy Additions Upon the General Salt Corrosion of Ti-12Zr-7Al

		Weight Gain (g/square inch) at 1200F				
		Air Flow (525 ml/minute)				Stagnant Furnace Atmosphere
Addition	Percent	2 hours	4 hours	6 hours	24 hours	24 hours
None		0.0046	0.0069	0.0092	0.0208	0.0284
Antimony	1.0	0.0041	0.0052	0.0063	0.0147	0.0511
Chromium	1.0	0.0043	0.0078	0.0104	0.0198	0.0540
Columbium	1.0	0.0071	0.0108	0.0133	0.0241	0.0272
Copper	1.0	0.0080	0.0120	0.0160	0.0433	0.0357
Gadolinium	0.1	0.0037	0.0037	0.0044	0.0102	0.0362
Indium	1.0	0.0064	0.0091	0.0109	0.0191	0.0298
Iron	1.0	0.0082	0.0119	0.0149	0.0276	0.0290
Manganese	1.0	0.0078	0.0110	0.0123	0.0168	0.0296
Molybdenum	1.0	0.0065	0.0129	0.0190	0.0653	0.0495
Nickel	1.0	0.0142	0.0178	0.0214	0.0374	0.0386
Oxygen	0.2	0.0051	0.0092	0.0112	0.0214	0.0585
Palladium	0.2	0.0052	0.0062	0.0073	0.0300	0.0117
Silicon	0.1	0.0051	0.0082	0.0103	0.0164	0.0322
Silver	1.0	0.0045	0.0099	0.0114	0.0220	0.0890
Tantalum	1.0	0.0055	0.0094	0.0102	0.0253	0.0553
Thorium	0.5	0.0073	0.0089	0.0113	0.0234	0.0730
Tin	1.0	0.0055	0.0086	0.0129	0.0270	0.0410
Vanadium	1.0	0.0072	0.0109	0.0135	0.0198	0.0365
Yttrium	0.1	0.0044	0.0055	0.0066	0.0132	0.0178
Yttrium	0.1	0.0013	0.0020	0.0027	0.0225	0.0171

TABLE XXXIV

Effect of Minor Alloy Additions Upon the General Salt Corrosion of Ti-8Al-1Mo-1V

		Weight Gain (g/square inch) at 1200F				
		Air Flow (525 ml/minute)				Stagnant Furnace Atmosphere
Addition	Percent	2 hours	4 hours	6 hours	24 hours	24 hours
None	-	0.0057	0.0132	0.0186	0.0795	0.0720
Antimony	1.0	0.0025	0.0063	0.0075	0.0150	0.1095
Chromium	1.0	0.0059	0.0108	0.0176	0.0960	0.1370
Columbium	1.0	0.0078	0.0137	0.0216	0.0745	0.0284
Copper	1.0	0.0045	0.0112	0.0191	0.0326	0.0980
Indium	1.0	0.0055	0.0082	0.0118	0.0282	0.1010
Iron	1.0	0.0031	0.0102	0.0163	0.0510	0.0771
Manganese	1.0	0.0150	0.0243	0.0326	0.1073	0.0240
Nickel	1.0	0.0031	0.0061	0.0069	0.0130	0.1210
Oxygen	0.2	0.0035	0.0063	0.0084	0.0197	0.0755
Palladium	0.2	0.0070	0.0181	0.0264	0.1360	0.0635
Silicon	0.1	0.0064	0.0077	0.0103	0.0334	0.0478
Silver	1.0	0.0042	0.0084	0.0126	0.0473	0.0957
Tantalum	1.0	0.0043	0.0069	0.0073	0.0128	0.0726
Thorium	0.5	0.0033	0.0041	0.0074	0.0287	0.0810
Tin	1.0	0.0023	0.0047	0.0081	0.0372	0.0779
Yttrium	0.1	0.0053	0.0071	0.0080	0.0115	0.0412
Zirconium	1.0	0.0086	0.0182	0.0231	0.0787	0.1035

TABLE XXXV

Effect of Minor Alloy Additions Upon the Salt Corrosion of Stressed Ti-12Zr-7Al Sheet

Alloy Addition	Amount %	Coating	Plastic Creep* %	Room Temperature Tensile Properties After Creep Exposure: Ultimate Tensile Strength ksi	0.2% Offset Yield Strength ksi	Elongation % in 0.6"	Reduction in Area %	Salt** Attack in Break
None	-	Salt	0.12	127.6	120.6	3.3	9.0	L
	-	None	0.03	143.0	139.9	11.7	45.6	
Antimony	1.0	Salt	0.00	150.6	143.0	5.0	12.7	VL-L
		None	0.05	160.5	135.9	10.0	24.7	
Chromium	1.0	Salt	0.00	167.9	152.9	1.7	10.3	L
		None	0.08	174.0	153.0	18.3	28.8	
Columbium	1.0	Salt	0.13	127.8	119.4	8.0	6.3	L
		None	0.04	138.1	129.0	18.3	32.5	
Copper	1.0	Salt	0.14	129.6	123.5	1.7	7.1	L
		None	0.12	153.3	142.3	18.3	38.8	
Gadolinium	0.1	Salt	0.07	155.9	150.2	0.0	6.3	L
		None	0.02	163.0	156.7	10.0	19.5	
Indium	1.0	Salt	0.16	109.5	103.8	3.3	3.8	L
		None	0.02	144.9	141.3	11.7	41.8	
Iron	1.0	Salt	Broke-67 hrs					
		Salt	0.14	152.2	144.9	1.0	6.7	L
		None	0.08	163.1	135.7	11.7	24.4	
Manganese	1.0	Salt	0.05	160.7	138.7	1.7	1.4	VL
		None	0.03	138.7	134.4	18.3	29.8	
Nickel	1.0	Salt	0.07	107.7	107.7	0.0	7.3	L
		None	0.00	160.4	147.9	8.3	13.4	
Oxygen	0.2	Salt	0.00	135.3	127.6	1.7	24.0	L
		None	0.05	154.5	146.4	18.3	32.1	

TABLE XXXV
(Continued)

Alloy Addition	Amount %	Coating	Plastic Creep* %	Room Temperature Tensile Properties After Creep Exposure: Ultimate Tensile Strength ksi	0.2% Offset Yield Strength ksi	Elongation % in 0.6"	Reduction in Area %	Salt** Attack in Break
Palladium	0.2	Salt	0.04	130.1	125.4	6.7	25.3	VL
		None	0.00	139.5	132.0	21.7	34.6	
Silicon	0.1	Salt	0.09	108.3	108.3	1.7	6.3	L
		None	0.05	148.9	143.3	11.5	36.0	
Silver	1.0	Salt	0.13	141.4	137.6	0.0	5.1	L-M
		None	0.00	156.5	152.5	16.7	45.7	
Thorium	0.5	Salt	0.13	123.9	115.2	3.3	1.4	L-M
		None	0.02	153.8	141.5	15.0	25.0	
Tin	1.0	Salt	0.13	138.9	132.1	1.7	4.0	L
		None	0.03	161.7	151.2	20.0	35.8	
Vanadium	1.0	Salt	0.06	162.3	155.5	10.0	17.3	VL
		None	0.06	162.8	154.7	20.0	31.7	
Yttrium	0.1	Salt	0.10	127.7	119.1	0.0	8.3	L-M
		None	0.30	158.1	148.3	15.0	48.2	

* Creep Conditions: 100 Hrs., 700F, 70 ksi Tensile Stress

** Code - See Table XX

TABLE XXXVI

Effect of Minor Alloy Addition Upon the Salt Corrosion of Stressed Ti-8Al-1Mo-1V Sheet

Alloy Addition	Amount %	Coating	Plastic Creep* %	Room Temperature Tensile Properties After Creep Exposure: Ultimate Tensile Strength ksi	0.2% Offset Yield Strength ksi	Elongation % in 0.6"	Reduction in Area %	Salt** Attack in Break
None	-	Salt	0.01	156.7	128.0	11.7	29.5	VL
	-	None	0.07	154.5	130.7	10.0	23.1	
Antimony	1.0	Salt	0.13	157.4	138.0	10.0	29.3	VL
		None	0.13	166.1	142.4	16.7	25.3	
Chromium	1.0	Salt	0.23	158.1	125.4	11.7	35.7	VL
		None	0.28	161.3	129.5	18.3	33.8	
Columbium	1.0	Salt	0.06	155.1	126.5	11.7	38.5	VL
		None	0.17	153.6	127.6	10.0	36.8	
Copper	1.0	Salt	0.17	155.8	132.7	6.7	18.2	L
		None	0.22	156.4	132.5	11.7	34.6	
Indium	1.0	Salt	0.08	155.4	132.2	11.7	39.7	VL
		None	0.19	156.5	132.5	15.0	36.7	
Iron	1.0	Salt	0.20	160.6	132.0	15.0	39.0	VL
		None	0.29	166.0	135.1	10.0	32.0	
Manganese	1.0	Salt	0.09	158.6	133.5	10.0	27.2	L
		None	0.13	166.5	135.8	18.3	30.0	
Nickel	1.0	Salt	Broke 75 hrs					
		Salt	0.48	154.3	141.9	1.7	2.7	L
		None	0.45	166.4	140.1	11.7	27.6	
Oxygen	0.2	Salt	0.09	174.3	160.0	5.0	6.5	L
		None	0.07	178.2	178.2	11.7	26.0	

TABLE XXXVI
(Continued)

Alloy Addition	Amount %	Coating	Plastic Creep* %	Room Temperature Tensile Properties After Creep Exposure: Ultimate Tensile Strength ksi	0.2% Offset Yield Strength ksi	Elongation % in 0.6"	Reduction in Area %	Salt** Attack in Break
Palladium	0.2	Salt	0.04	157.1	133.7	10.0	31.5	VL
		None	0.06	154.1	132.3	11.7	35.9	
Silicon	0.1	Salt	0.04	158.3	131.4	13.3	34.6	VL
		None	0.07	154.8	154.8	11.7	37.7	
Silver	1.0	Salt	0.10	160.1	140.1	10.0	16.0	VL-L
		None	0.07	162.3	139.9	16.7	34.6	
Thorium	0.5	Salt	0.03	151.9	128.6	3.3	12.7	VL
		None	0.06	153.1	125.2	6.7	13.6	
Tin	1.0	Salt	0.20	158.9	134.5	6.7	13.6	VL
		None	0.20	157.3	130.1	16.7	35.4	
Yttrium	0.1	Salt	0.12	156.8	153.0	6.7	15.9	VL
		None	0.08	155.6	139.7	8.3	30.0	
Zirconium	1.0	Salt	0.01	158.5	132.0	15.0	24.1	VL
		None	0.12	164.6	154.0	15.0	26.3	

* Creep Conditions: 100 Hrs, 700F, 70 Ksi Tensile Stress

** Code - See Table XX

TABLE XXXVII

General Salt Corrosion Tests of Selected Alloys

Alloy	Weight Gain (g/square inch)				
	Air Flow (525 ml/minute)				Stagnant Furnace Atmosphere
	2 hours	4 hours	6 hours	24 hours	24 hours
Ti-12Zr-7Al	0.0067	0.0098	0.0124	0.0311	0.0036
Ti-12Zr-7Al-1Mn	0.0182	0.0298	0.0418	0.1222	0.0245
Ti-12Zr-7Al-0.2Pd	0.0069	0.0112	0.0150	0.0348	0.0196
Ti-12Zr-7Al-0.1Y	0.0082	0.0172	0.0258	0.0579	0.0201
Ti-10Zr-7Al	0.0053	0.0089	0.0112	0.0208	0.0208
Ti-8Al-1Mo-1V	0.0060	0.0112	0.0133	0.0236	0.0193
Ti-8Al-1Mo-1Mn-1V	0.0215	0.0395	0.0541	0.1034	0.1054
Ti-8Al-1Mo-1V-0.2Pd	0.0071	0.0111	0.0141	0.0307	0.0231
Ti-8Al-1Mo-1V-0.1Y	0.0047	0.0069	0.0090	0.0236	0.0032
Ti-8Al-1Mo-1Cb	0.0052	0.0112	0.0175	0.0885	0.0229

TABLE XXXVIII

Salt-Creep Corrosion Behavior of Selected Alloys

Alloy Addition	Amount %	Coating	Plastic Creep* %	Room Temperature Tensile Properties After Creep: Ultimate Tensile Strength ksi	0.2% Offset Yield Strength ksi	Elongation % in 0.6"	Reduction in Area %	Salt** Attack in Break
Ti-12Zr-7Al Series								
None	-	Salt	0.02	134.8	129.5	3.3	6.3	L-M
	-	None	0.07	142.6	137.8	18.3	32.1	
		As Annealed	-	141.5	134.0	16.7	31.3	
Manganese	1.0	Salt	0.10	103.7	103.7	1.7	2.5	L-M
		None	0.14	166.5	151.7	16.7	27.7	
		As Annealed	-	167.7	149.7	15.0	28.9	
Palladium	0.2	Salt	0.01	160.0	146.1	13.3	22.5	VL
		None	0.08	163.2	147.6	16.7	24.7	
		As Annealed	-	161.2	143.6	16.7	31.7	
Yttrium	0.1	Salt	0.02	145.6	137.7	11.7	23.8	VL
		None	0.05	146.3	139.3	16.7	31.7	
		As Annealed	-	145.1	135.9	15.0	34.1	
Ti-10Zr-7Al		Salt	0.02	154.2	134.7	15.0	26.5	VL
		None	0.07	154.8	135.4	16.7	24.1	
		As Annealed	-	154.3	133.1	16.7	28.0	

TABLE XXXVIII
(Continued)

Alloy Addition	Amount %	Coating	Plastic Creep* %	Room Temperature Tensile Properties After Creep: Ultimate Tensile Strength ksi	0.2% Offset Yield Strength ksi	Elongation % in 0.6"	Reduction in Area %	Salt** Attack in Break
Ti-8Al-1Mo-1V Series								
None	-	Salt	0.07	156.9	135.0	11.7	37.5	VL
	-	None	0.12	159.6	135.7	15.0	33.7	
	As Annealed		-	160.1	140.8	13.3	25.9	
Manganese	1.0	Salt	0.20	164.9	139.3	10.0	17.1	VL
		None	0.21	164.5	140.6	11.7	25.3	
	As Annealed		-	160.5	142.7	15.0	22.9	
Palladium	0.2	Salt	0.03	159.8	138.8	13.3	30.5	VL
		None	0.05	162.7	135.6	13.3	39.8	
	As Annealed		-	163.3	139.8	15.0	32.5	
Yttrium	0.1	Salt	0.11	159.6	131.6	13.3	26.5	VL
		None	0.23	162.9	133.0	13.3	24.1	
	As Annealed		-	161.5	140.4	15.0	25.0	
Ti-8Al-1Mo-1Cb		Salt	0.07	155.0	134.2	11.7	23.8	VL
		None	0.16	157.1	134.6	13.3	26.2	
	As Annealed		-	156.8	136.0	13.3	27.4	

*Salt-creep and creep specimens tested at 700F and 70 ksi for 100 hours.
**Code - See Table XX.

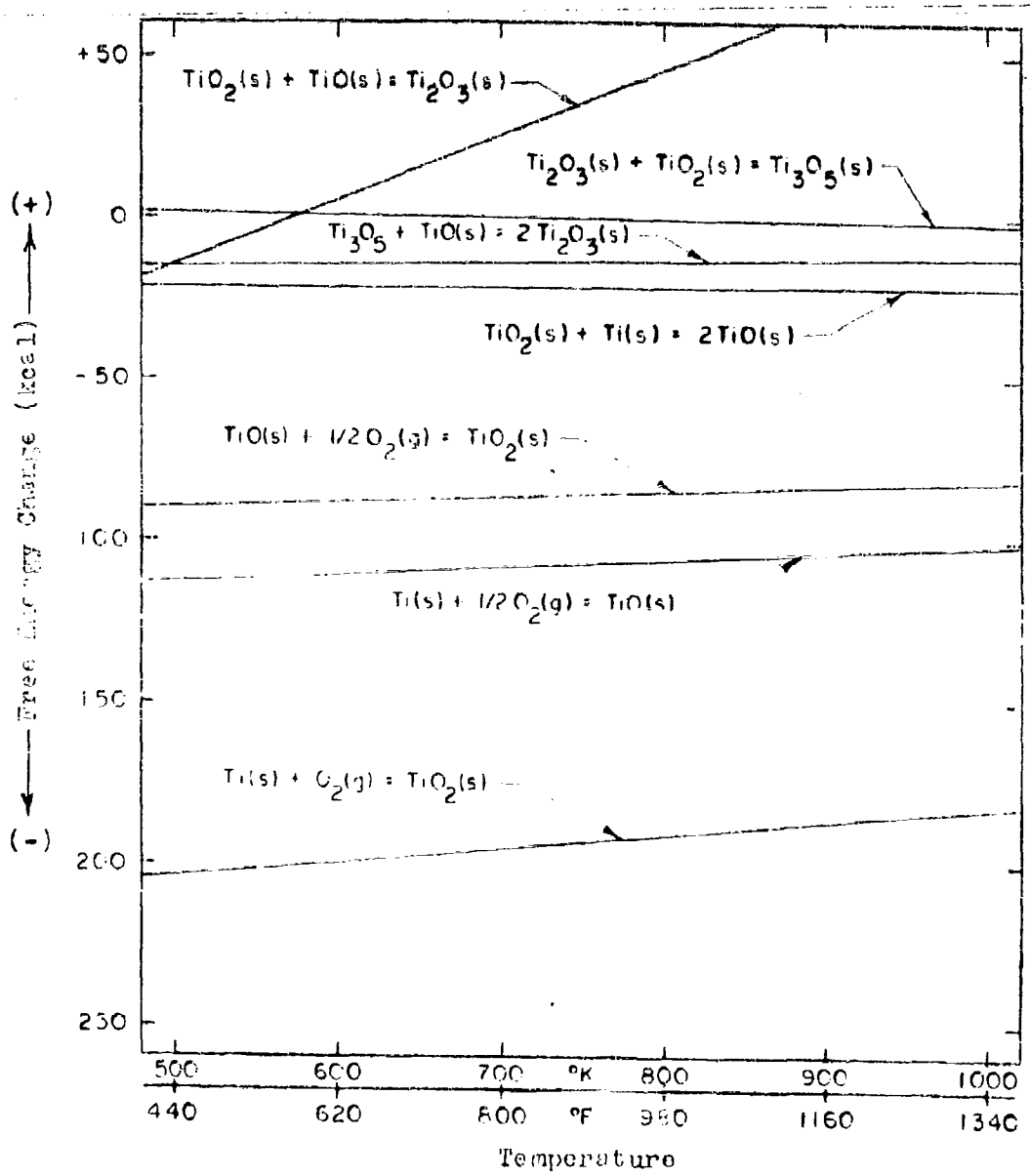

Figure 1: The Relationship Between Free Energy Changes and Temperature for Reactions of Compounds of Titanium and Oxygen. (Ref. 100)

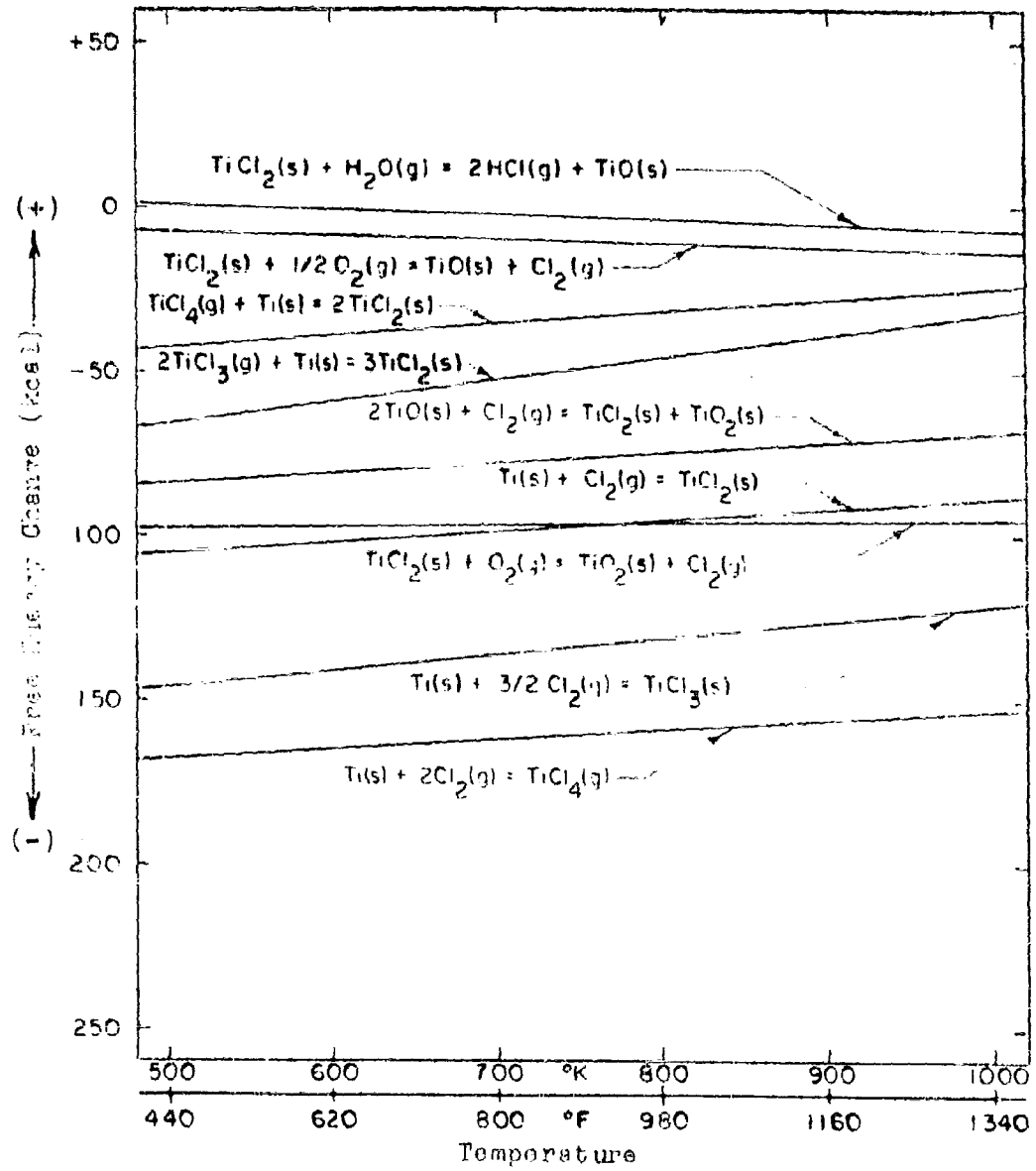

Figure 2: The Relationship Between Free Energy Changes and Temperature for Reactions of Compounds of Titanium, Oxygen, and Chlorine. (Ref. 100)

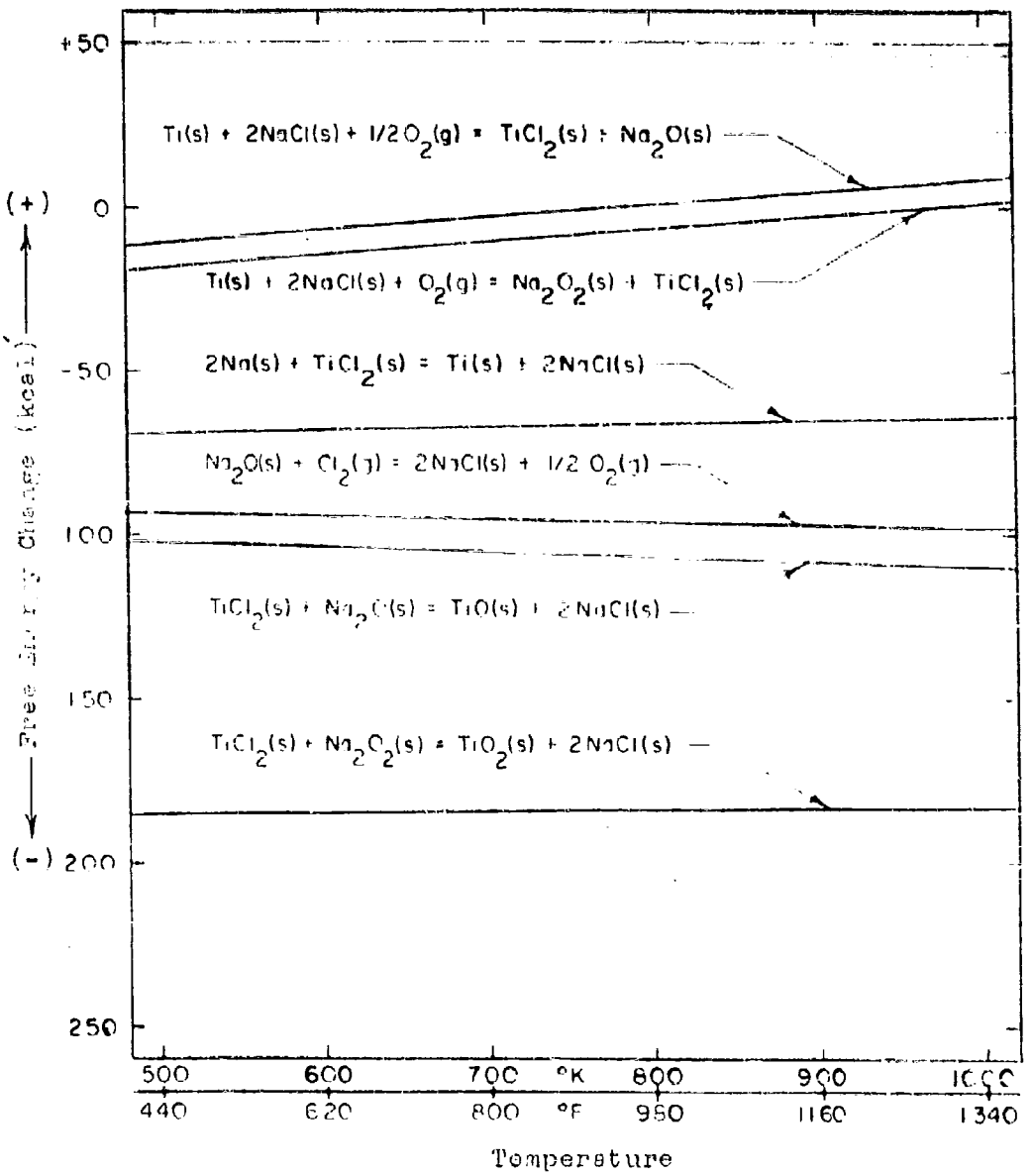

Figure 3: The Relationship Between Free Energy Changes and Temperature for Reactions of Compounds of Titanium, Oxygen, Chlorine and Sodium. (Ref. 100, 101, 102)

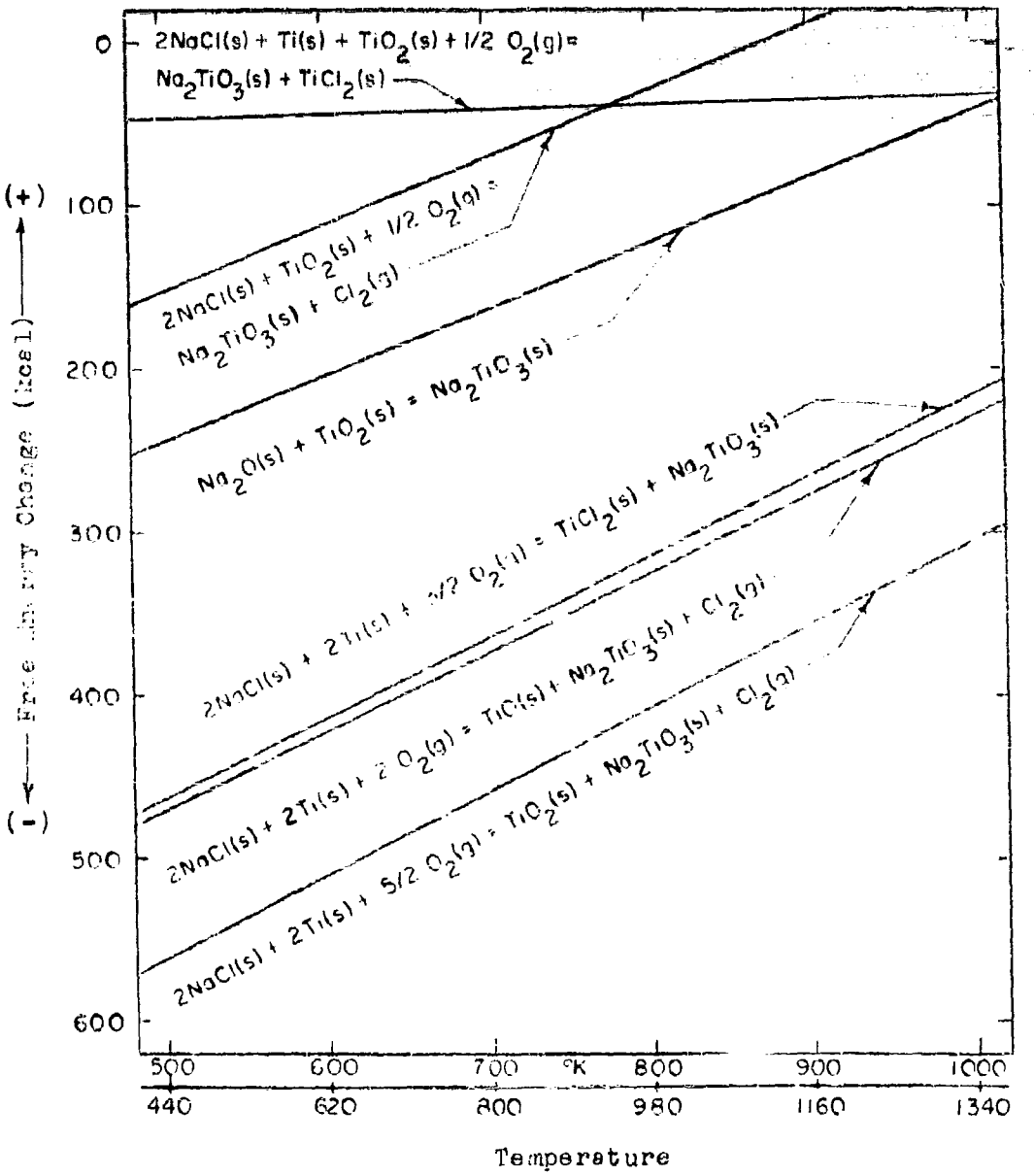

Figure 4: The Relationship Between Free Energy Changes and Temperature for Reactions of Compounds of Titanium, Oxygen, Chlorine and Sodium Showing Titanate Formation. (Ref 1, 100, 101, 102)

Figure 5

Attack of Sodium Chloride on Ti-12Zr-7Al Sheet After 100 Hours at 900F. Dark Blister Corrosion Product Underlying Sodium Chloride Crystals is Largely TiO_2. 20X

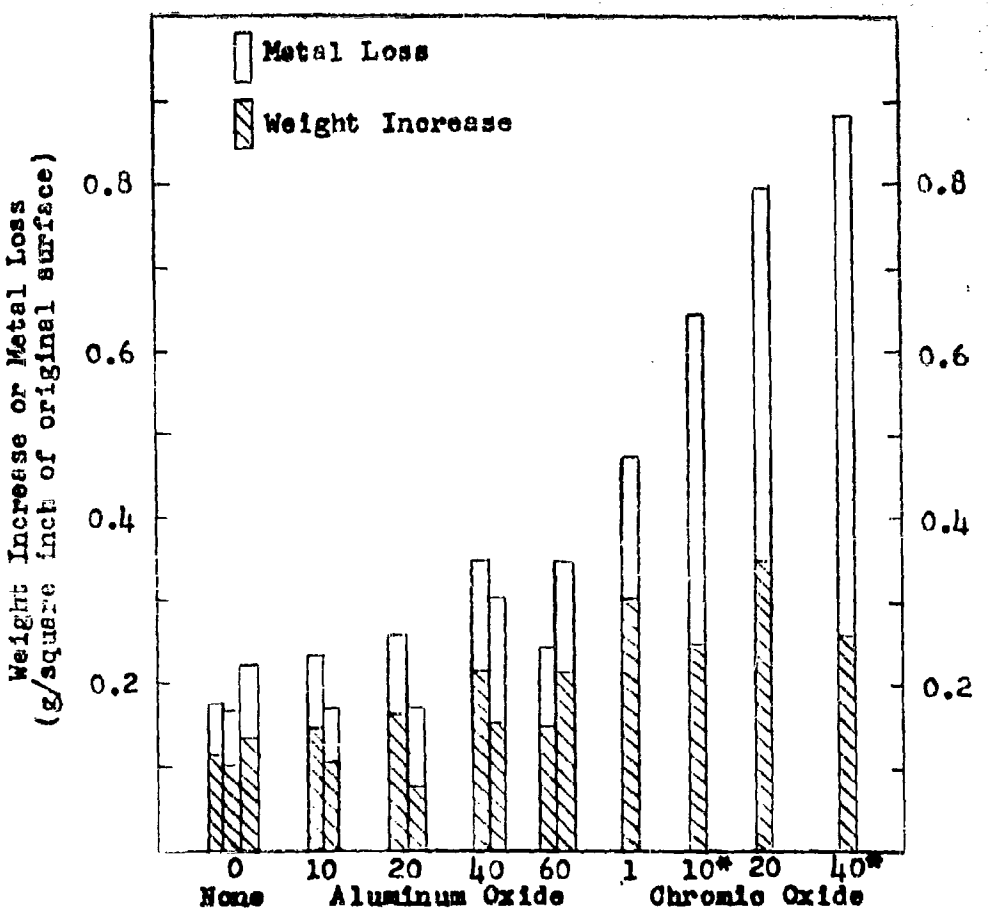

Figure 6: Effect of Additions of Aluminum Oxide and Chromic Oxide to Salt Upon the Corrosion of Titanium

*Weight increase higher than indicated since corrosion products were not all recovered.

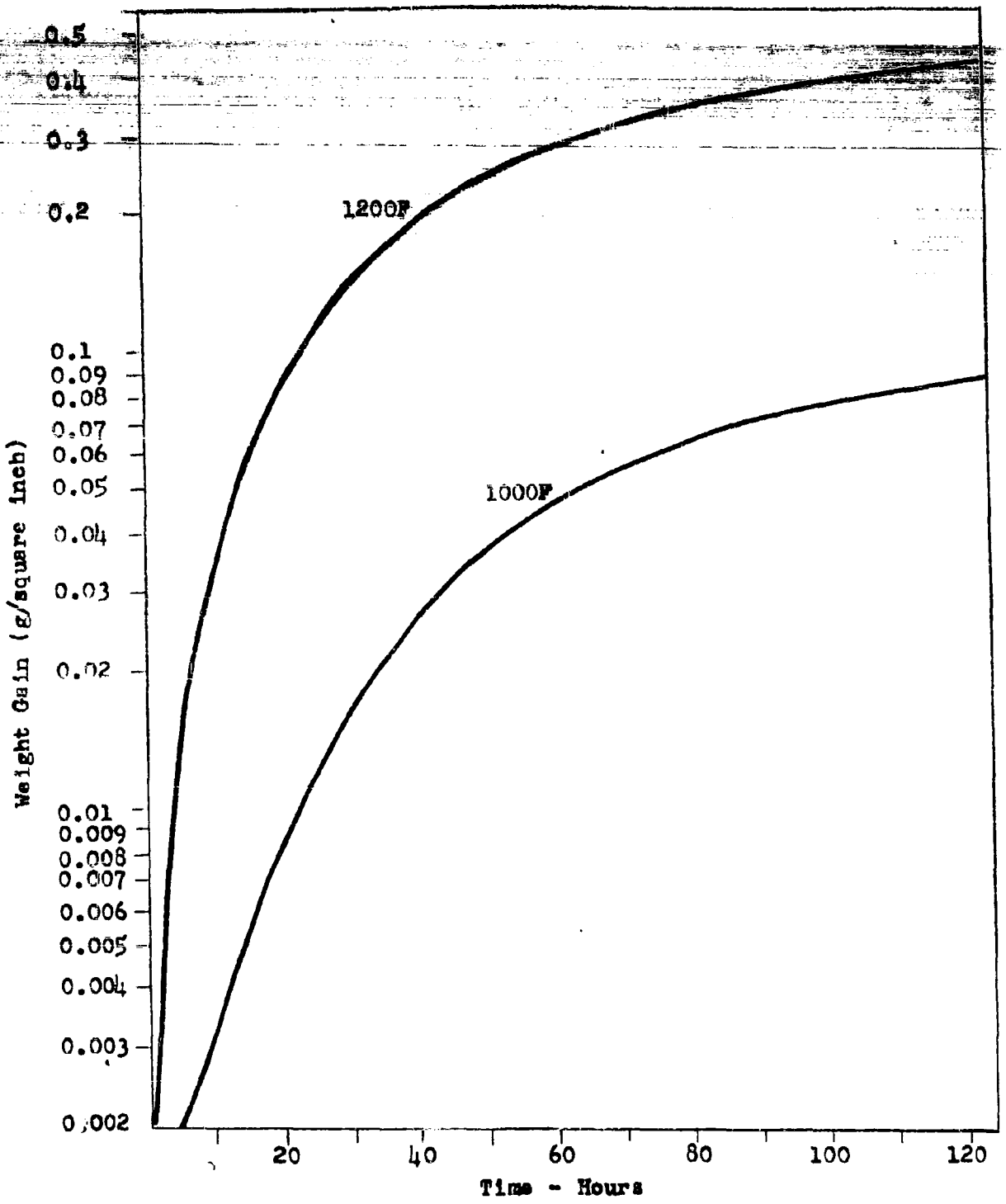

Figure 7: The Accelerated Oxidation of Commercially Pure Titanium (A70) when Liberally Coated with Sodium Chloride.
NOTE: A salt-free sample tested at 1000F for 118 hours and a salt-coated sample tested at 800F for 152 hours, gained less than 0.001 g/square inch.

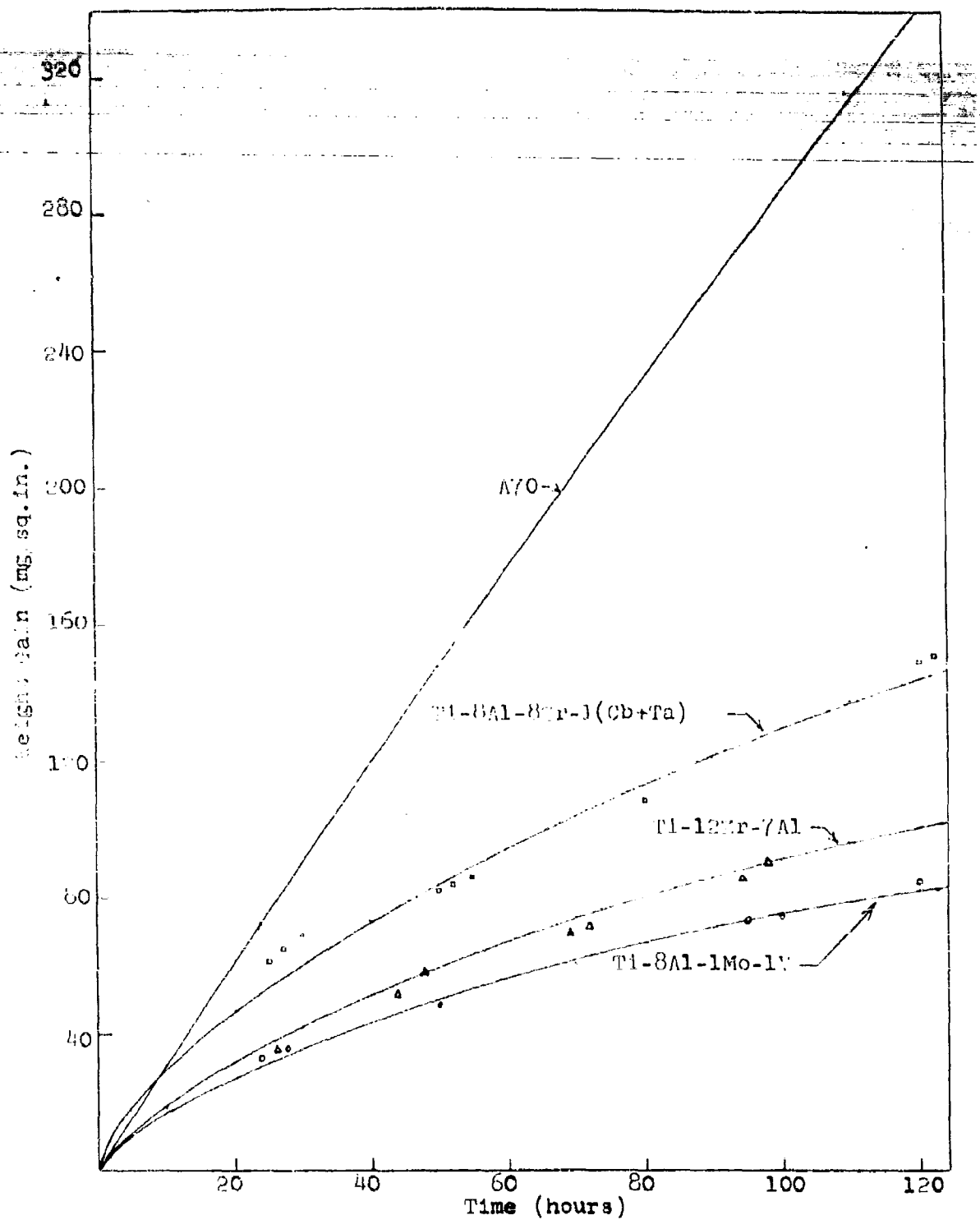

Figure 8: The Accelerated Oxidation of Salt Coated Titanium Alloys at 1200F

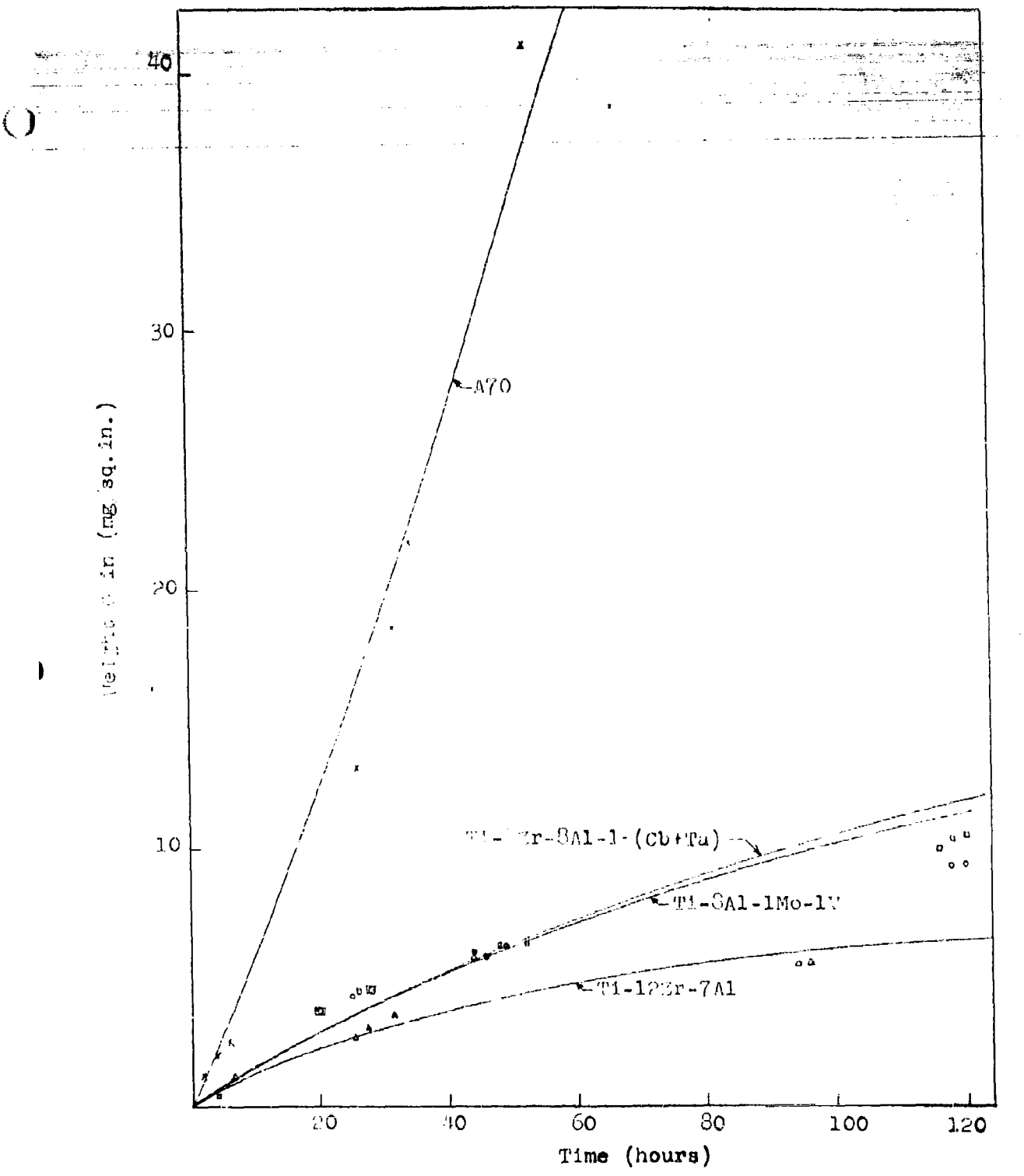

Figure 9: The Accelerated Oxidation of Salt Coated Titanium Alloys at 1000F.

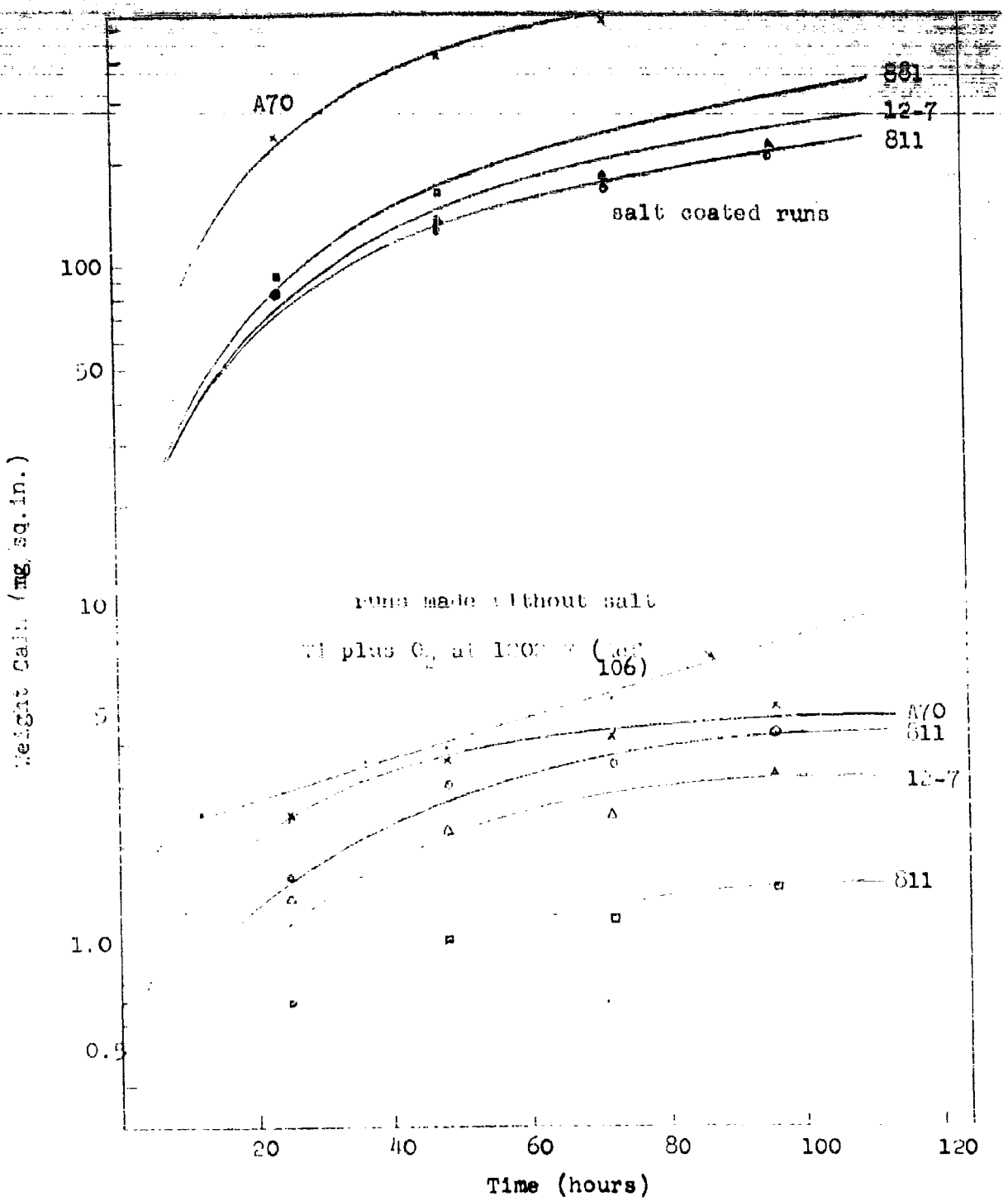

Figure 10: A Comparison of Salt Corrosion and Normal Oxidation of Titanium Alloys at 1200F

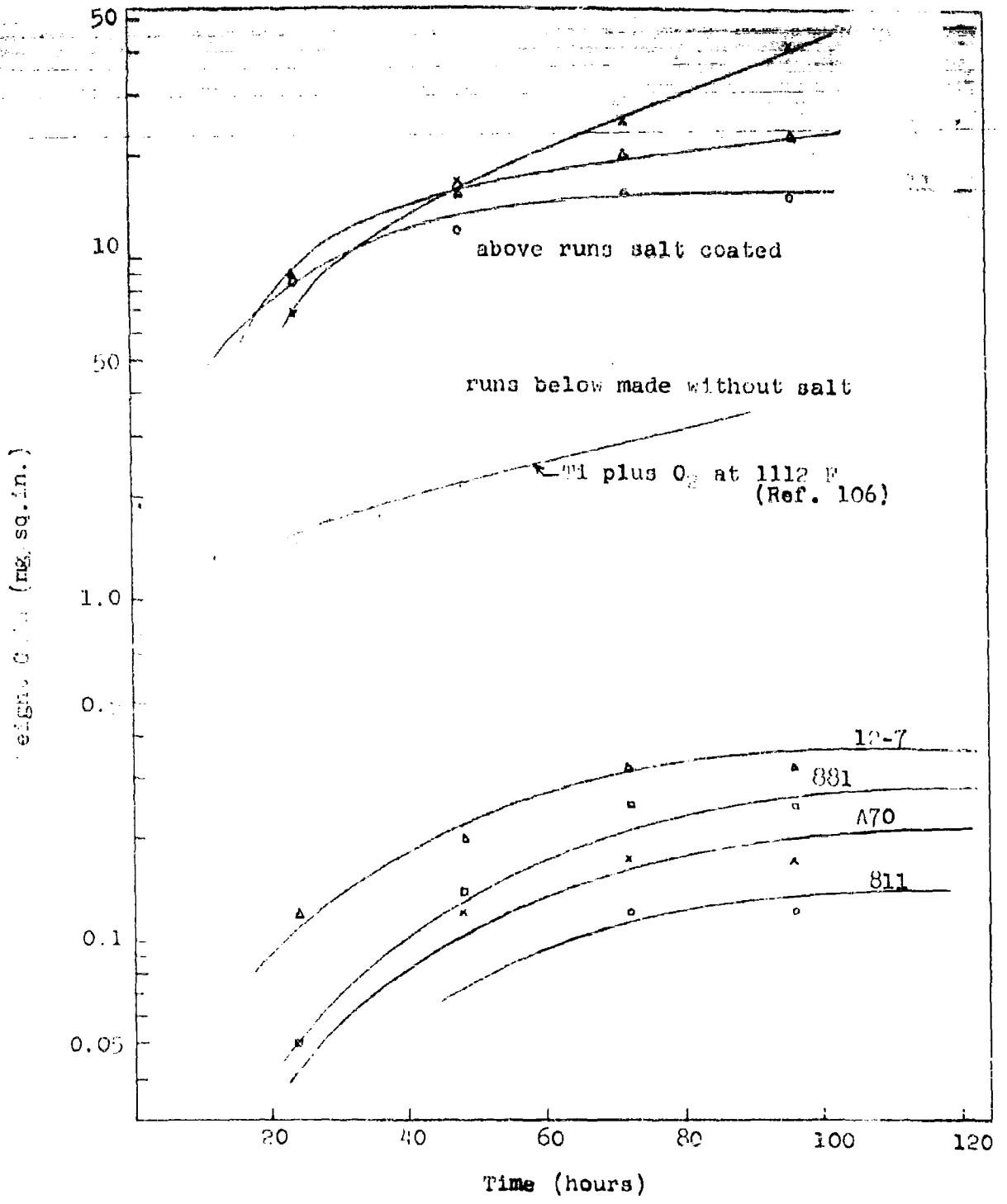

Figure 11: A Comparison of Salt Corrosion and Normal Oxidation of Titanium Alloys at 1000F

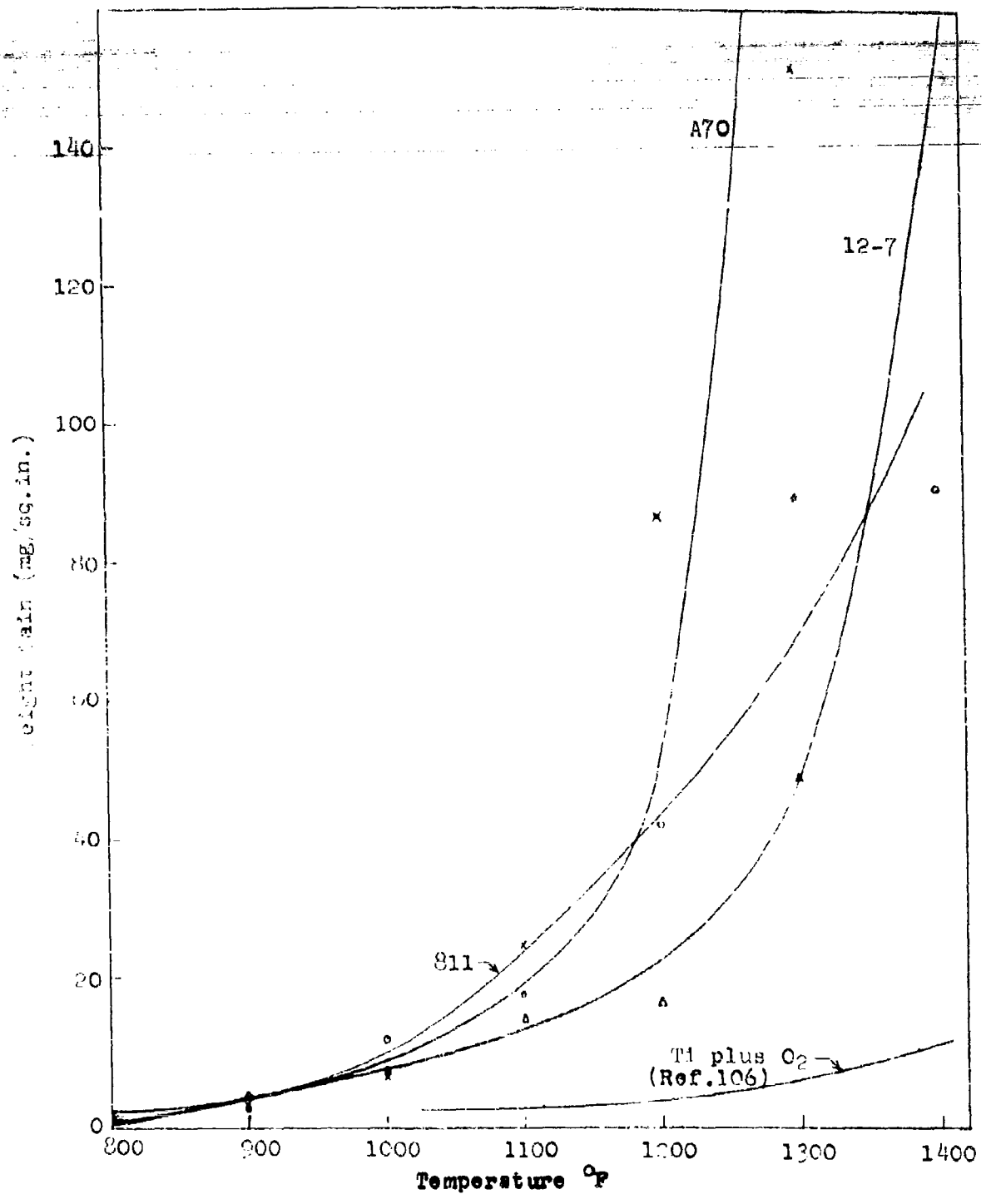

Figure 12: The Effect of Temperature Upon Salt Coated Titanium Alloys Exposed for 16-Hours

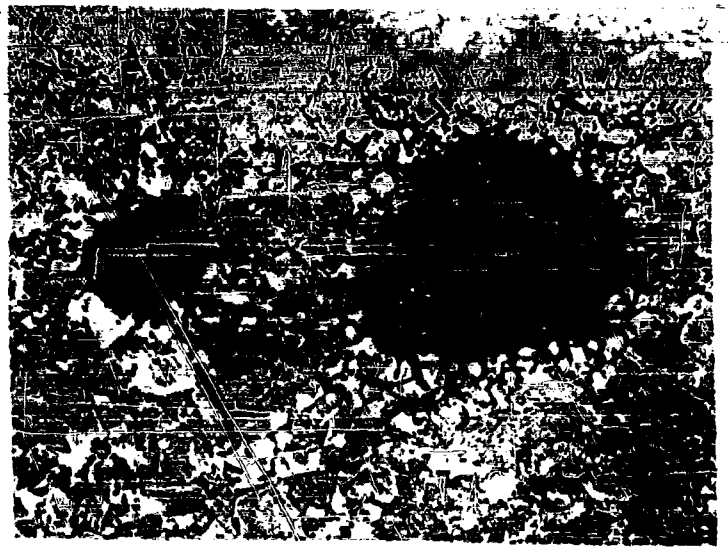

Figure 13

Intergranular Pitting Attack on Surface of Salt-Coated Ti-12Zr-7Al Sheet Exposed 100 Hours at 800F Without Stress. Sheet Condition: Hot Rolled at 1800F and Annealed 1 Hour at 1650F. 300X

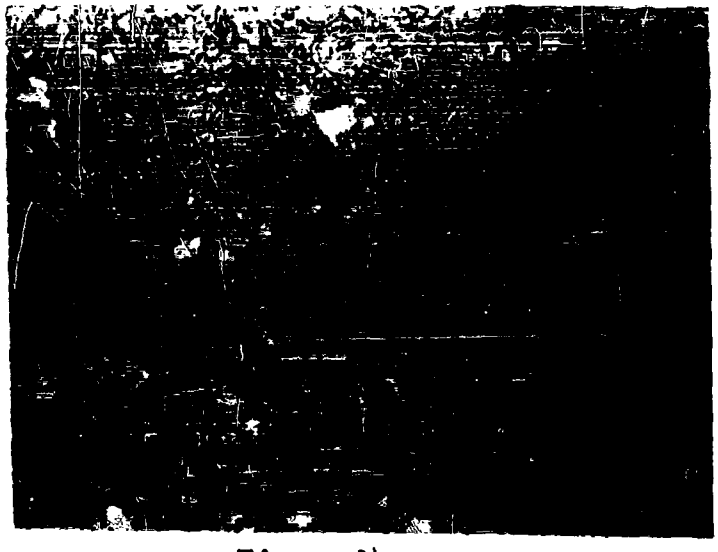

Figure 14

Intergranular Attack on Surface of Salt-Coated Ti-12Zr-7Al Sheet Exposed 22 Hours at 800F With 80 ksi Tensile Stress. Sheet Condition Same as Figure 13. 300X

NOTE: All Metallographic Samples in this Report Etched With 1HF-2HNO_3.

Figure 15

Intergranular Attack on Surface of Salt-Coated Ti-12Zr-7Al Bar Exposed 100 Hours at 800F Without Stress. Bar Condition: Hot Rolled at 1950F and Annealed 1 Hour at 1650F. 300X

Figure 16

Transgranular Cracking on Surface of Salt-Coated Ti-12Zr-7Al Bar Exposed 66 Hours at 800F With 80 ksi Tensile Stress. Bar Condition Same as Figure 15. 300X

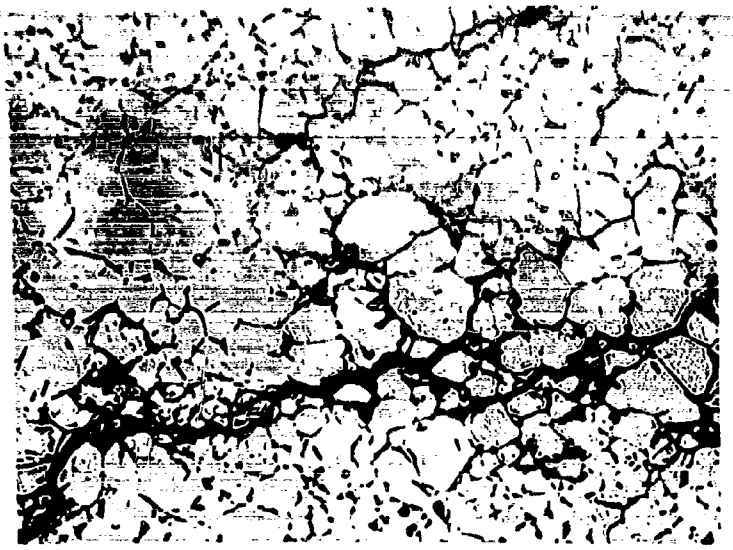

Figure 17

The Surface of a Salt-Corroded Tensile Sample of Ti-12Zr-7Al Sheet. The Sample was Coated with Salt and Exposed 100 Hours at 900F with 30 ksi Tensile Stress. 300X

Figure 18

Intergranular Attack on the Surface of a Bend-Stressed Sample of Annealed Ti-12Zr-7Al Sheet Heated in Dry Air Containing 1% Cl_2 from Room Temperature to 500F and Held a Few Minutes. 300X

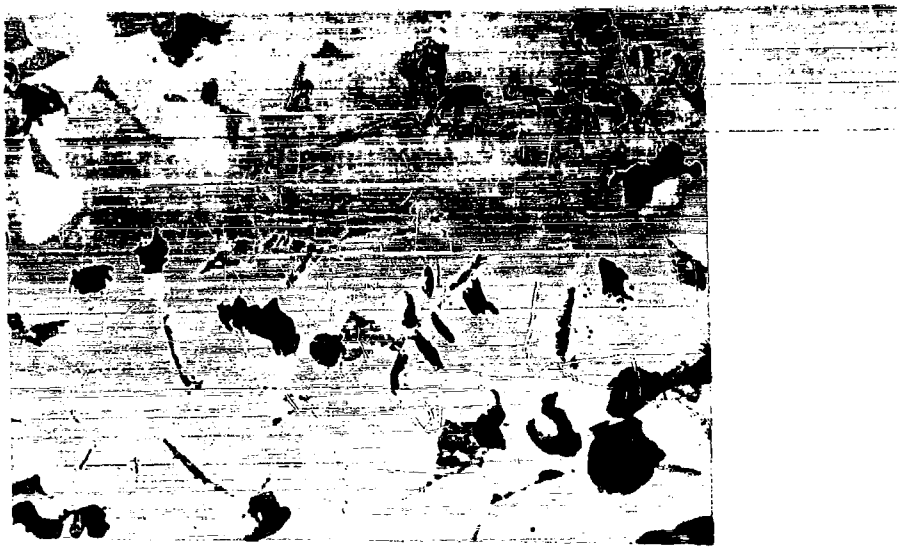

Figure 19

Random Attack on the Surface of a Bend-Stressed Sample of Ti-12Zr-7Al Sheet Exposed to an Aqueous Solution of 5%HCl for 20 Days Without Failure. Sheet Held 16 Hours at 1800F (alpha + beta region) Before Exposure 300X

Figure 20

Same Bend Stress and HCl Exposure as Figure 19 Except Sheet Held 4 Hours at 1900F (Beta Region) Before Exposure. Sheet Failed Instantaneously by Stress Corrosion Cracking. Cracks are Observed to be Transverse to Alpha Platelets. 300X

Figure 21

A Sample of Ti-8Al-1Mo-1V Showing an Area of Selective Attack. The Specimen has been Exposed at 1900F for 10 Hours and Stressed in 5% HCl for 5 Days at 78 ksi. 5X

Figure 22

A Sample of Ti-8Al-1Mo-1V Showing Crack Passing Through the Specimen. The Specimen had been Exposed at 1900F for 10 Hours and Stressed in 5% HCl for 5 Days at 78 ksi. 5X

Figure 23

A Sample of Ti-8Al-1Mo-1V Showing Origin of Cracks in Primary Alpha Platelets. The Specimen had been Exposed at 1900F for 10 Hours and Stressed in 5% HCl Solution for 5-1/6 Days at 78 ksi. 500X

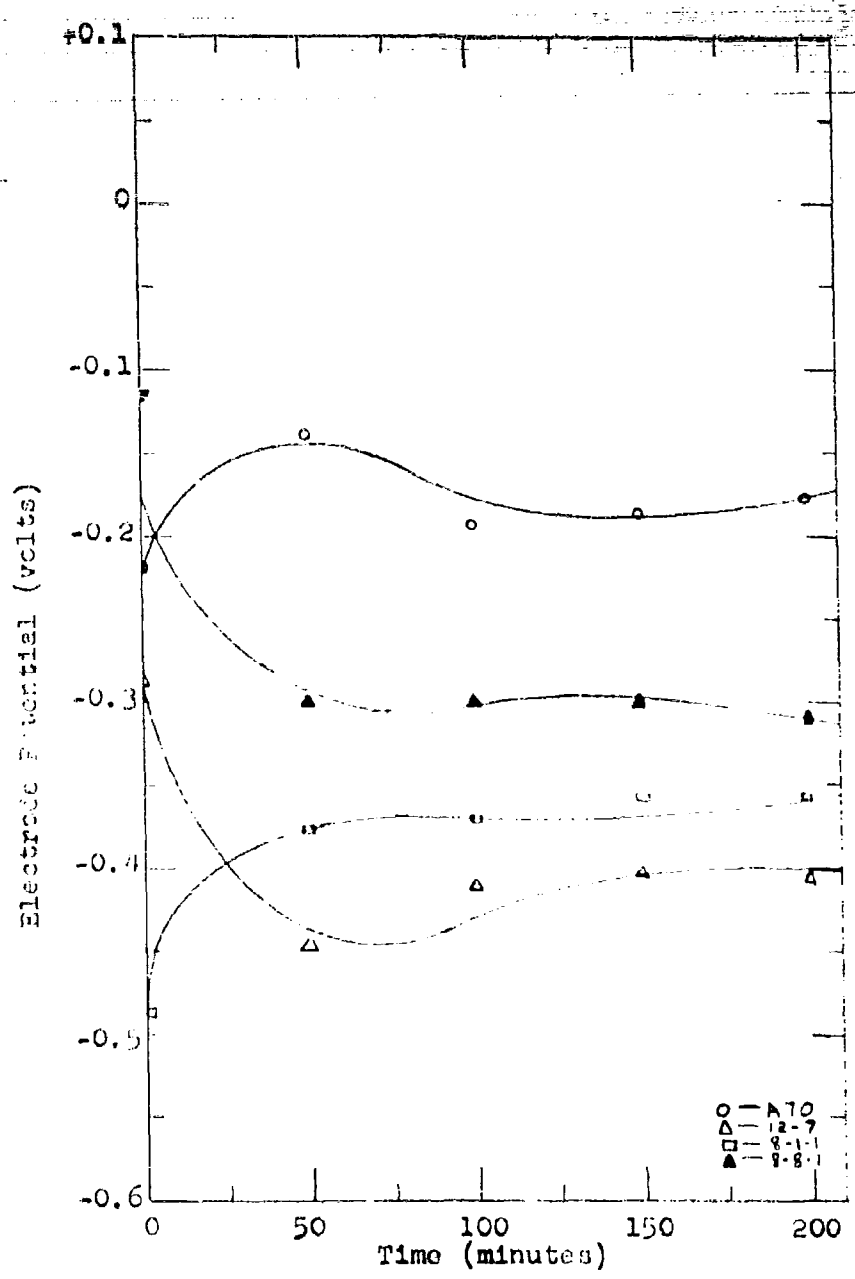

Figure 24: Time - Potential Curve for Titanium Alloys in 5% HCl Solution. Solution was Agitated at Room Temperature by an Argon Flow.

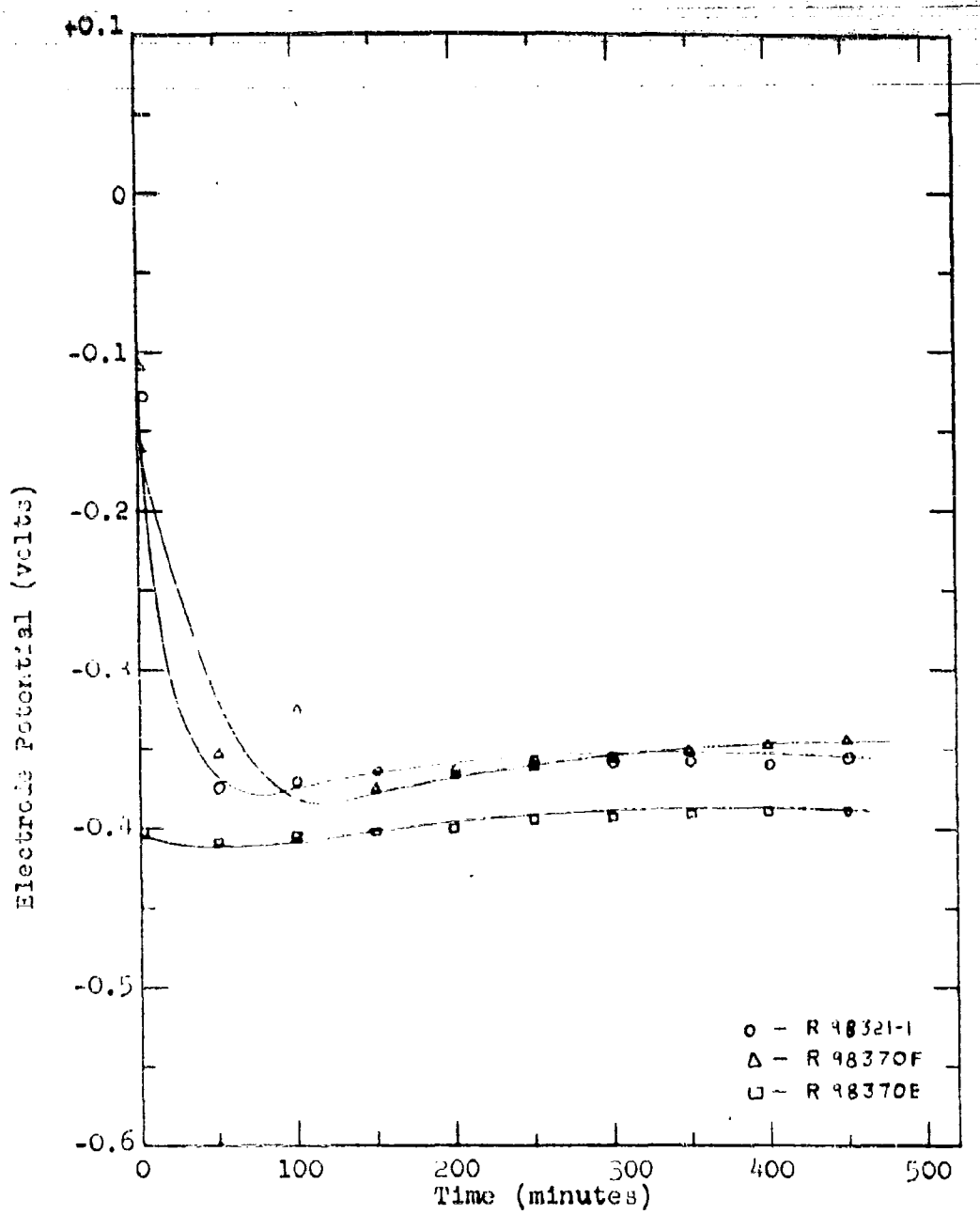

Figure 25: Time - Potential Curves for Several Heats of Ti-12Zr-7Al in 5% HCl Solution. Heats R98321-1 and R98370F Processed Below 1700F. Heat R98270E Hot Rolled at 1950F. Samples Annealed for 1 Hour at 1650F and Air Cooled.

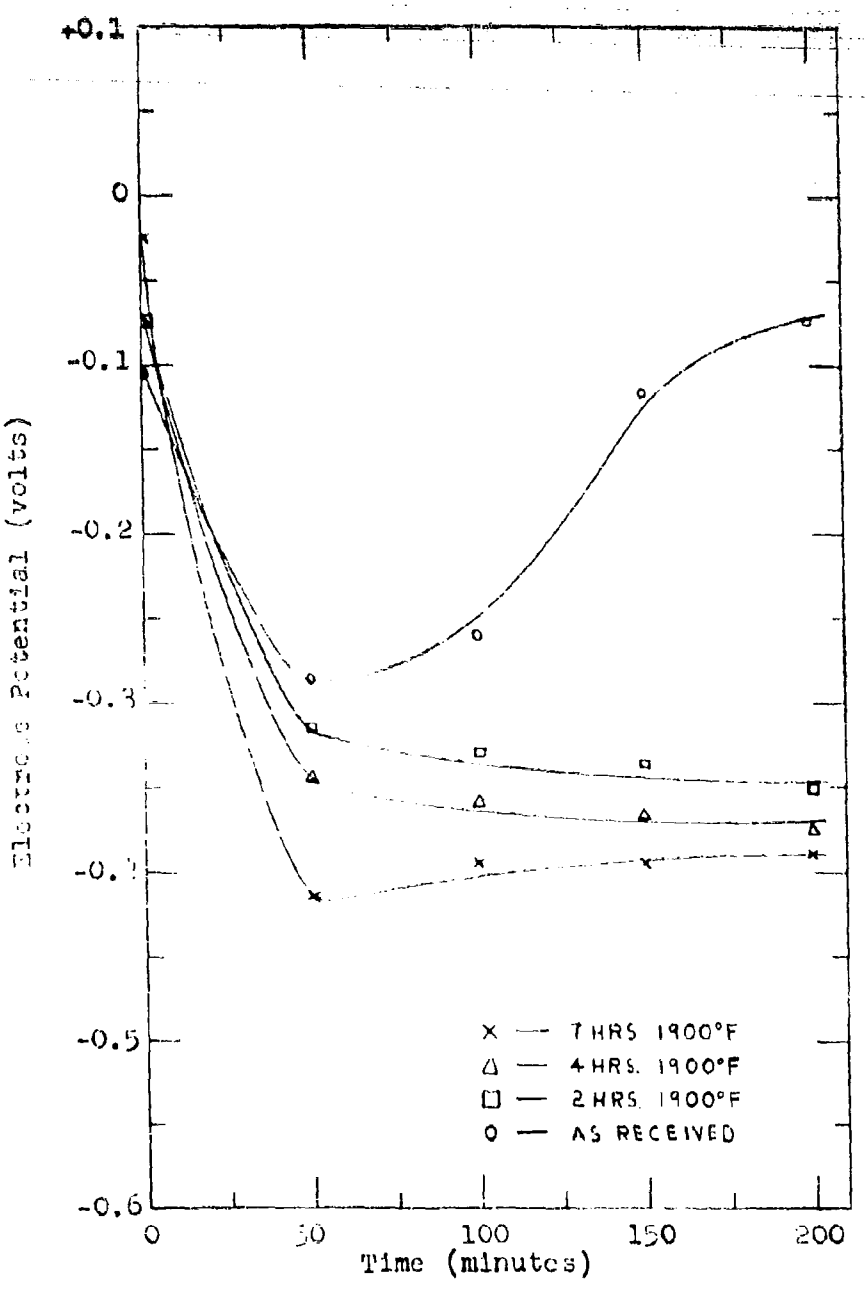

Figure 26: Time - Potential Curves for A70 in Stagnant 5% HCl Solution Showing Effect of High-Temperature Exposure. Samples Previously Stressed in 5% HCl with Cracking of of Sample Exposed for 7 Hours.

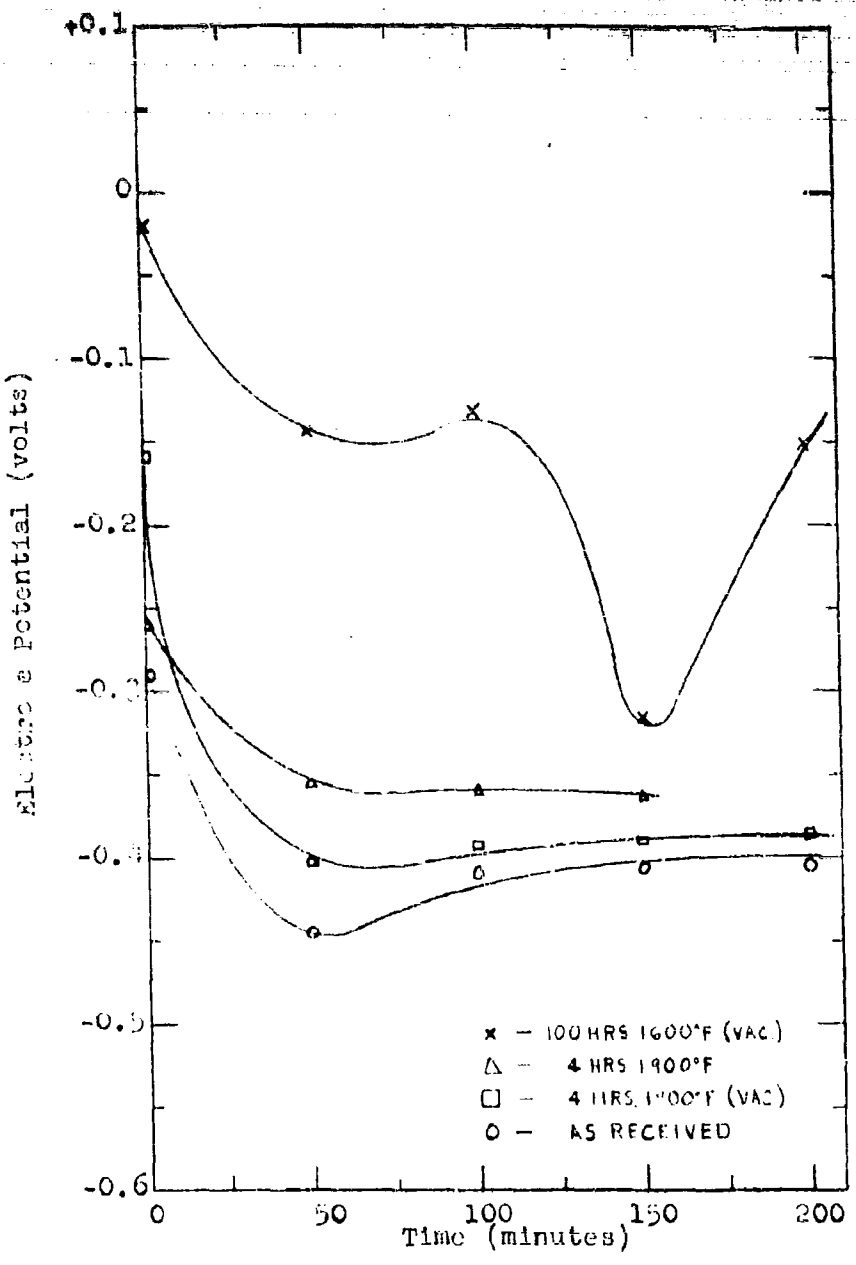

Figure 27: Time - Potential Curves of Ti-12Zr-7Al from Stress Corrosion Tests. Sample Exposed for 4 Hours at 1900F Cracked. Potential Measurements Made in 5% HCl Solution Agitated by an Argon Flow at Room Temperature

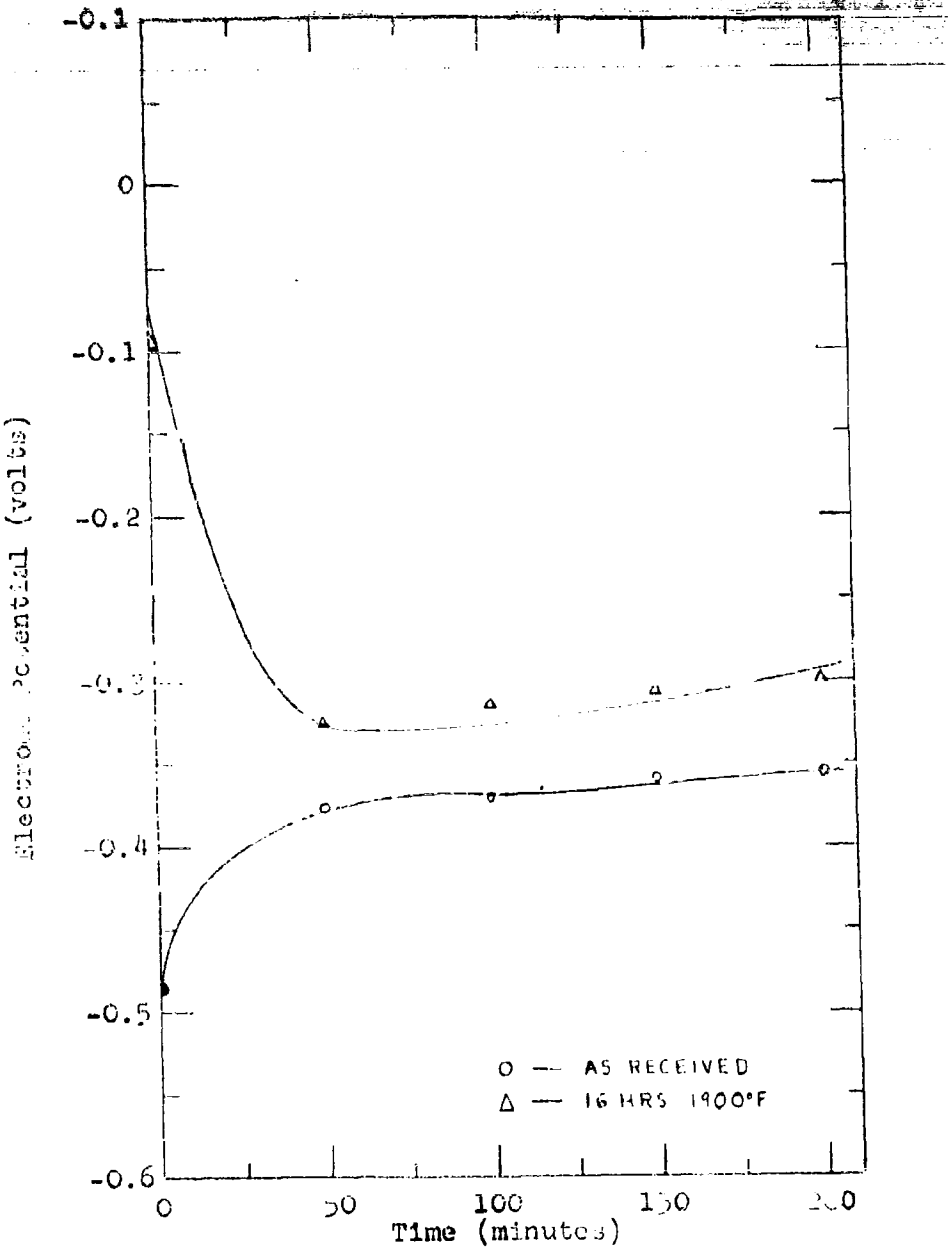

Figure 28: **Time - Potential Curves of Ti-8Al-1Mo-1V From Stress Corrosion Tests. Sample Exposed 16 Hours at 1900F Cracked. Potential Measurements Made in 5% HCl Solution Agitated by an Argon Flow at Room Temperature.**

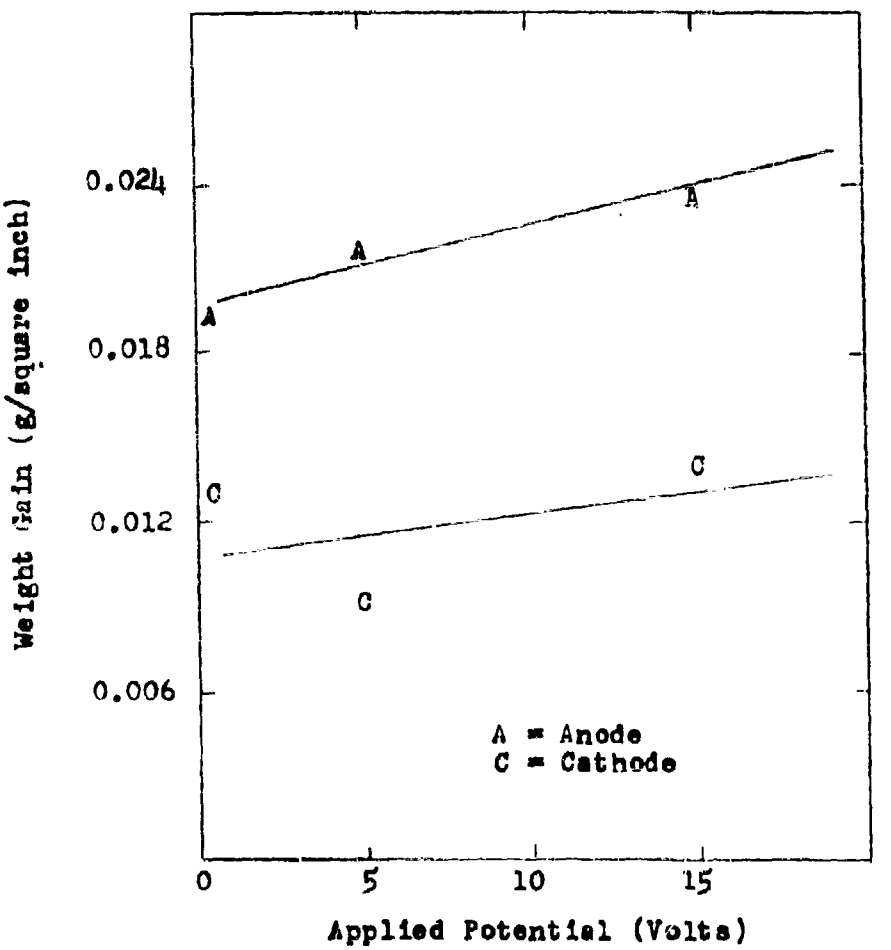

Figure 29: Weight Increase of Titanium Electrodes in Salt as a Function of the Applied Voltage. (Electrodes held at indicated voltage for 4 hours at 1200F)

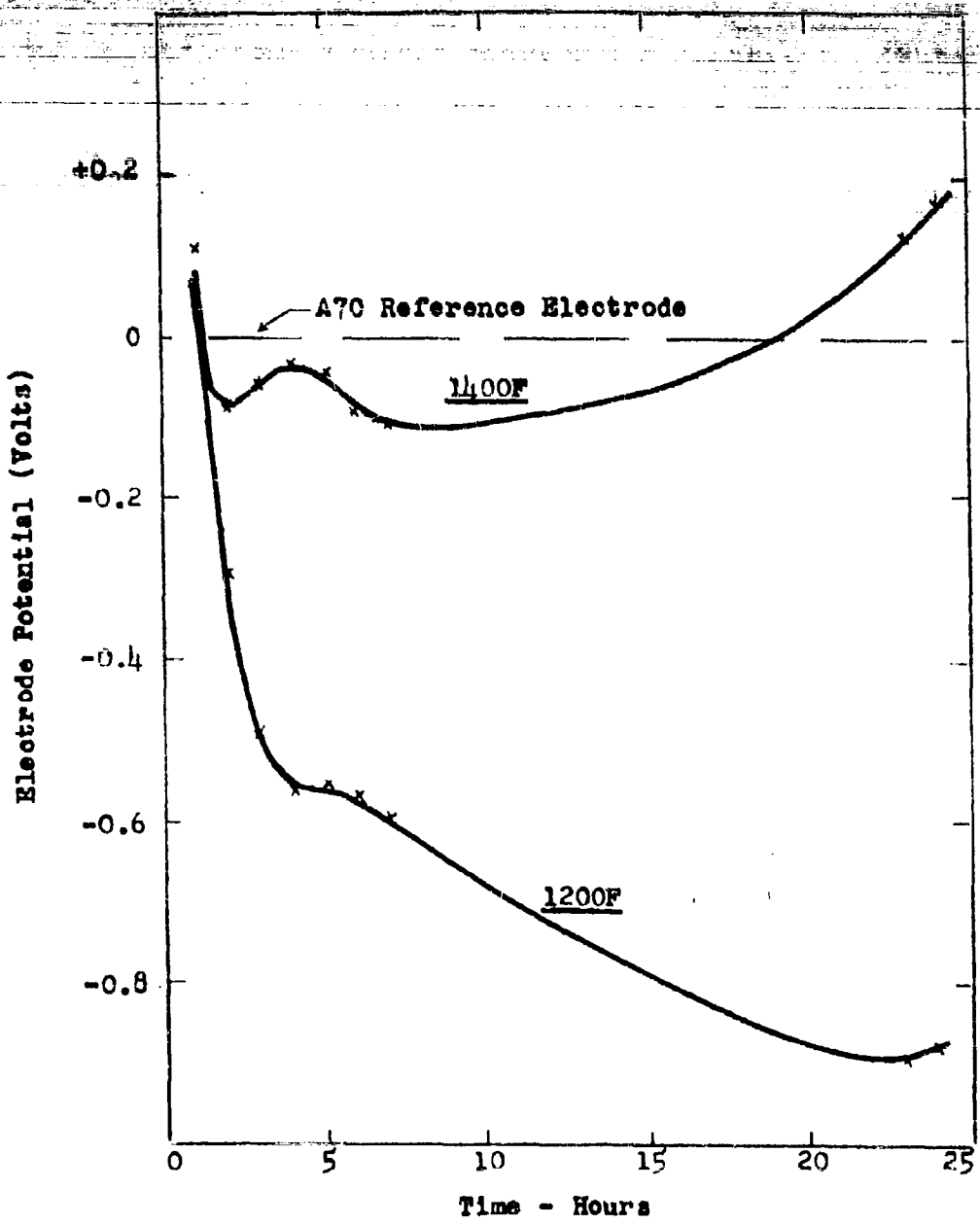

Figure 30: Electrode Potentials of B120VCA Relative to an A70 Reference Electrode Measured in Sodium Chloride at the Temperatures Indicated in the Presence of Air.

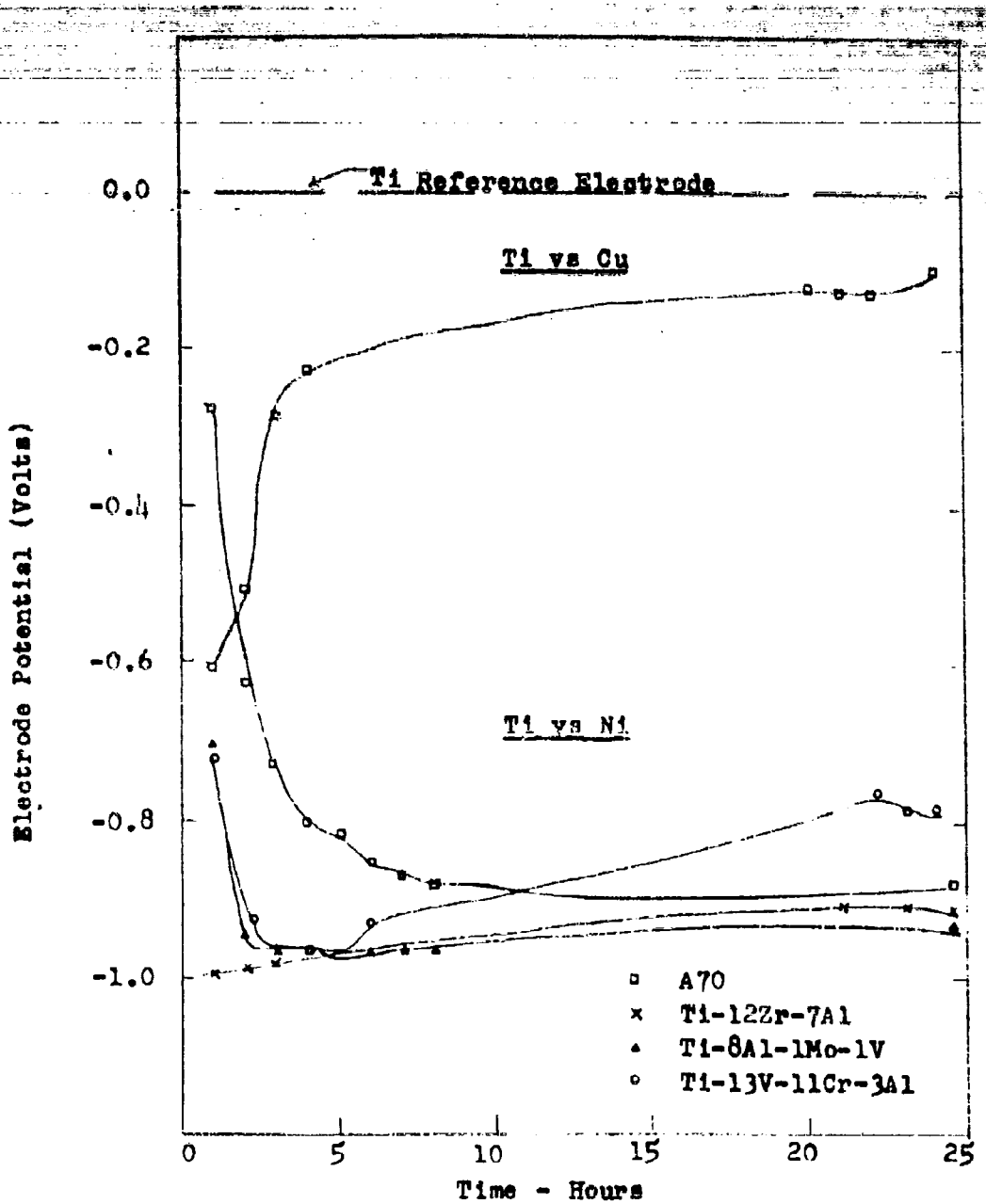

Figure 31: Electrode Potentials of Titanium and Titanium Alloys Relative to Copper and Nickel in Sodium Chloride at 1200F in the Presence of Air

Ti-12Zr-7Al
(Heat R98321, 0.050" Sheet
HR 1800F, Anneal 1 Hr 1600F)

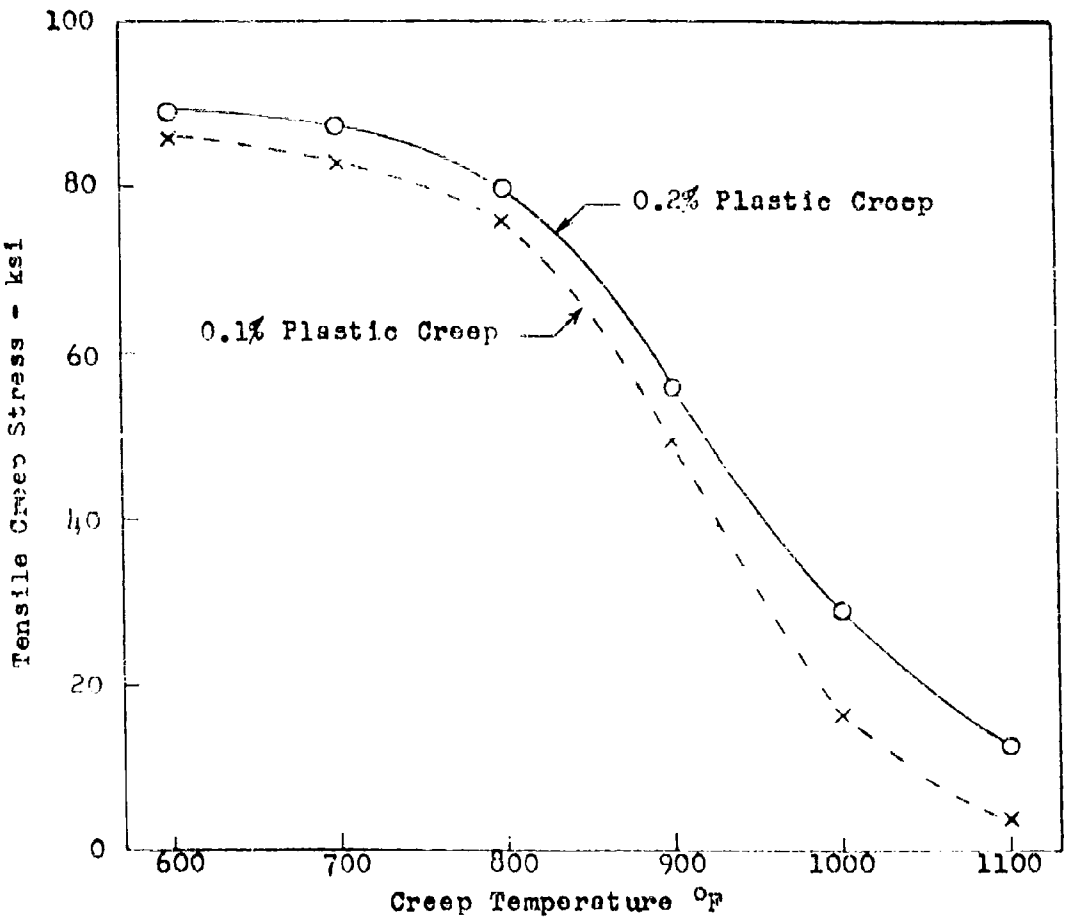

Figure 32: Temperature Vs Creep Stress to Give 0.1 and 0.2% Plastic Strain in 100 Hours. Ti-12Zr-7Al Sheet.

Ti-12Zr-7Al
(Heat R98370, 7/8" Diameter Rod
HR 1950F, Anneal 1 Hr 1650F)

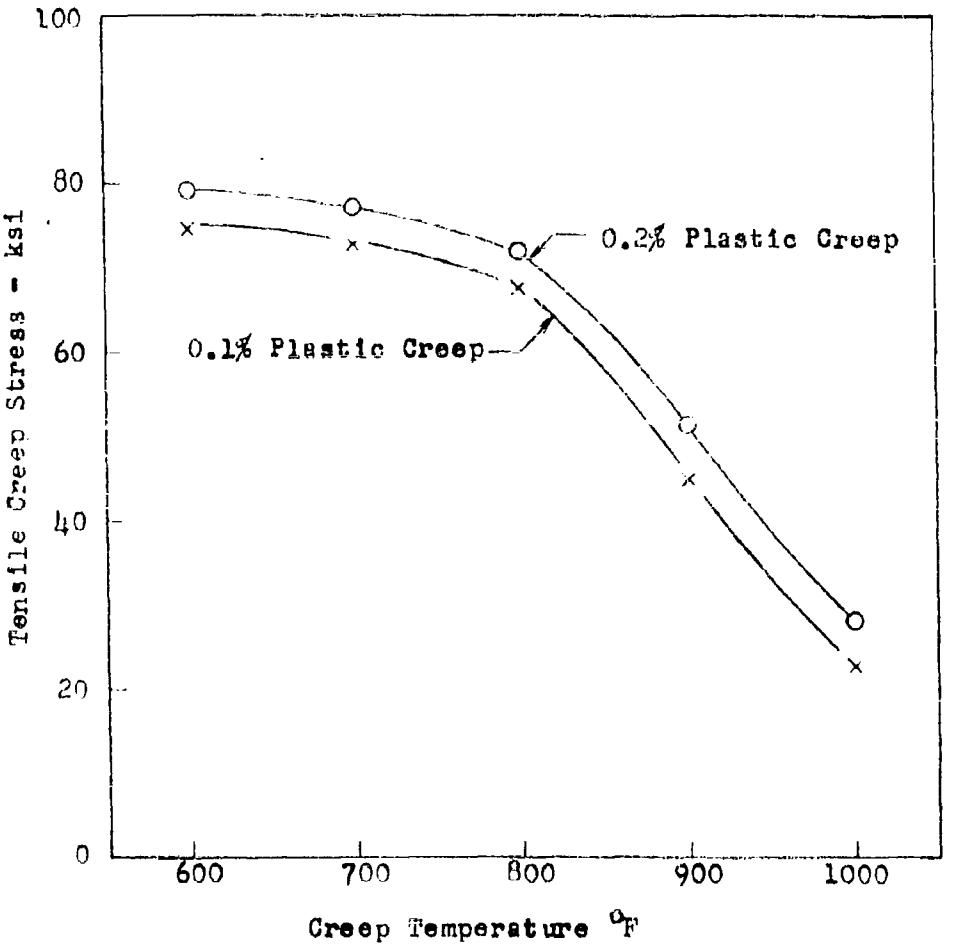

Figure 33: Temperature Vs Creep Stress to Give 0.1 and 0.2% Plastic Strain in 100 Hours. Ti-12Zr-7Al Rod.

Ti-8Al-1Mo-1V
(Heat R98369, 7/8" Diameter Rod,
HR 1950F, Anneal 1 Hr 1800F + 8 Hrs 1100F)

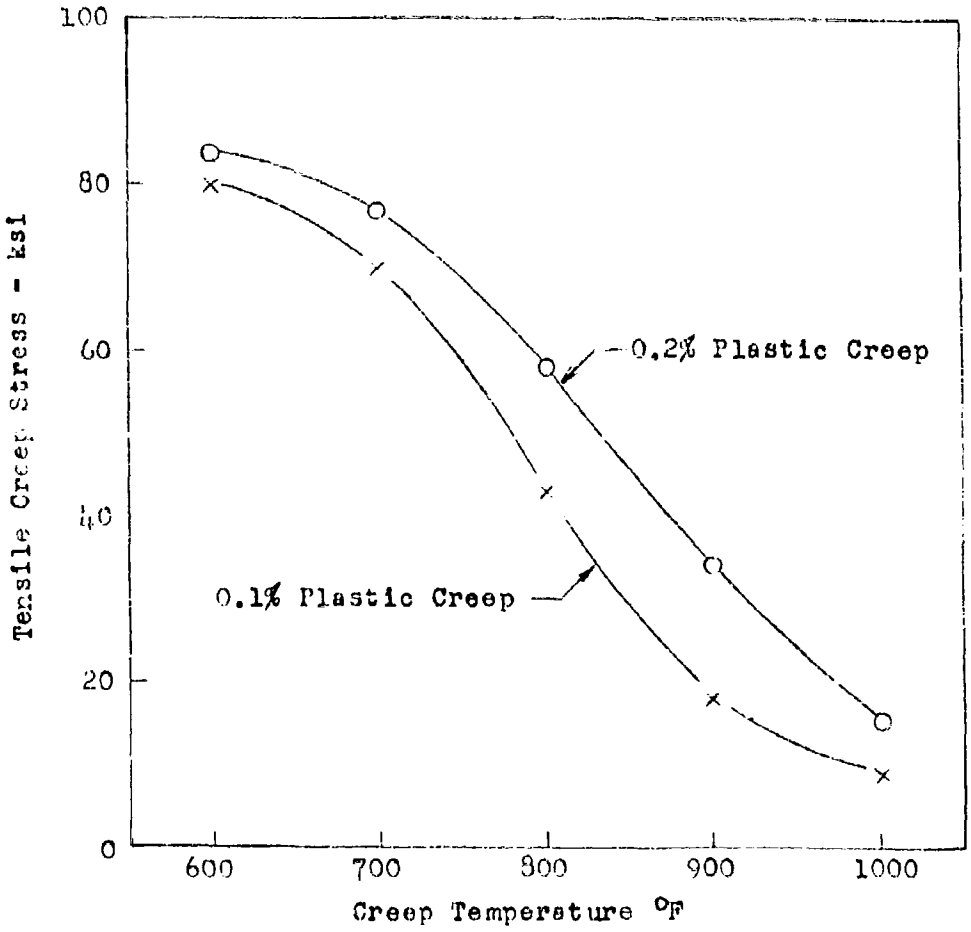

Figure 34: Temperature Vs Creep Stress to Give 0.1 and 0.2% Plastic Strain in 100 Hours. Ti-8Al-1Mo-1V Rod.

Ti-6Al-4V
(C120AV)
(Heat G5895, 0.050" Sheet, Mill Annealed)

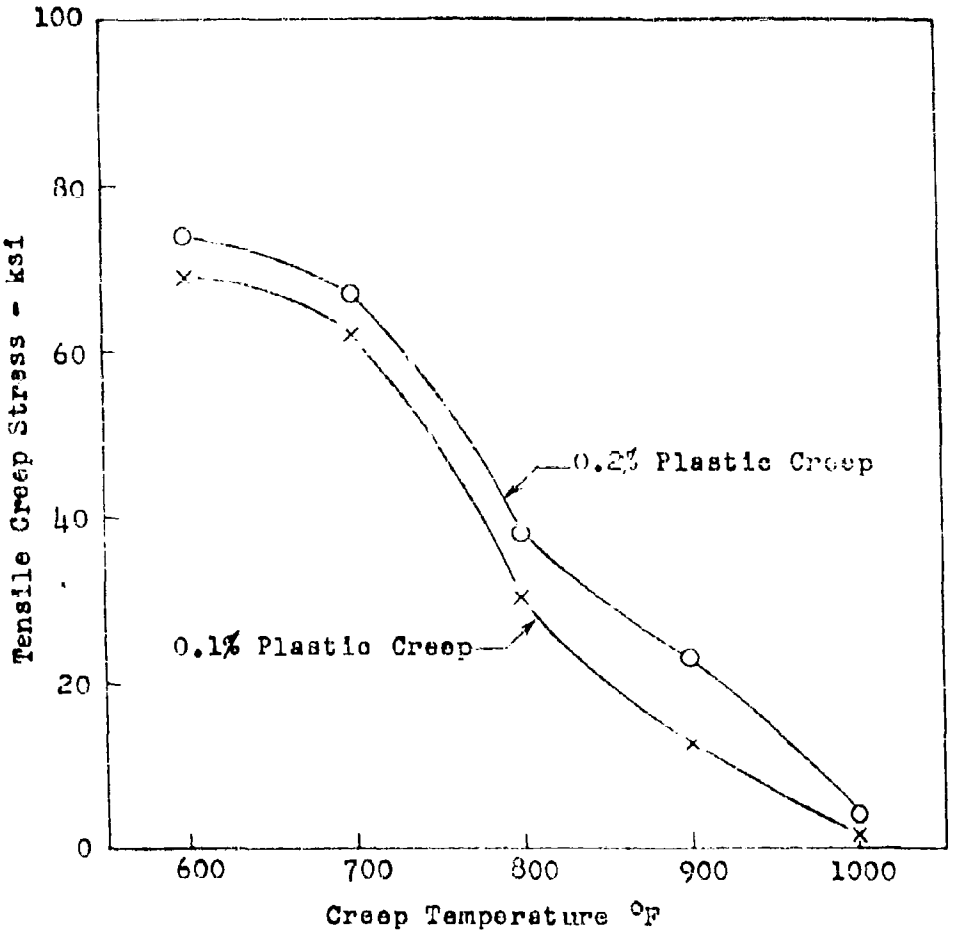

Figure 35: Temperature Vs Creep Stress to Give 0.1 and 0.2% Plastic Strain in 100 Hours. Ti-6Al-4V (C120AV) Sheet.

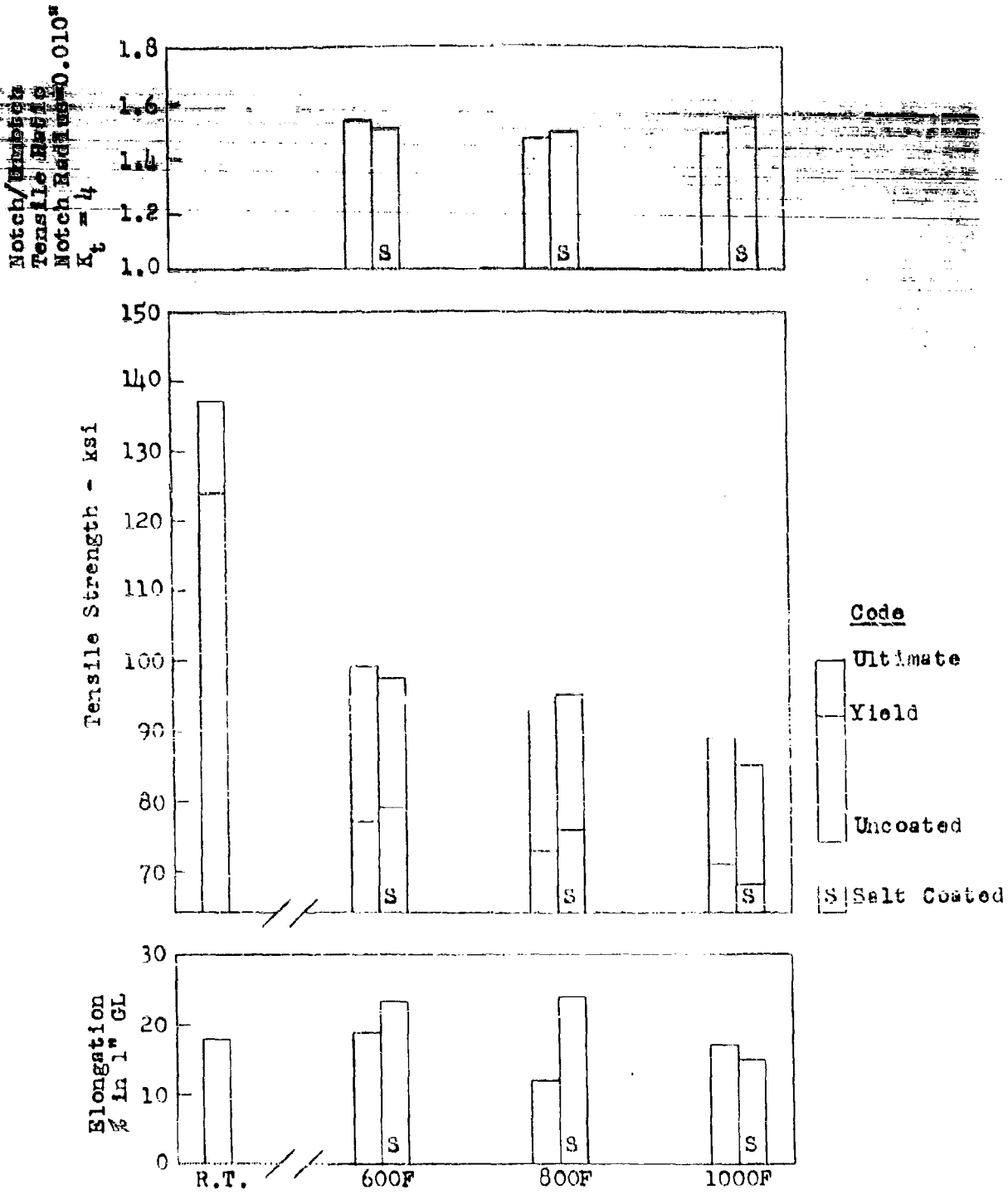

Figure 36: Effect of Salt on the Notched and Unnotched Hot Tensile Strength of Beta-Processed Ti-12Zr-7Al Rod. (7/8" Diameter, HR 1950F, Ann. 1 Hr 1650F, Av. of 2 Tests.)

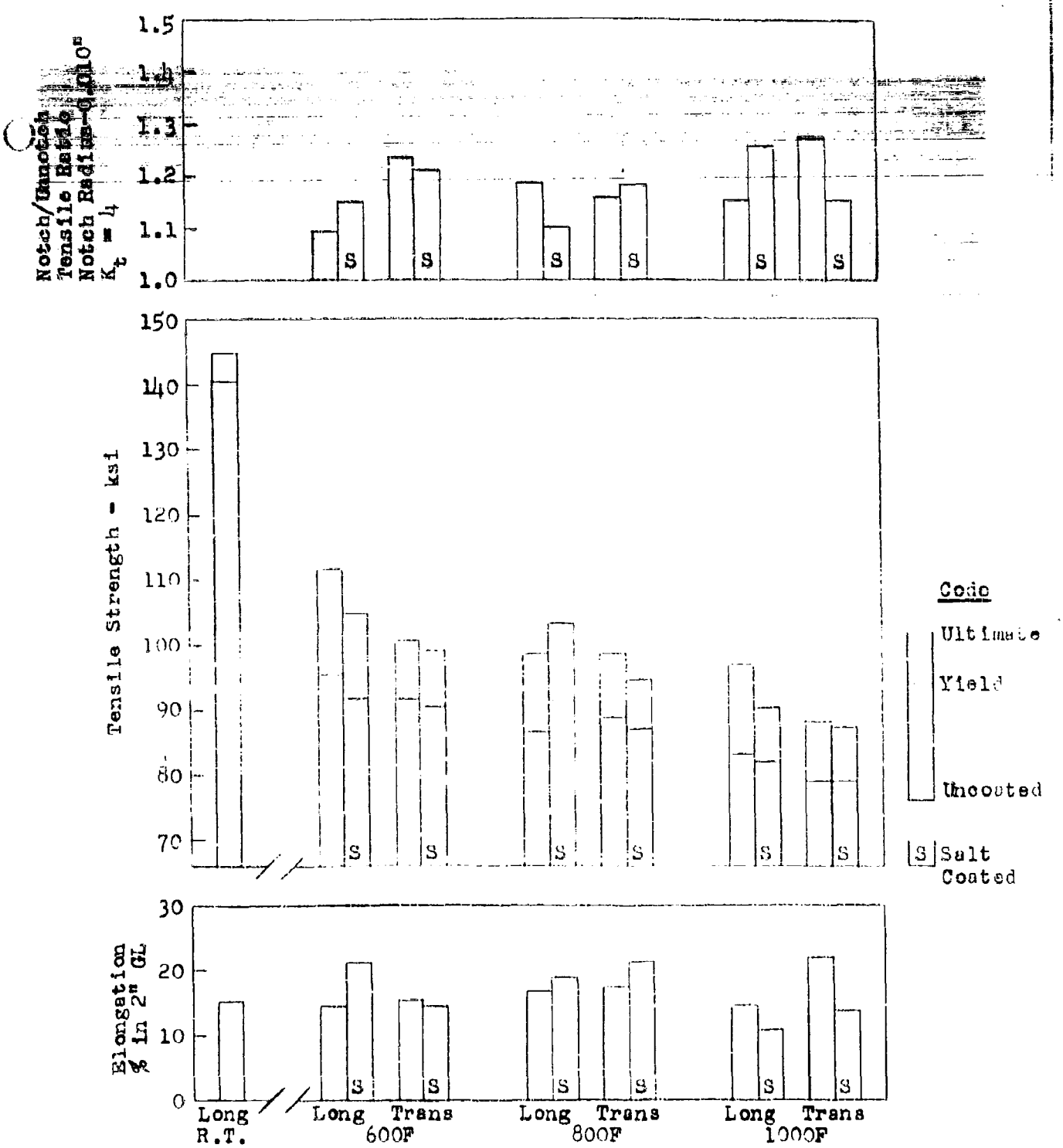

Figure 37: Effect of Salt on the Notched and Unnotched Hot Tensile Strength of Alpha-Processed Ti-12Zr-7Al Sheet. (0.050" thick, HR 1650F, Ann. 2 Hrs 1500F, Av. of 2 Tests.)

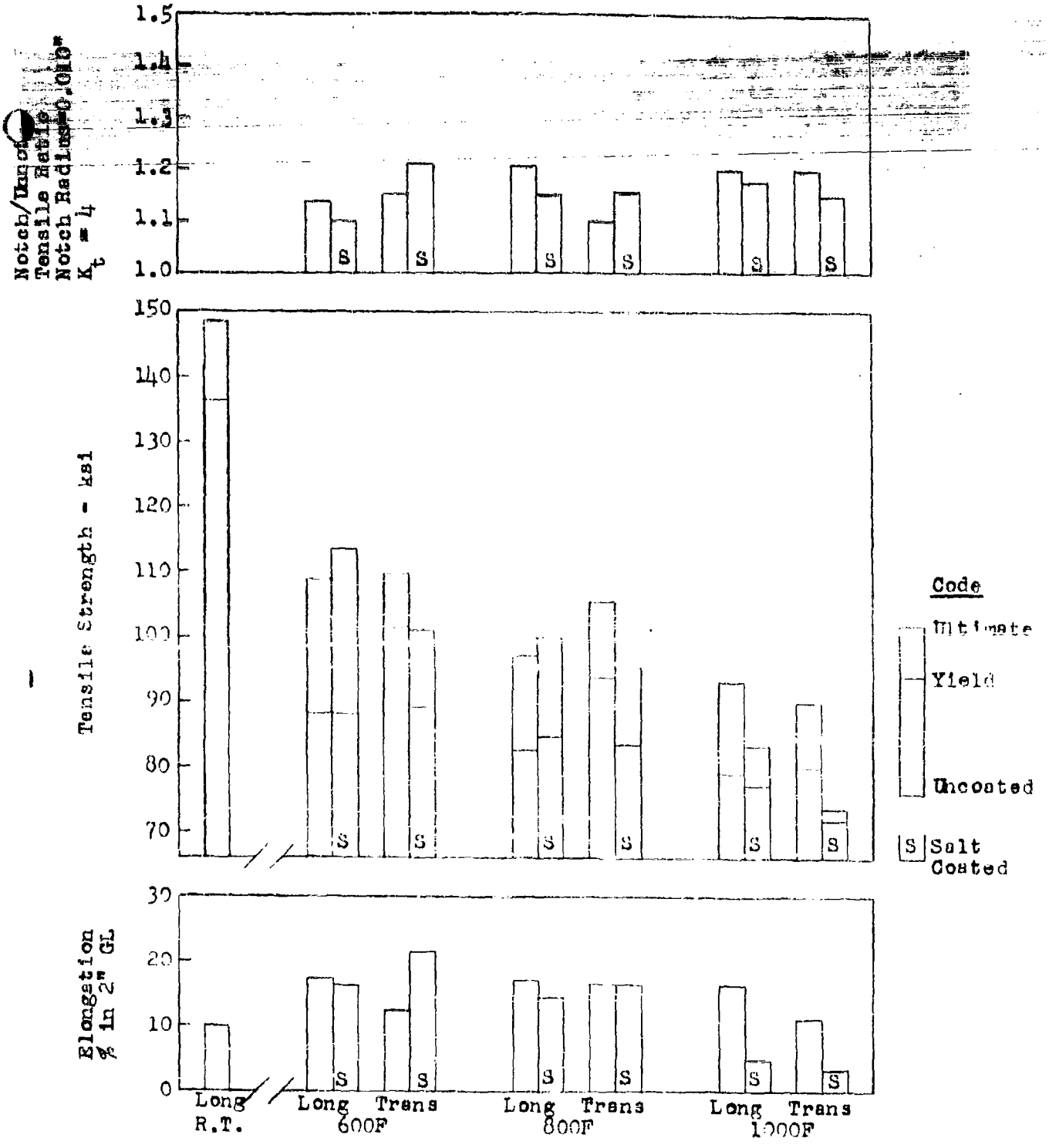

Figure 38: Effect of Salt on the Notched and Unnotched Hot Tensile Strength of Alpha-Plus-Beta-Processed Ti-12Zr-7Al Sheet. (0.050" thick, HR 1800F, Ann. 1 Hr. 1650F, Av. of 2 Tests)

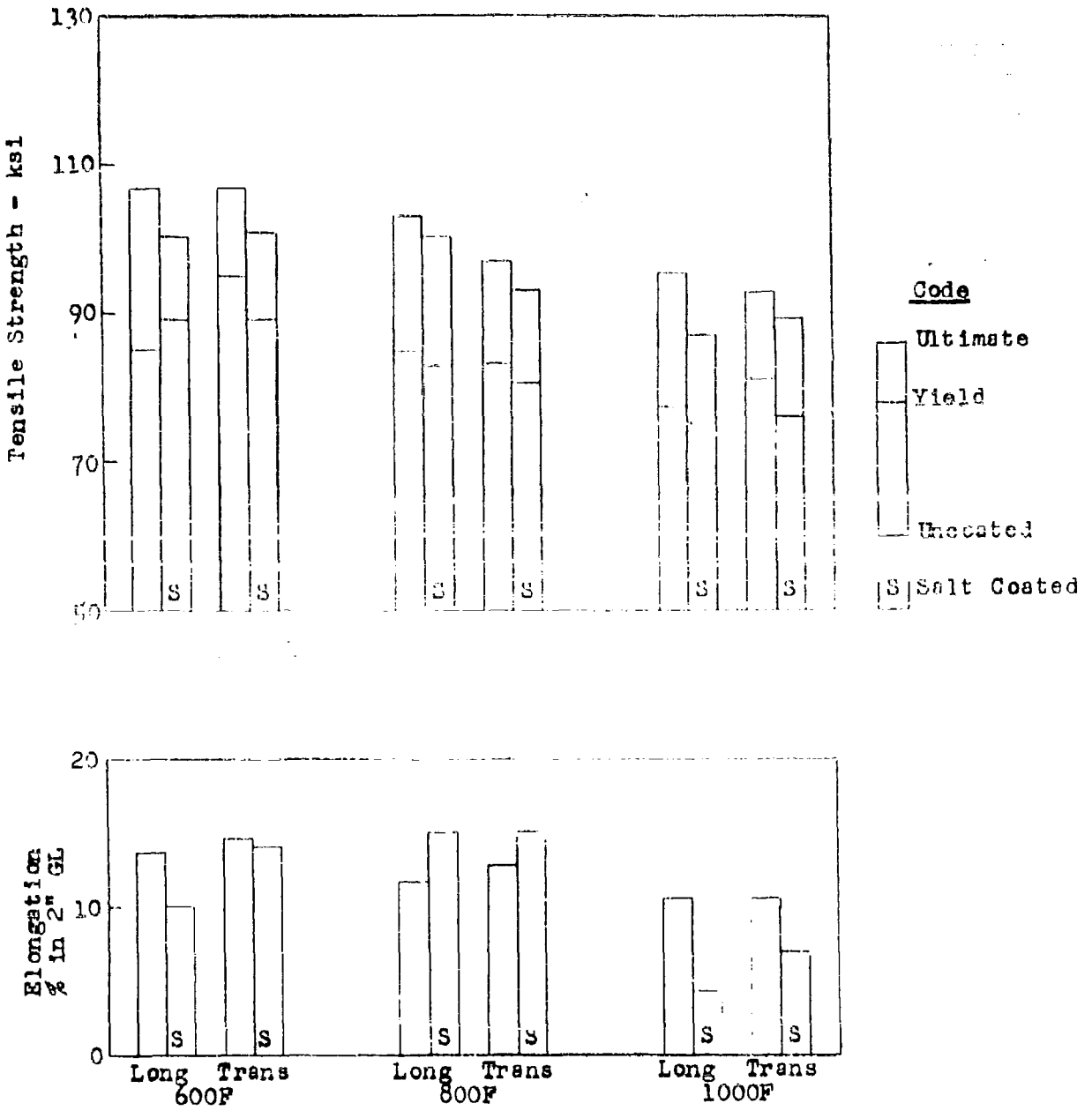

Figure 39: Effect of Salt on the Hot Tensile Strength of Longitudinal and Transverse Welds on Ti-12Zr-7Al Sheet. (0.050" thick, HR 1800F, Ann. 1 Hr. 1650F, Av. of 2 Tests.)

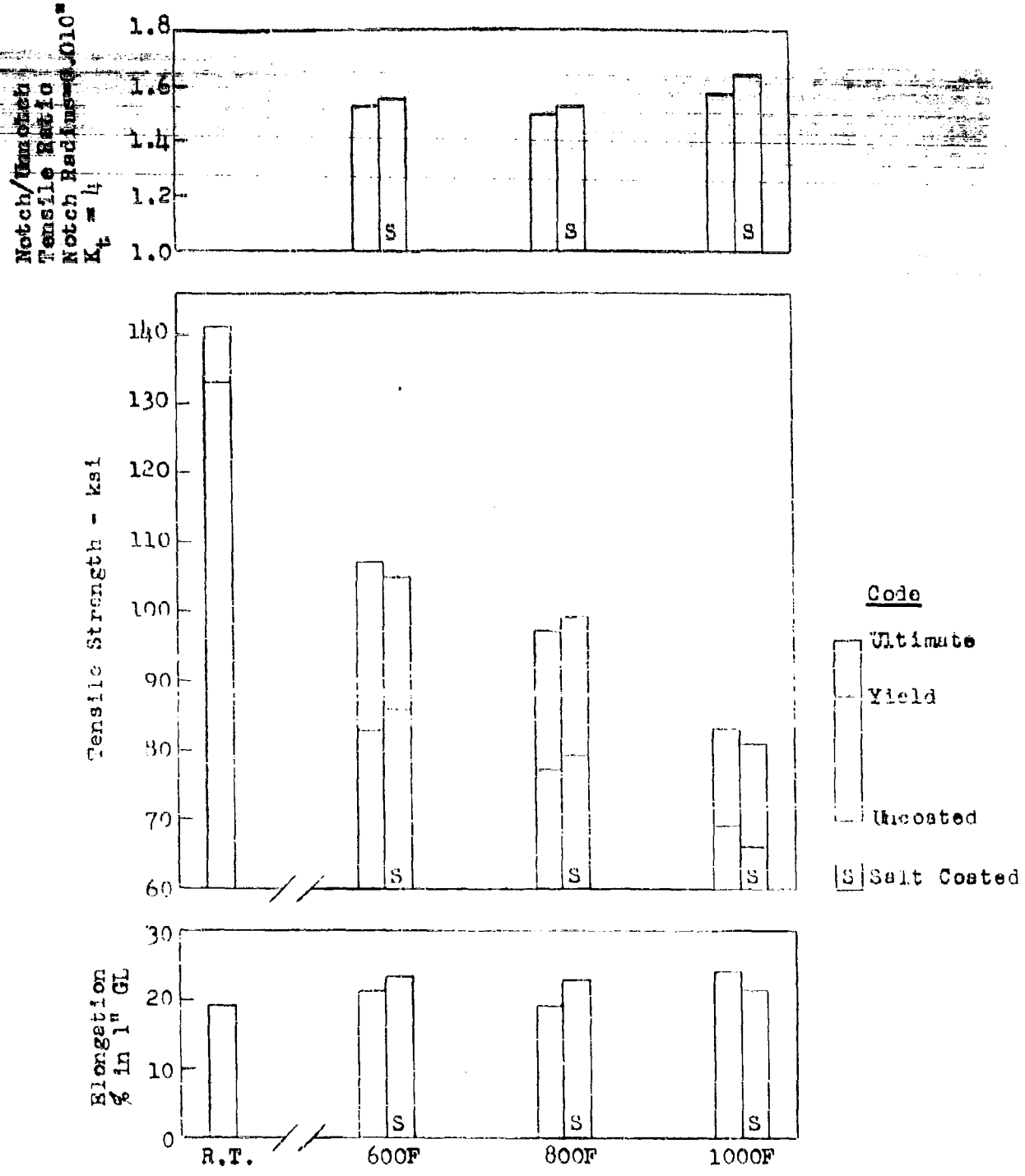

Figure 40: Effect of Salt on the Notched and Unnotched Hot Tensile Strength of Beta-Processed Ti-8Al-1Mo-1V Rod. (7/8" Diameter, HR 1950F, Ann. 1 Hr. 1800F + 8 Hrs. 1100F, Av. of 2 Tests.)

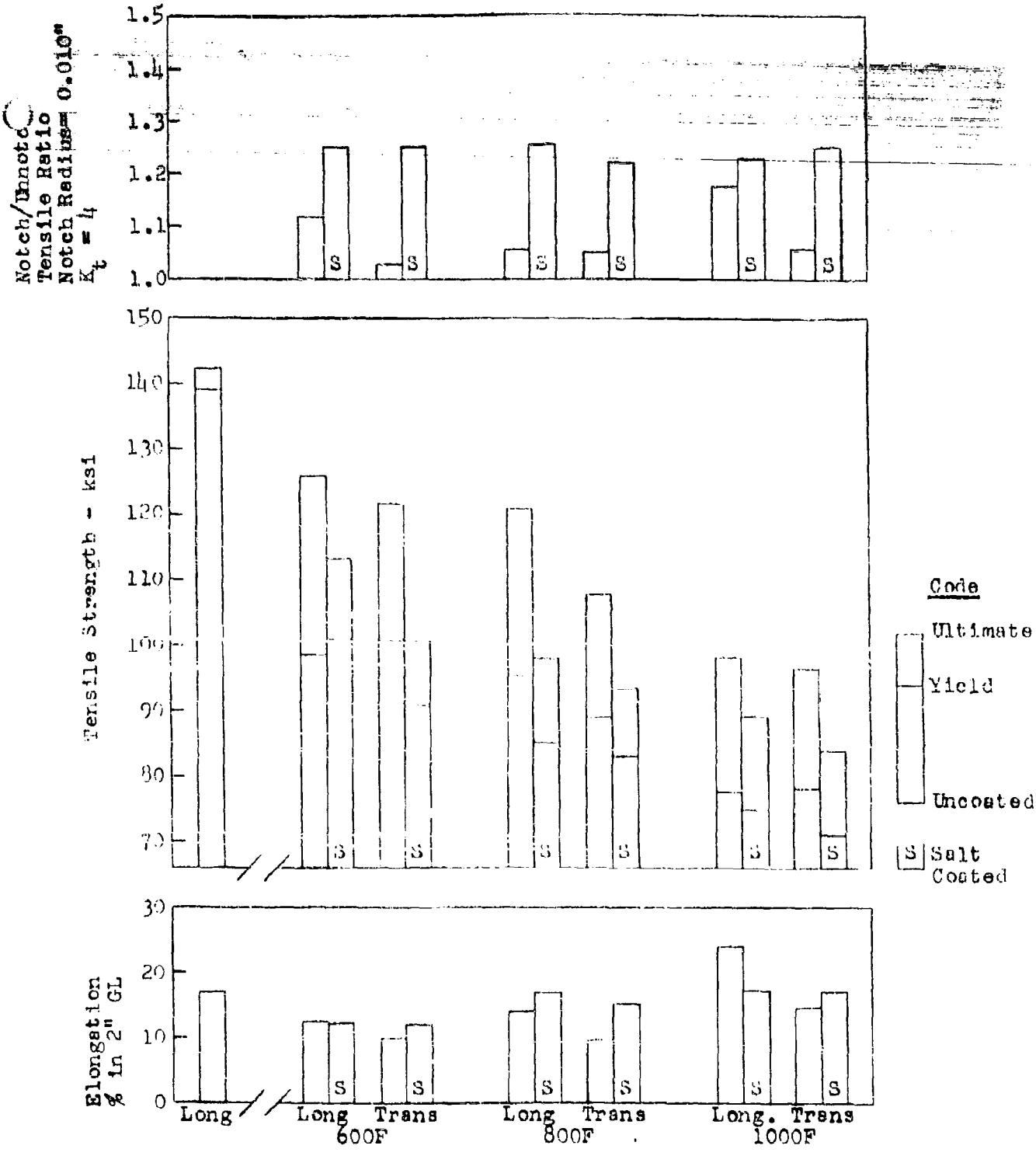

Figure 41: Effect of Salt on Notched and Unnotched Hot Tensile Strength of Alpha-Processed Ti-8Al-1Mo-1V Sheet. (0.050" thick, HR 1650F, Ann. 1 Hr. 1600F + 8 Hrs. 1100F, Av. of 2 Tests.)

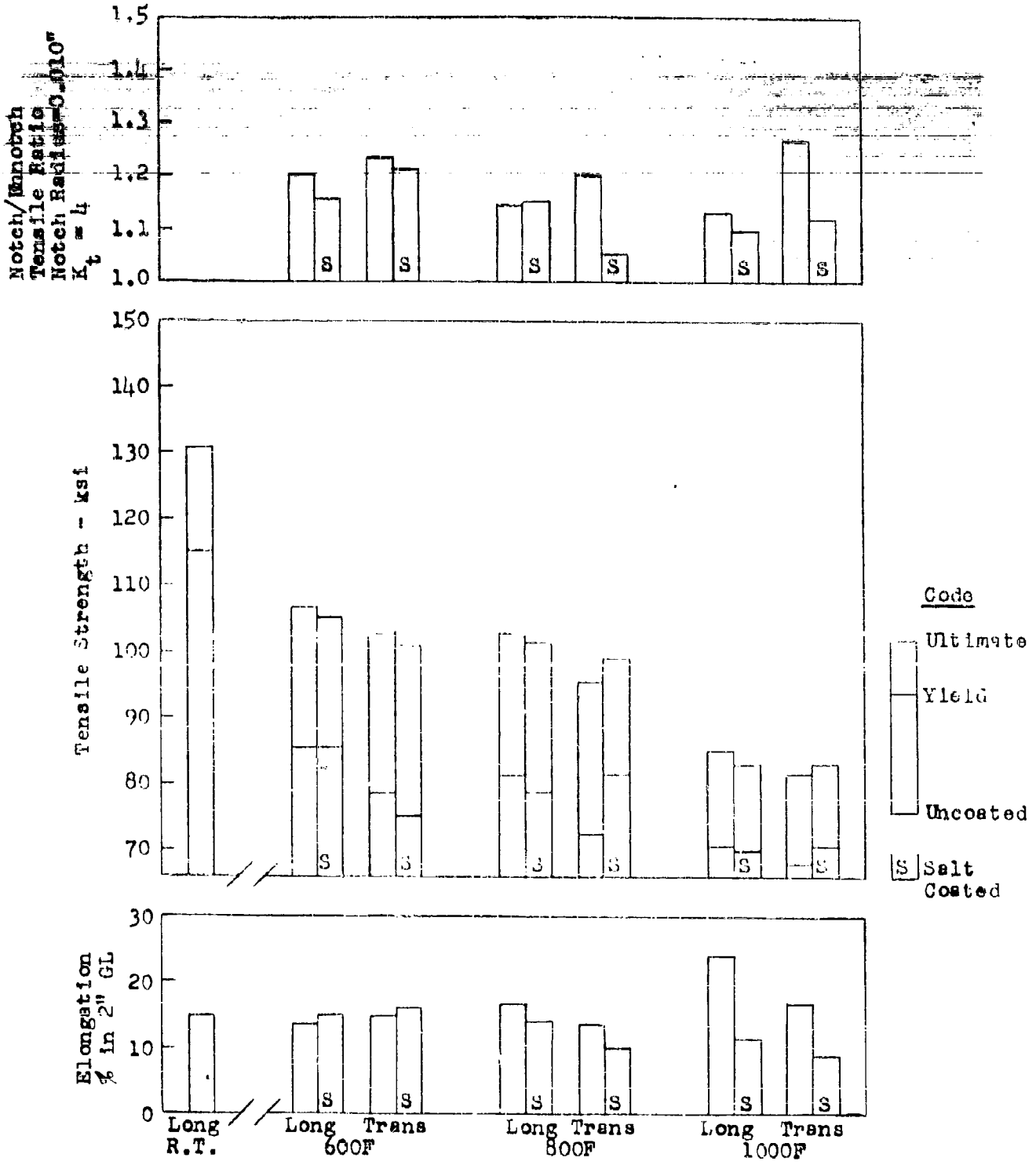

Figure 42: Effect of Salt on Notched and Unnotched Hot Tensile Strength of Alpha-Plus-Beta-Processed Ti-8Al-1Mo-1V Sheet. (0.050" thick, HR 1800F, Ann. 1 Hr 1800F + 8 Hrs. 1100F, Av. of 2 Tests.)

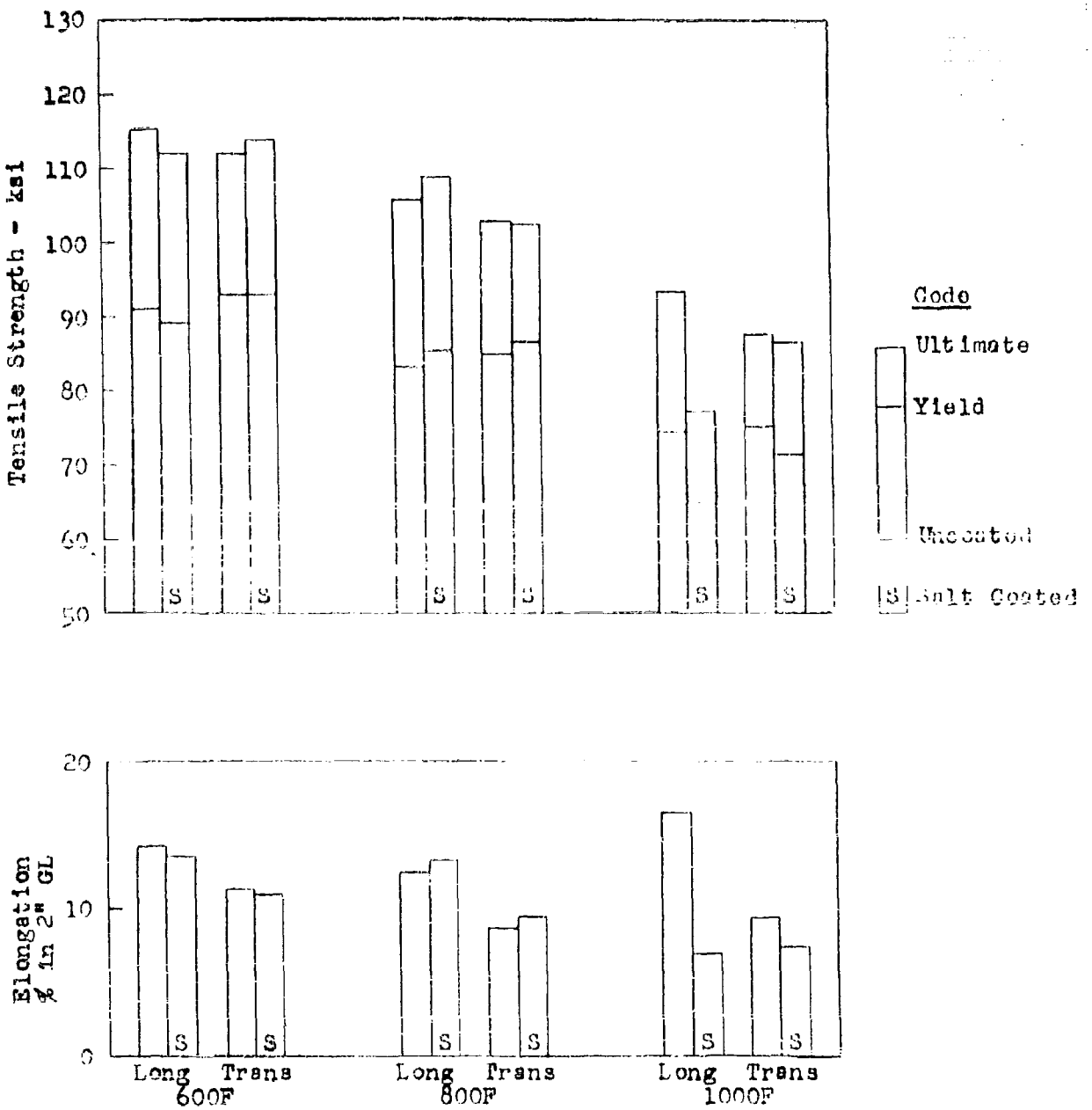

Figure 43: Effect of Salt on the Hot Tensile Strength of Longitudinal and Transverse Welds on Ti-8Al-1Mo-1V Sheet. (0.050" thick, HR 1800F, Ann. 1 Hr. 1800F + 8 Hrs. 1100F, Av. of 2 Tests.)

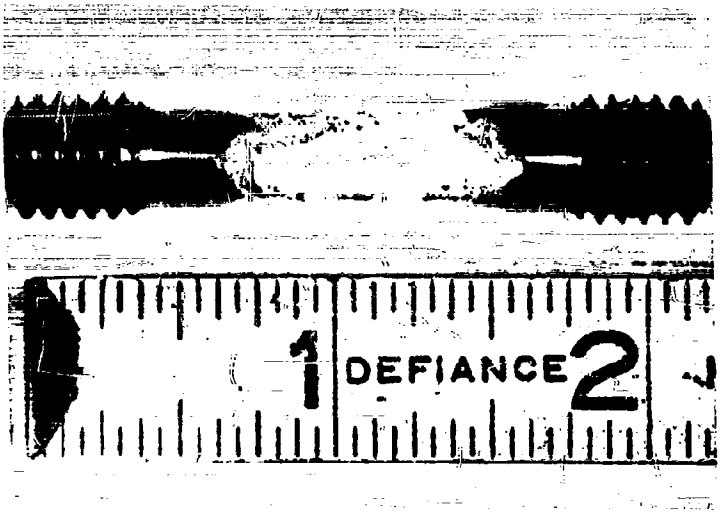

Figure 44

A Salt-Coated Ti-8Al-1Mo-1V Round Tensile Specimen After 100-Hours Exposure at 600F Under 79 ksi Stress 2X

Temp °F	Stress ksi
600	79
700	77
800	43
900	40

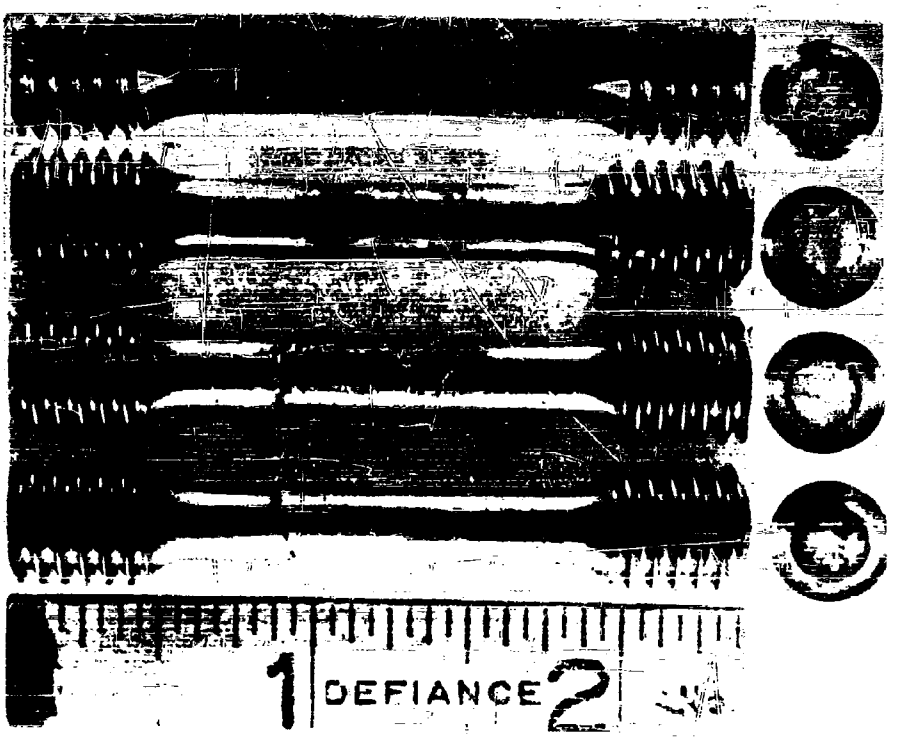

Figure 45

Condition of Ti-8Al-1Mo-1V Round Tensile Specimens After Salt Exposure at Temperature and Stress Indicated. Samples were Tensile Tested After Creep Exposure.

Figure 46

Intergranular Salt Attack on Surface of Ti-6Al-4V After 100 Hours at 800F and 39 ksi Stress. Preferential Attack of the Dark-Etching Beta + Alpha Transformation Structure is Noted. 500X

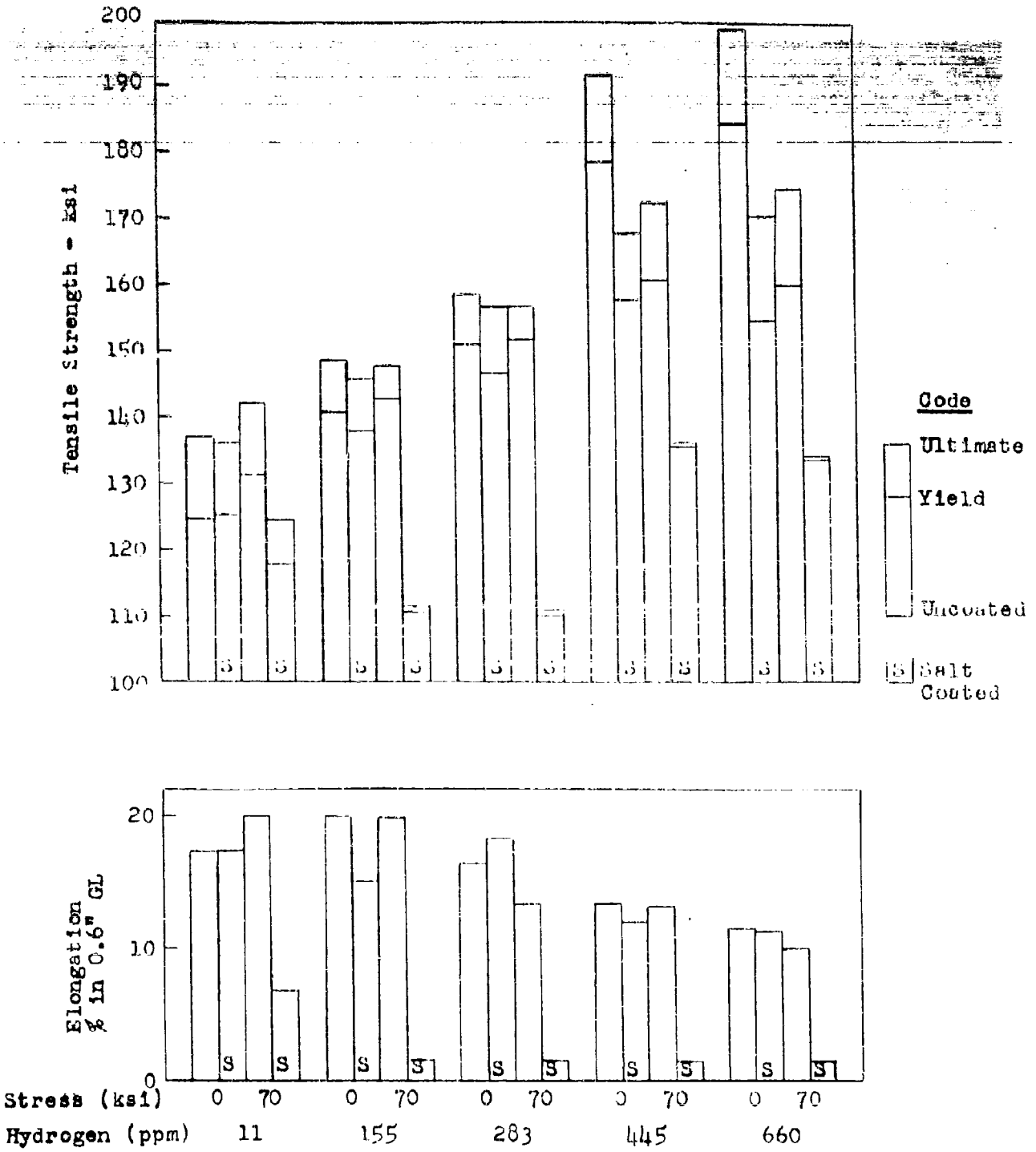

Figure 47: Effect of Hydrogen on the Tensile Stability of Ti-12Zr-7Al Sheet After 100 Hours Exposure at 700F as Influenced by Salt and Stress

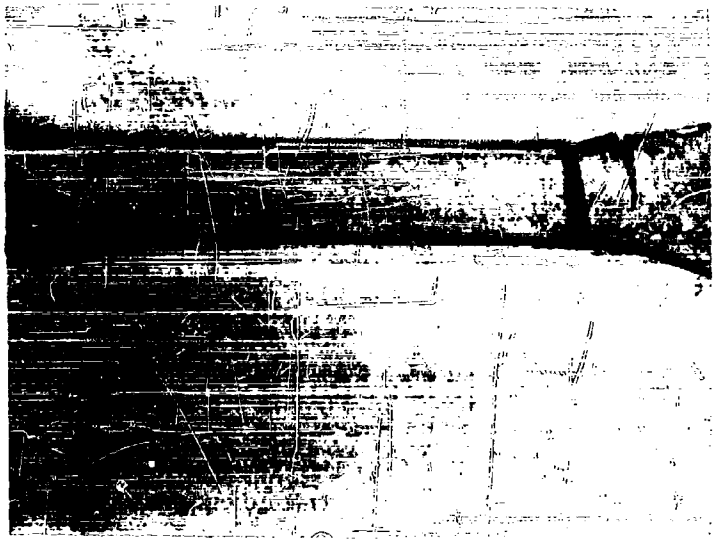

Figure 48

Al-Dip Ti-12Zr-7Al Sheet Tensile Specimen Which Failed after 116-Hour Salt-Creep Exposure at 1000F and 8 ksi Stress. Cracks Propagated From Edges where Aluminum Coating was Less than 0.0005" Thick. 4X

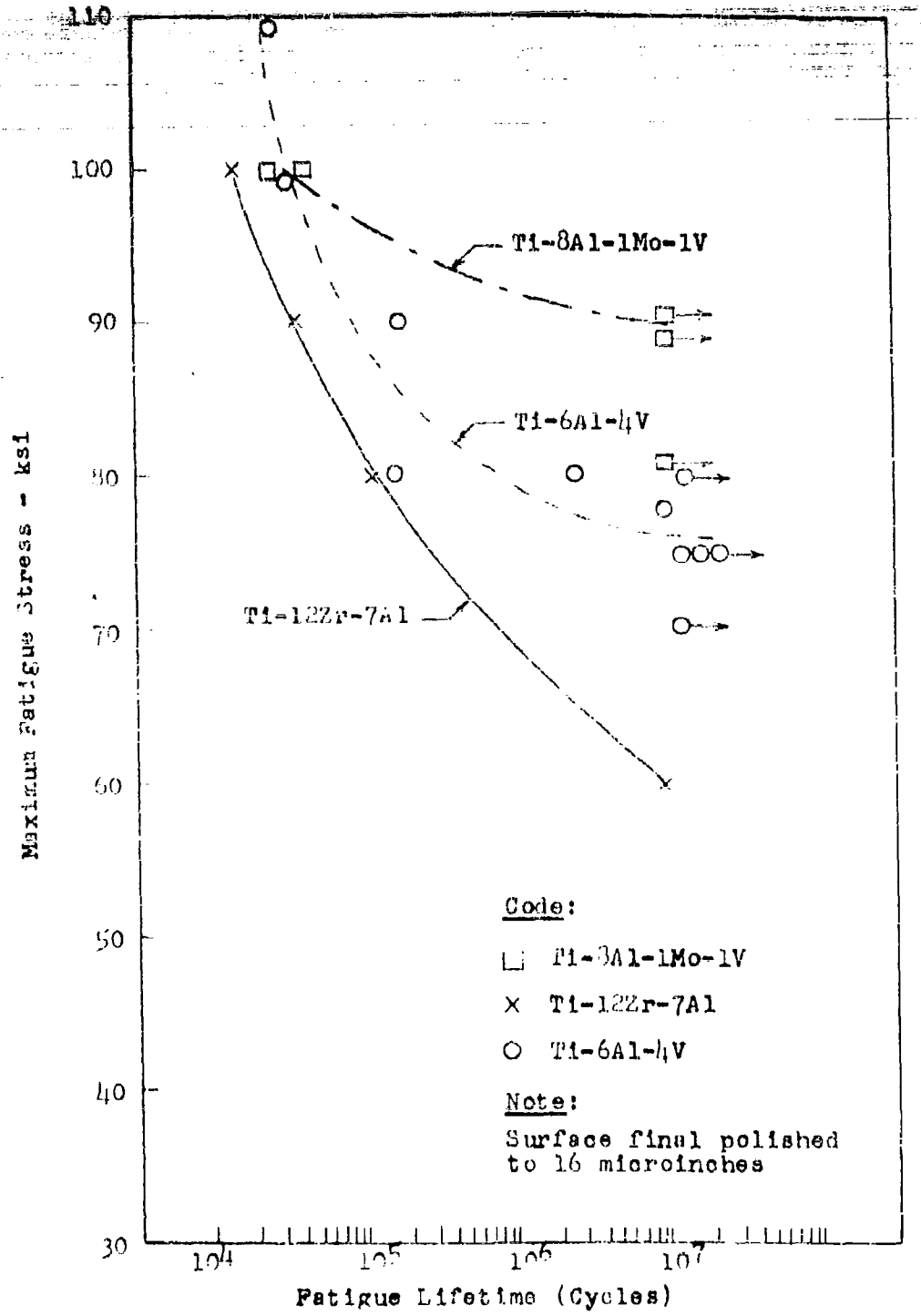

Figure 49: Rotating-Beam Fatigue Properties of Ti-12Zr-7Al, Ti-8Al-1Mo-1V and Ti-6Al-4V

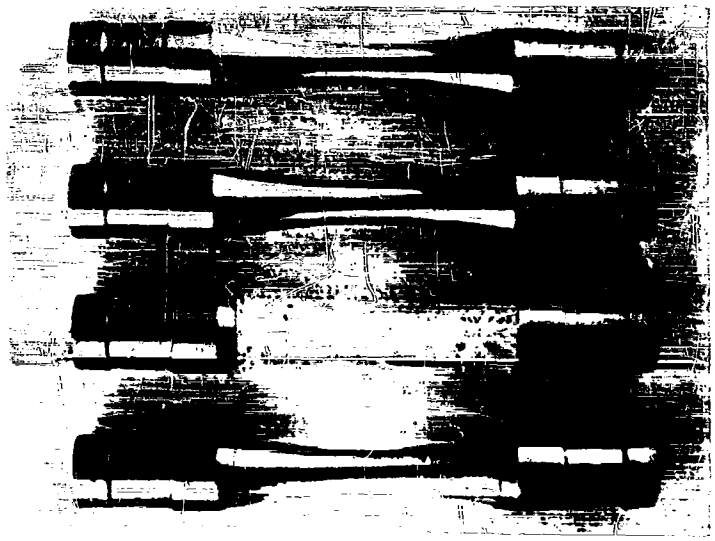

As Machined

Nickel Plated

Al Flame Spray

Al Dip

Figure 50

Rotating-Beam Fatigue Samples in the As-Machined and Coated Conditions Prior to Testing. 1X

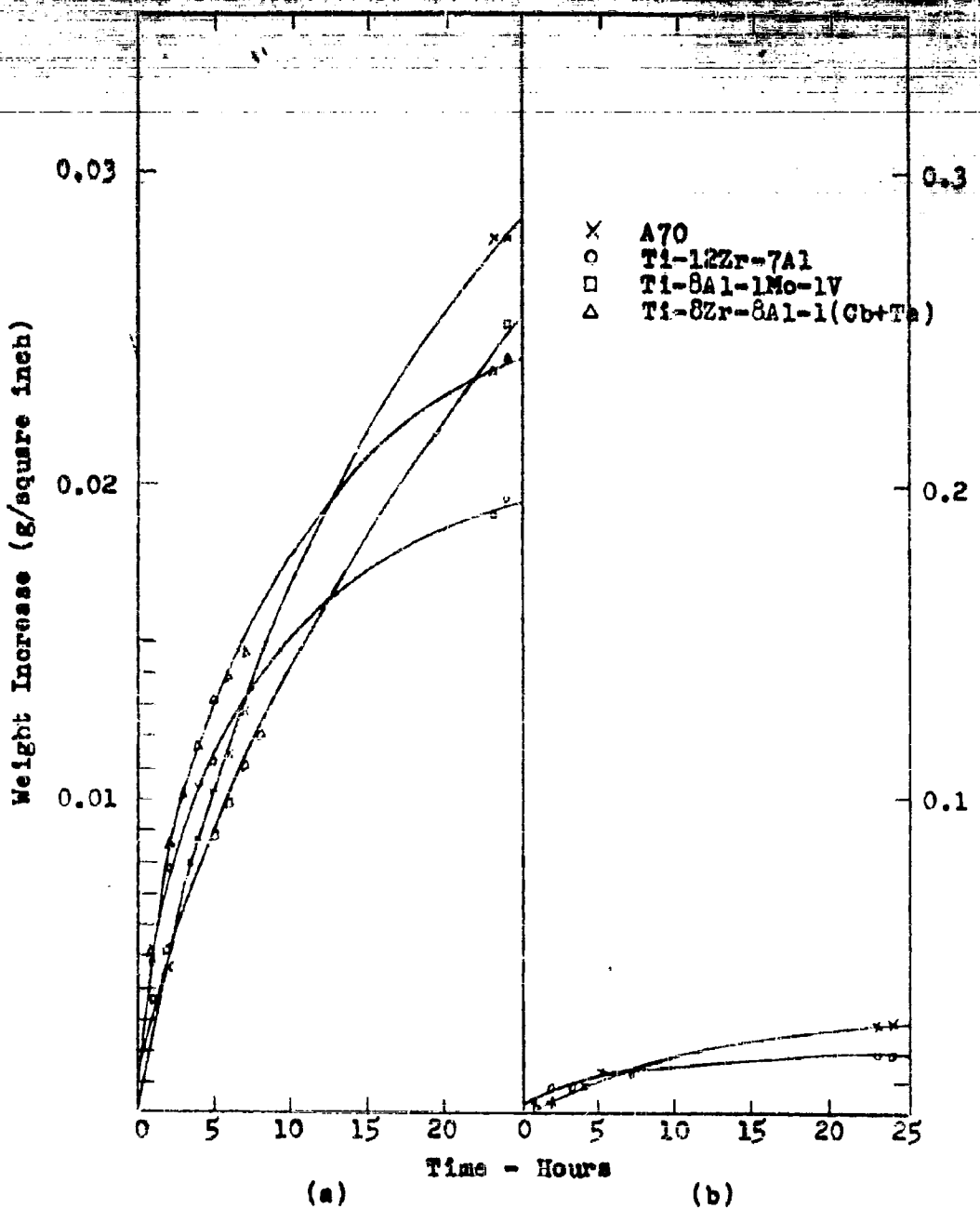

Figure 51: Weight Increase of Salt-Coated Super-Alpha Alloys with Time at 1200F

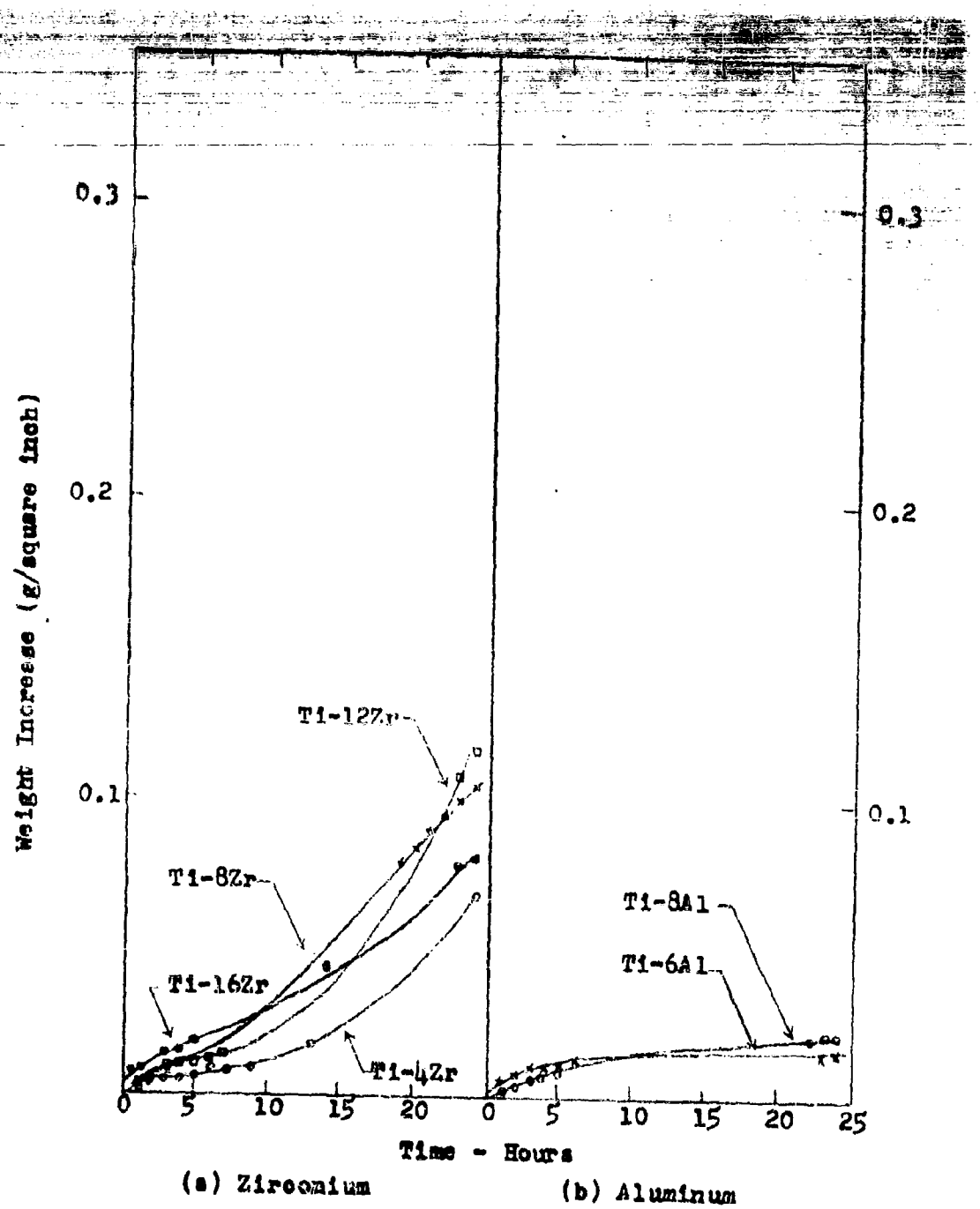

Figure 52: Rate of Salt Corrosion of Ti-Zr and Ti-Al Binary Alloys at 1200F

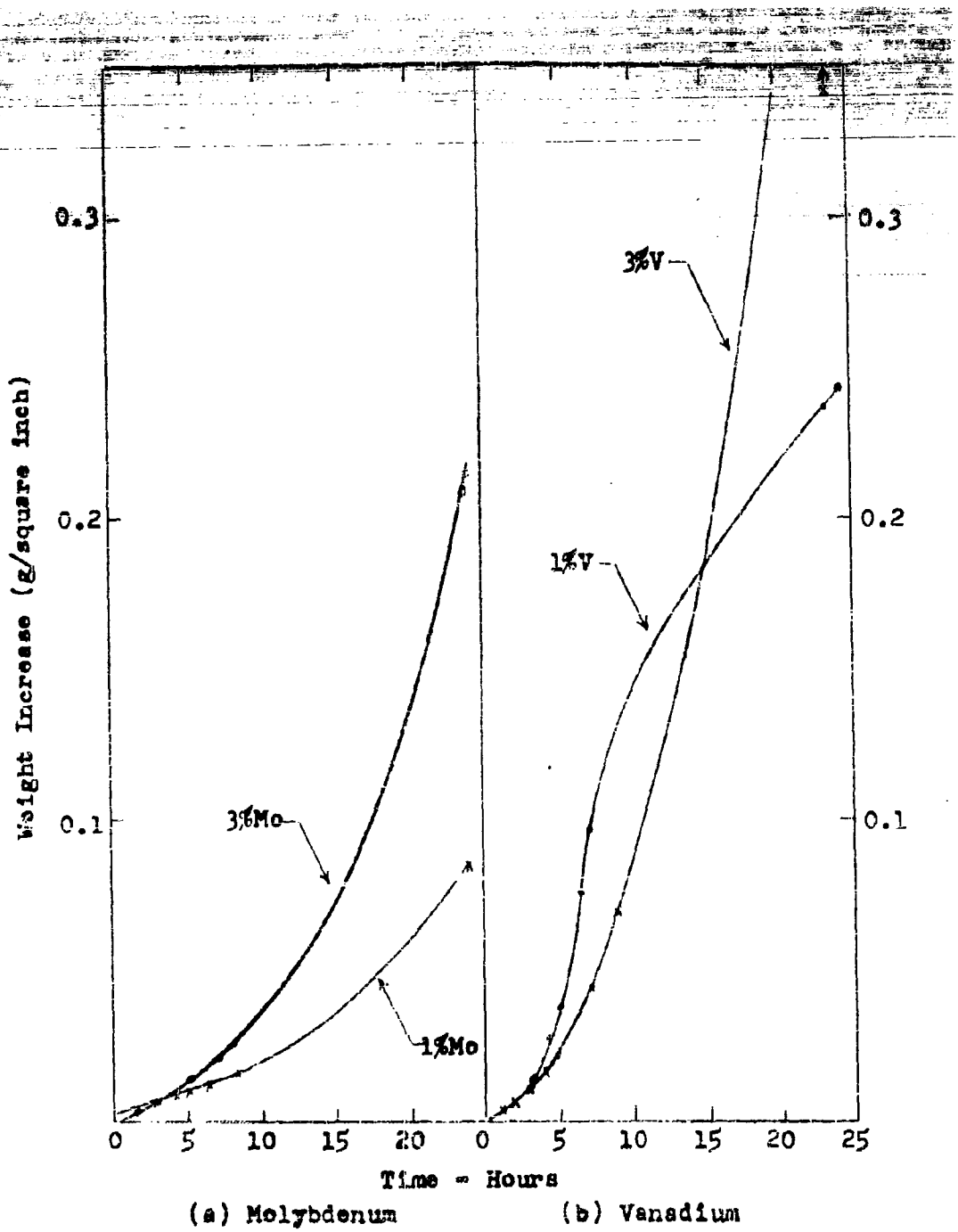

Figure 53: Rate of Salt Corrosion of Ti-Mo and Ti-V Binary Alloys at 1200F

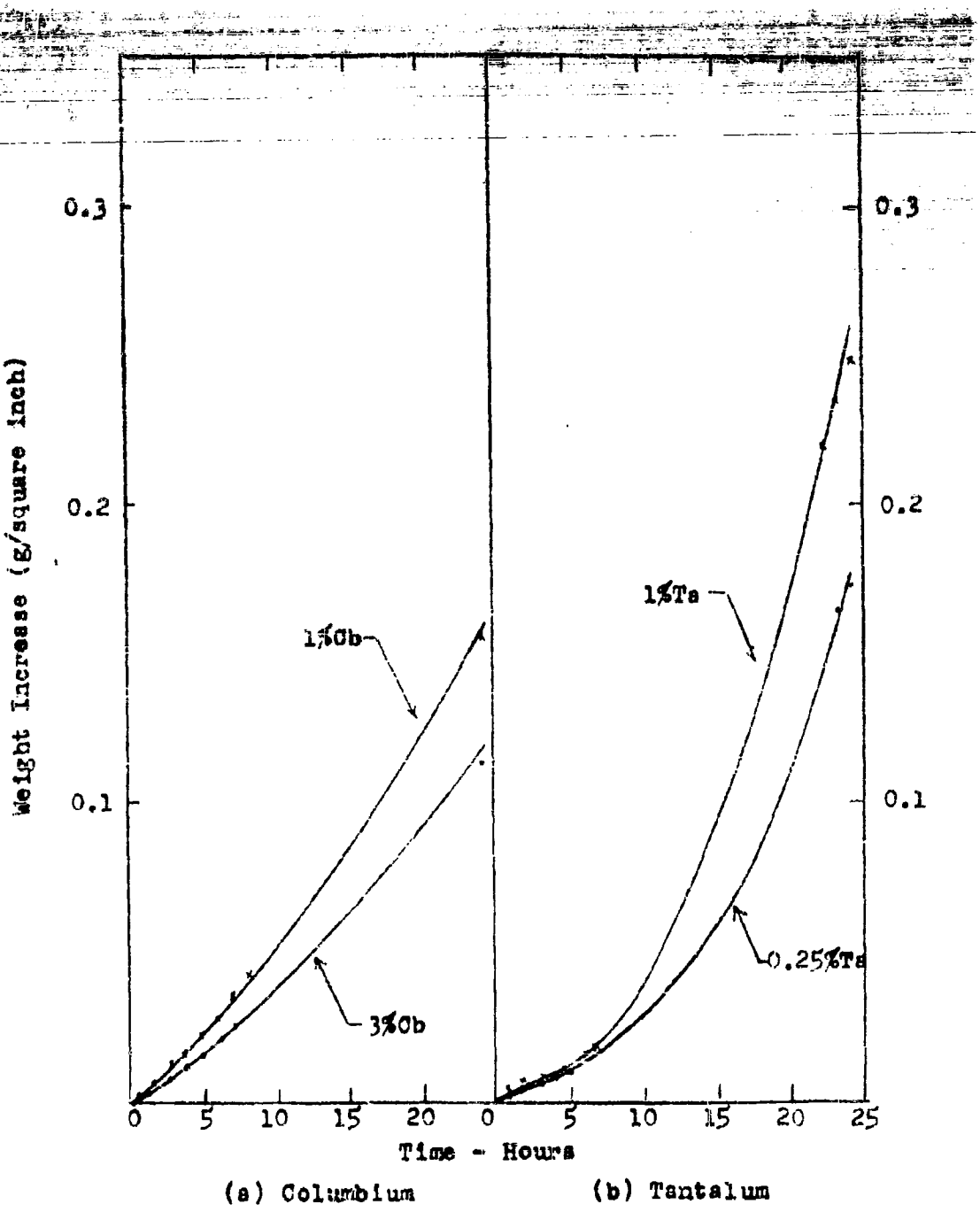

Figure 54: Rate of Salt Corrosion of Ti-Cb and Ti-Ta Binary Alloys at 1200F

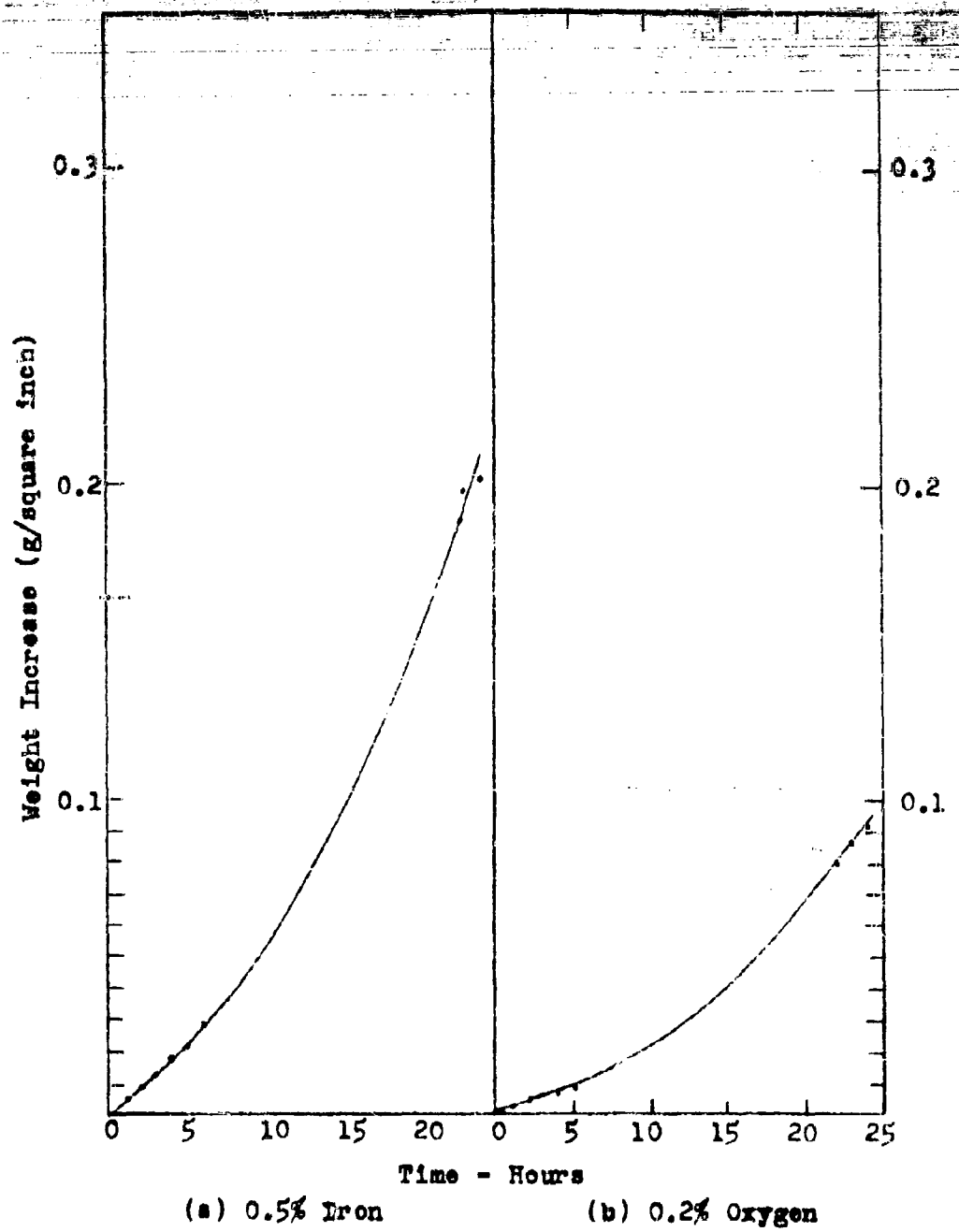

Figure 55: Effect of Iron and Oxygen Upon the Salt Corrosion of Titanium at 1200F

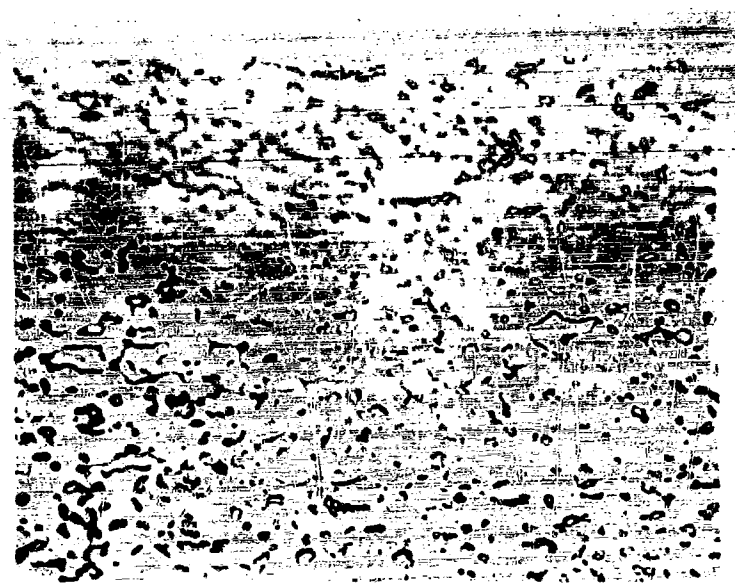

a) Equiaxed Beta Particles, Approaching Fully Annealed Structure. Salt Test Gave 0.0795 g./sq.in. Weight Gain in 24 Hours. 1000X

b) Fine Beta Particles. Structure is Incompletely Annealed. Salt Test Gave 0.0253 g./sq.in. Weight Gain in 24 Hours. 1000X

Figure 56

Effect of Microstructure on the General Salt Corrosion of Ti-8Al-1Mo-1V Sheet

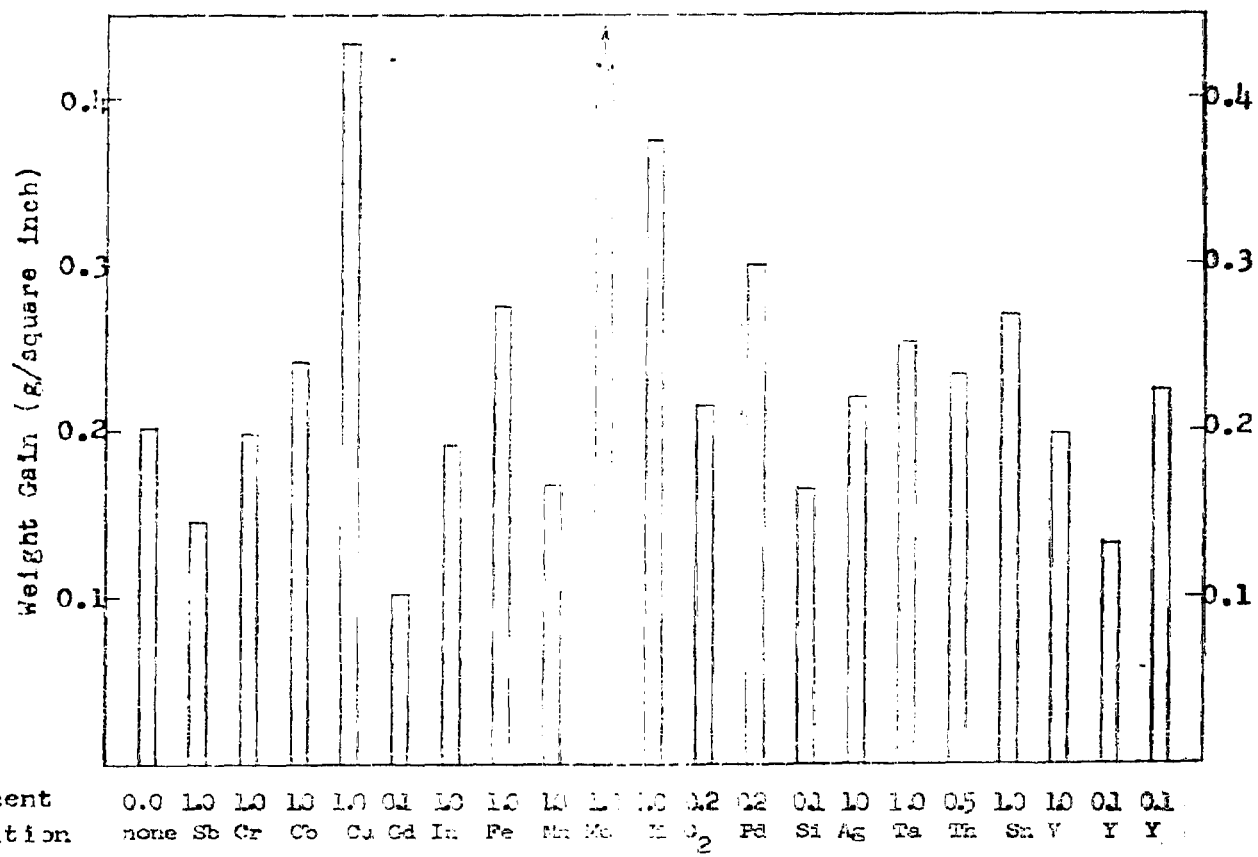

Figure 57: Effect of Minor Alloy Additions Upon the General Salt Corrosion of Ti-12Zr-7Al. Data are from Tests of 24-Hour Duration at 1200F in an Air Stream of 525 ml/minute.

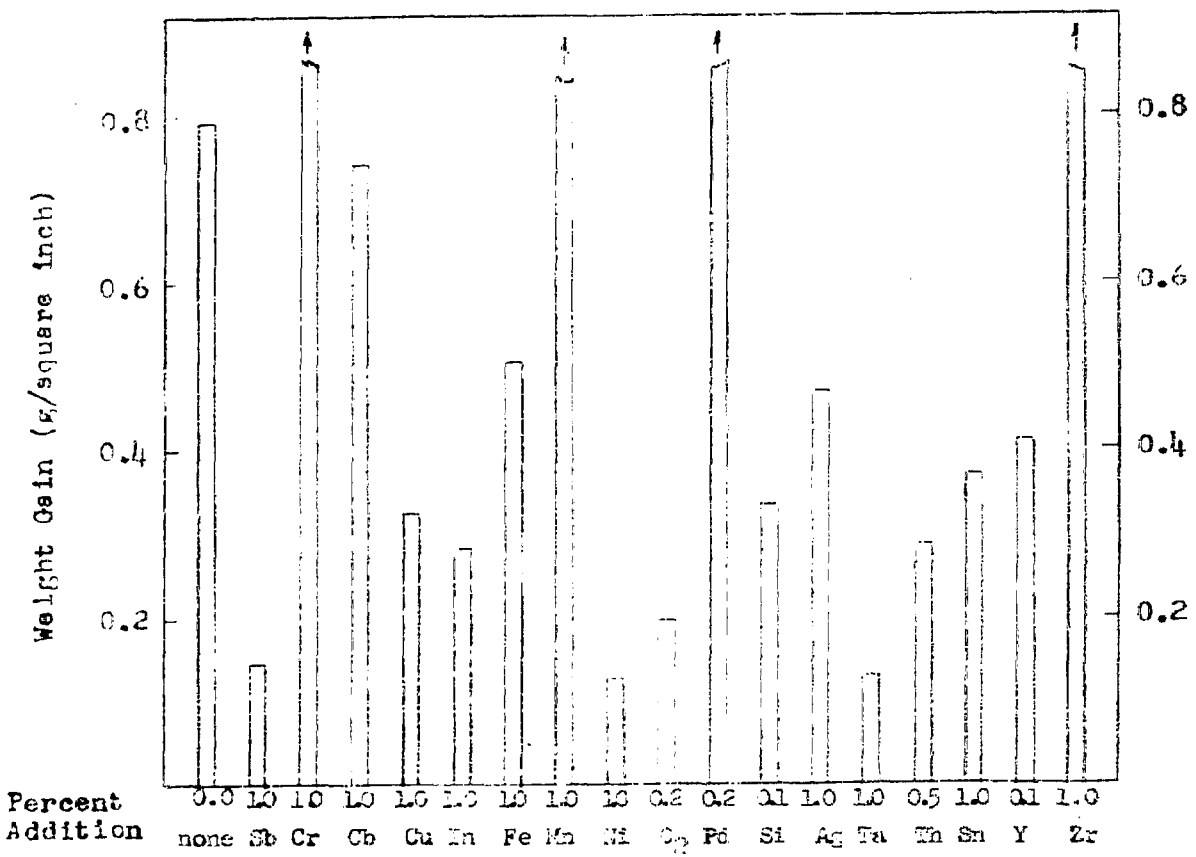

Figure 58: Effect of Minor Alloy Additions Upon the General Salt Corrosion of Ti-8Al-1Mo-1V. Data are from Tests of 24-Hour Duration at 1200F in an Air Stream of 525 ml/minute.

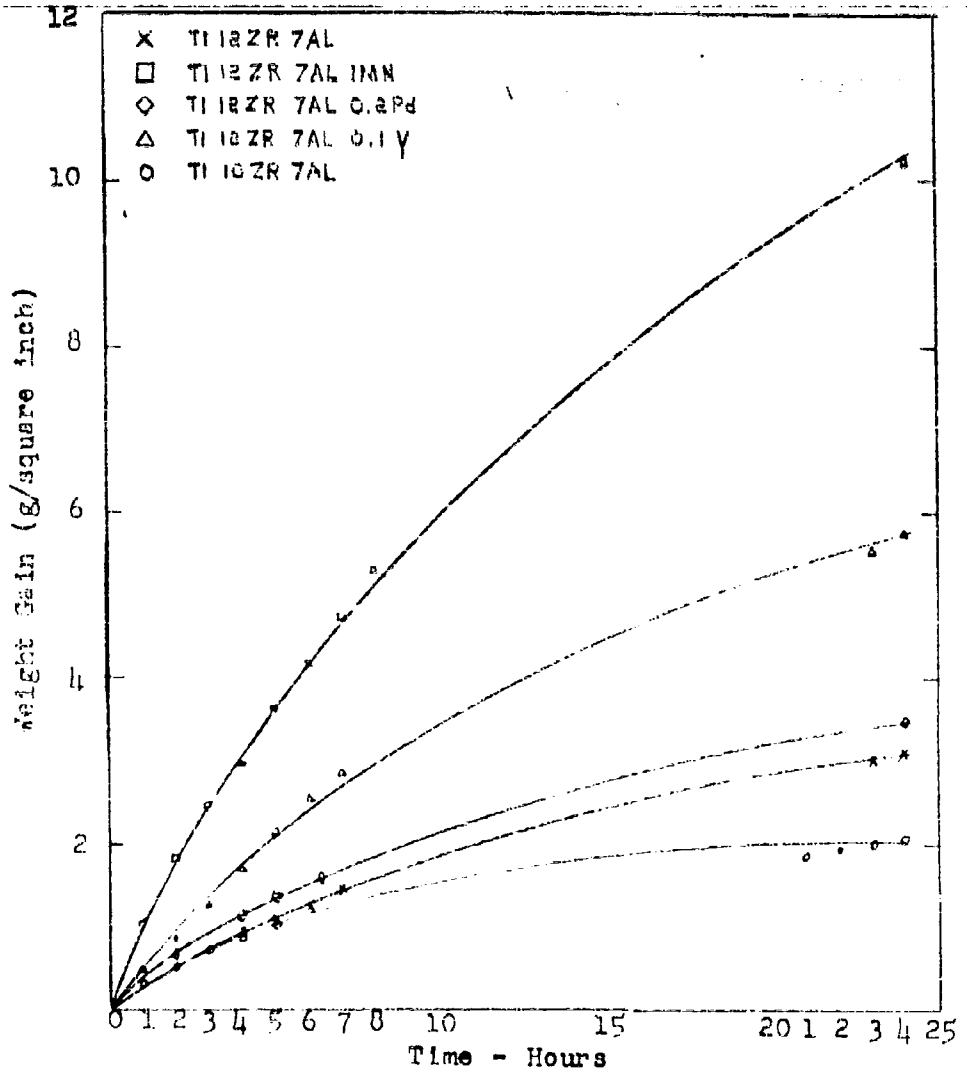

Figure 59: Rate of Corrosion of Selected Alloys of the Ti-12Zr-7Al Series

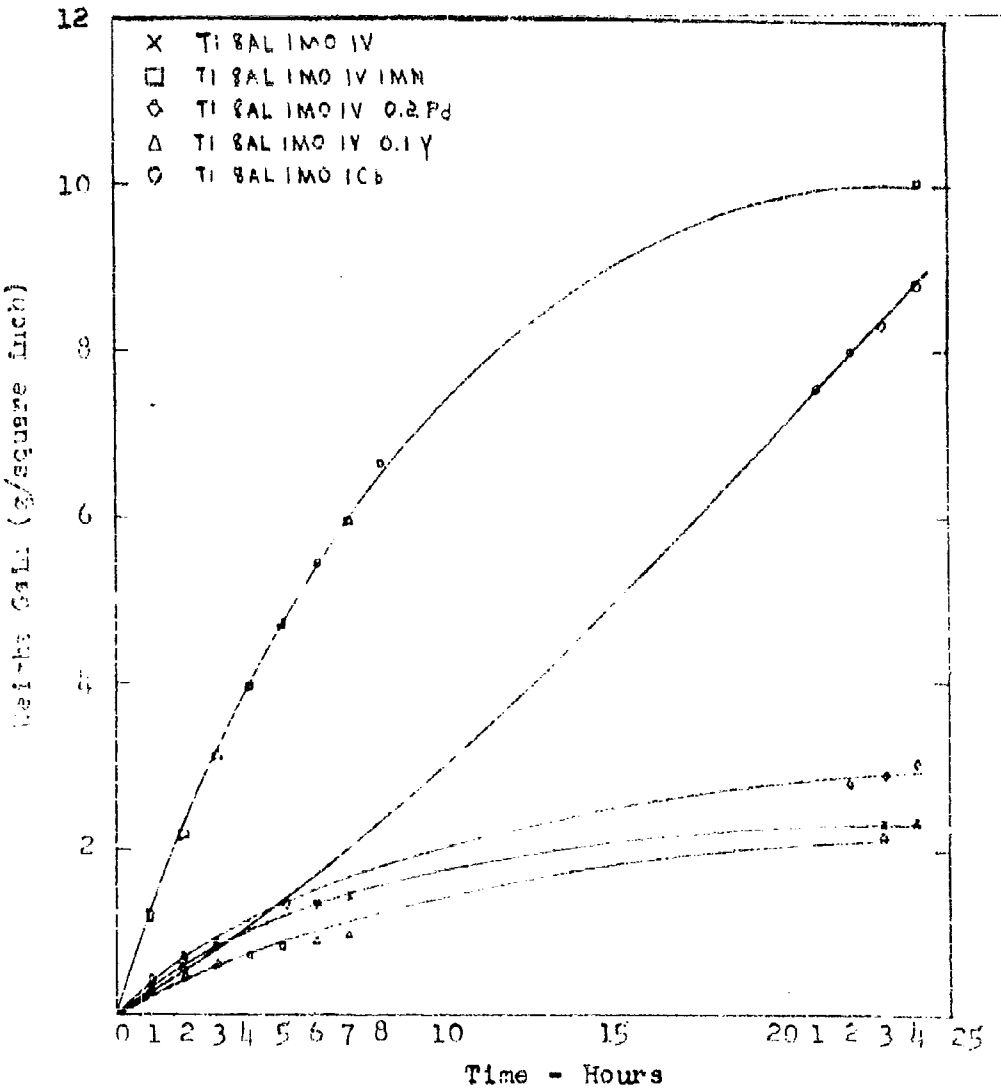

Figure 60: Rate of Corrosion of Selected Alloys of the Ti-8Al-1Mo-1V Series

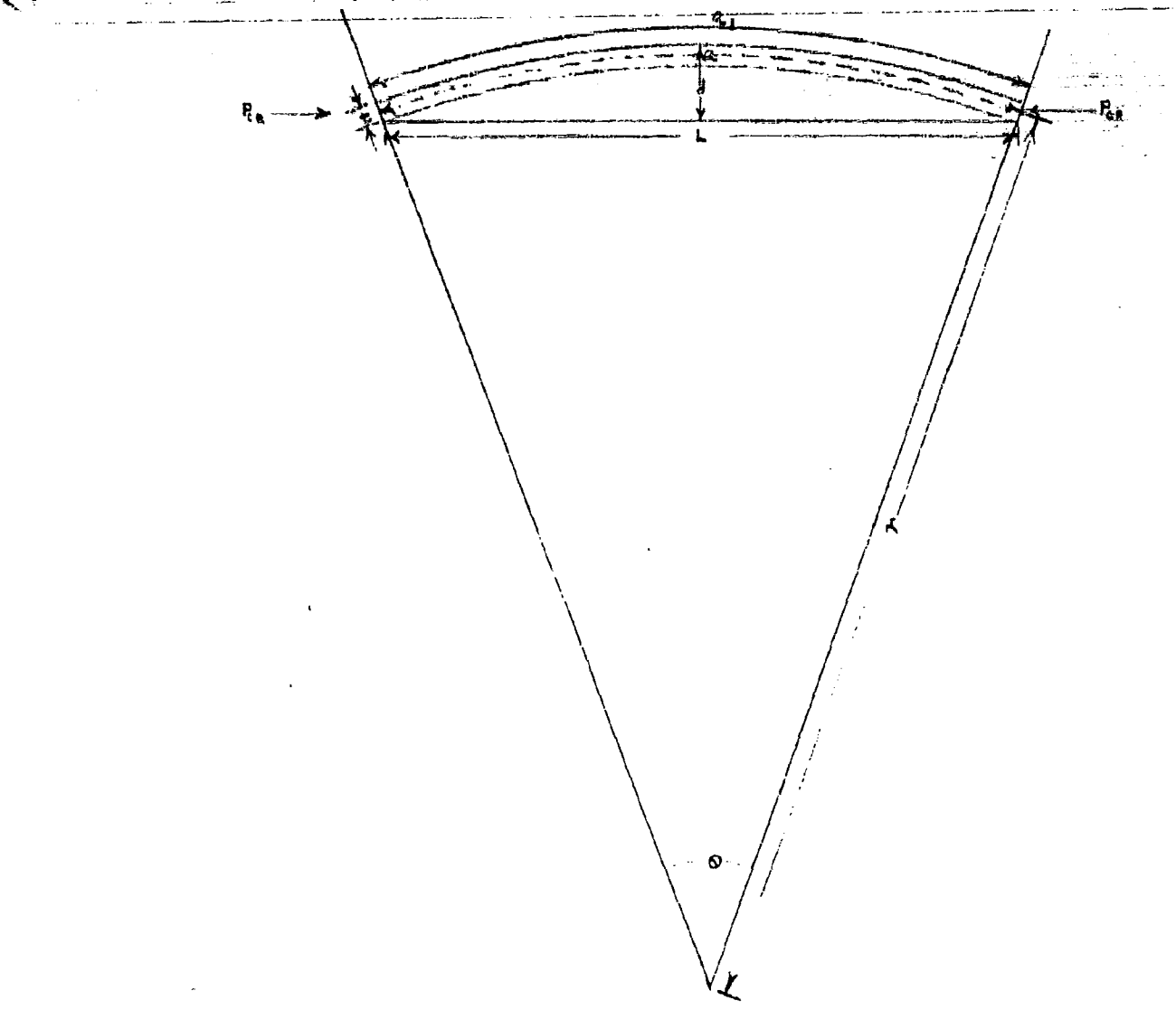

Figure 61: Geometrical Construction of Stressed Specimen

DISTRIBUTION LIST

Chief, Bureau of Naval Weapons
Department of the Navy
Materials Division
Washington 25, D. C. VIA
Inspector of Naval Material
401 Old Post Office Building
Pittsburgh 19, Pennsylvania

Mr. R. W. Crozier
Executive Director
Materials Advisory Board
National Academy of Sciences
2101 Constitution Avenue
Washington 25, D. C.

Dr. R. I. Jaffee
Battelle Memorial Institute
505 King Avenue
Columbus 1, Ohio

Dr. George Gerard
Professor of Aeronautical Engineering
New York University
New York 53, New York

Mr. T. H. Gray
Assistant Chief Metallurgist
Boeing Aircraft Corporation
Seattle 24, Washington

Dr. Donald McPherson, Manager
Metallurgical Research Dept.
Armour Research Foundation
10 West 35th Street
Chicago 16, Illinois

Director, Metallurgical Research Laboratories
Syracuse University Research Institute
Syracuse, New York

Mr. S. V. Arnold
Physical Metallurgy Division
Watertown Arsenal Laboratory
Watertown, Massachusetts

Mr. Howard Middendorp
Wright Air Development Center
Wright-Patterson Air Force Base
Ohio

Mr. L. L. Gould
Materials Advisory Board
National Research Council
2101 Constitution Avenue
Washington 25, D. C.

Mr. W. H. Sharp, Metallurgist
Engineering Department
Pratt & Whitney Aircraft Corp.
East Hartford 8, Connecticut

Mr. L. P. Spalding, Director of Laboratories
North American Aviation, Inc.
International Airport
Los Angeles 45, California

Mr. Robert Wischer
Chief Research Engineer
Republic Aviation Corporation
Farmingdale, L. I., New York

Dr. William Youden, Consultant
National Bureau of Standards
Washington 25, D. C.

Mr. H. D. Kessler
Titanium Metals Corporation of America
P. O. Box 718
Toronto, Ohio

Mr. S. R. Seagle, Supervisor
Sponsored Research
Reactive Metals, Inc.
Niles, Ohio

Commander
Headquarters Air Materiel Command
Wright-Patterson AFB, Ohio
ATTN: MCPBM, Mr. Robert T. Jamison

DISTRIBUTION LIST
(Continued)

Mr. H. R. Ogden
Defense Metals Information Center
Battelle Memorial Institute
505 King Avenue
Columbus 1, Ohio

Mr. John H. Garrett
Chief Materials Division Office
Director of Research and Engineering
The Pentagon-Washington 25, D. C.

Convair Astronautics
A Division of General Dynamics Corporation
P. O. Box 166
San Diego 12, California
ATTN: Mr. A. Hurlich
Materials Research Group
Department 592-10

Mr. S. R. Carpenter
Producibility Supervisor
Mail Zone 6-148
Convair
A Division of General Dynamics Corporation
San Diego 12, California

Republic Steel Company
Massillon, Ohio
ATTN: Mr. H. O. Mattes

Mr. P. J. Hughes
Lockheed Aircraft Corporation
Structural Research Laboratory
Marietta, Georgia

Commanding Officer
Diamond Ordnance Fuze Lab
ATTN: Tech. Ref. Sec. ORDTL 012
Washington 25, D. C.

Naval Air Materiel Center
Aeronautical Materials Laboratory
Philadelphia 12, Pennsylvania

Crucible Steel Company of America

Bureau of Ships (Code 343)
Navy Department
Washington 25, D. C.

Naval Research Laboratory
Washington 25, D. C.

Office of Naval Research (Code 423)
Washington 25, D. C.

National Aeronautical & Space Admin.
1520 H Street NW
Washington 25, D. C. (3 copies)

Aerospace Industries Associated
7660 Beverly Boulevard
Los Angeles 36, California
ATTN: Mr. H. D. Moran (10 copies)

Executive Office of the President
Office of Defense Mobilization
ATTN: Mr. J. H. Stehmen
Washington, D. C.

Department of Commerce, Business Defense Supply Agency
Washington, D. C.
ATTN: Mr. H. Cullen

Grumman Aircraft Engineering Corp.
Bethpage, Long Island, New York
ATTN: Mr. F. X. Drumm
Engineering Material Group

North American Aviation Corp.
Columbus, Ohio
ATTN: Mr. Paul Maynard
Engineering Materials Group

Chance Vought Aircraft, Inc.
Dallas, Texas
ATTN: Mr. John Seeger
Engineering Materials Group

Titanium Metals Corporation of America
233 Broadway, New York 17, N. Y.
ATTN: Mr. Ward W. Minkler